UNIVERSITÀ DEGLI STUDI DI PADOVA

DIPARTIMENTO DI INGEGNERIA INDUSTRIALE

CORSO DI LAUREA MAGISTRALE IN CHEMICAL AND PROCESS ENGINEERING

Tesi di Laurea Magistrale in

Chemical and Process Engineering

Design of an advanced control system and a dual-horizon optimizer for a refinery thermal cracking furnace through predictive fouling modeling

Relatore: Prof. Massimiliano Barolo

Correlatore: Ing. Luca Barboni

Laureando: MATTEO UJKA

ANNO ACCADEMICO 2022 – 2023

Abstract

In industrial processes, such as oil refining, after addressing the fundamental requirements of ensuring the essential functionality and safety of the control system through the basic control layer, the next step involves process optimization. Advanced process control (APC) applications enable the stabilization of operations and the achievement of measurable economic goals. Notably, APC applications often rely on model predictive control (MPC). The success of MPC is rooted in its ability to provide a systematic and standardized approach to multivariable process control, incorporating constraints and utilizing models derived from experimental tests. Additionally, it can employ non-linear models, such as those derived from system physics, to predict future process behavior.

This Thesis addresses the design of an APC system with a dual-horizon optimizer for a refinery thermal cracking process through predictive fouling modeling. The APC models developed are divided into:

• short-term models, developed using AspenTech's DMC3™ software, with the aim of providing short-term predictive control;

• a long-term model based on a time series model, developed in MATLAB, for predicting furnace fouling.

Both models are equipped with an optimizer to achieve short-term objectives, including maximizing yields while adhering to safety, environmental, and process constraints, as well as long-term objectives to ensure fouling control to reach the end of the run at the set conditions. The project was carried out at API Refinery of Ancona S.p.A., located in Falconara Marittima (AN), Italy, in collaboration with Aspen Technology. The results obtained from the predictive fouling model simulations highlight the possibility of providing a reliable prediction, suggesting a long-term optimization that can yield an increase of over 1% in production, with a substantial economic return. This allows the project to proceed to the commissioning phase for the online implementation of the APC by 2024, along with further model development in collaboration with AspenTech through the utilization of deep learning neural networks.

Table of Contents

List of symbols

Acronyms

ARIMA	=	autoregressive integrated moving average
CCR	=	Conradson carbon residue
CV	=	controlled variable
DCS	=	distributed control system
DMC	=	dynamic matrix control
FFWDV	=	feed-forward disturbance variable
FC	=	flow controller
FI	=	flow indicator
FT	=	flow transmitter
FOP	=	furnace outlet pressure
FOT	=	furnace outlet temperature
HGO	=	heavy gas oil from atmospheric distillation column
HGOVB	=	heavy gas oil from visbreaking after-vacuum flash unit
HVBGO	=	heavy visbreaking gas oil after atmospheric distillation
PSHH	=	high pressure block
HPTC	=	high pressure thermal cracking
HLL	=	higher liquid level
IVP	=	initial value problem
LVGO	=	light vacuum gas oil
LLL	=	lower liquid level
MAN	=	manual

MP = medium pressure

MAN = manual

MPC = model predictive control

PID = partial-integral-derivative control

PI = pressure indicator

PIC = pressure indicator controller

PI = pressure indicator

PSV = pressure safety valve

PV = process value

RSP = remote set-point

SP = set-point

XY = solenoid valve of the pressure control system of the furnace

PID = partial-integral-derivative control

SS = steady-state

TC = temperature control

TI = temperature indicator

SEV = thermal cracking severity

F-1815 = thermal cracking furnace tag

K-UOP = UOP characterization factor

TSHH = ultra-high temperature block

SS = steady-state

VB = visbreaking

VGC = viscosity gravity constant

Introduction

The necessity to stabilize operations and achieve quantifiable economic goals has led to the application of advanced process control (APC), with particular reference to model predictive control (MPC). MPC allows for the optimization and enhancement of the efficiency, safety, and profitability of industrial processes. One of the major sectors where APCs are employed is petrochemical refineries, where optimizing processes presents one of the main challenges.

The API Refinery of Ancona S.p.A., located in Falconara Marittima (AN), Italy, is a hydroskimming-thermal-cracking type of refinery. It employs a noncatalytic thermal cracking process to fractionate heavy gas oil into lighter distillates, increasing the overall refinery conversion. Since one of the major limitations of a thermal cracking unit is the fouling of furnace pipes due to coke deposition, especially as process severity and conversion increase, it is essential to control the severity of thermal cracking to maximize conversion and simultaneously manage pipe fouling to ensure the end-of-run conditions are met while adhering to safety, environmental, and process constraints. The current project aims to address this need through the design of an advanced process control system and dual-horizon optimizer for the thermal cracking furnace, incorporating predictive fouling modeling specific to the API refinery furnace (F-1851). The dynamic matrix control (DMC) software provided by AspenTech, with whom the project collaborates, is used for the design of the APC system, while MATLAB is utilized for the predictive fouling model. The thesis is structured into five chapters, following the chronological development of the project:

- Chapter 1 provides the necessary elements for understanding the thermal cracking process, including reactions and variables influencing its thermodynamics and kinetics, with a particular focus on coke formation;
- Chapter 2 offers a detailed description of the plant under examination, including its basic control system and an exploration of the unit's current management;
- in Chapter 3, the steps taken for the design of the APC are defined, combining theoretical considerations with practical implementation aspects. This involves using an MPC-based APC with the DMC3 software provided by AspenTech;
- Chapter 4 describes short-term and long-term models, providing examples for the former and extensive discussion regarding the underlying model choices, construction, operation, and results for the latter. The chapter also outlines the entire control system architecture;
- Chapter 5 offers a description of the dual-horizon optimization system, distinguishing between short-term and long-term optimization, and includes an analysis of yields and benefits in comparison to the long-term model.

A final section provides the conclusions of the study.

Chapter 1

The thermal cracking process

The thermal cracking is a noncatalytic heating process of hydrocarbons at temperatures above 400°C based on the decomposition of long hydrocarbon chains in spontaneous, nonselective reactions that produce hydrocarbon molecules of different molecular weights and boiling points. Different types of hydrocarbons, such as paraffins, aromatics, naphthenes, olefins and hetero-aromatic compounds, behave differently when subjected to this process. The purpose of this chapter is to present thermal cracking by analyzing the chemistry, kinetics and fundamental aspects that characterize the process.

1.1 Decomposition of hydrocarbons

Thermal decomposition of hydrocarbons, referred to as thermal cracking, begins at temperatures above 400°C, with decomposition rates increasing as compound structure and molecular weight increase. Decomposition leads to the formation of smaller molecules that can, depending on the availability of hydrogen, form saturated hydrocarbons, olefins, aromatic compounds, or even leading to the formation of larger molecules than the starting molecules. Each class of hydrocarbons undergoes different reaction pathways when subjected to thermal cracking. Specifically, it can be summarized according to the reactions proposed by Murphree e Ciprios (1962), and Asinger (1968), the following statements:

- paraffins undergo dehydrogenation reactions that cause their progressive reduction in size into shorter chains and olefins;
- olefins undergo decomposition to paraffins and olefins with lower boiling points, polymerization and isomerization, leading to the formation of naphthenes and unsaturated cyclic compounds, then to the subsequent formation of aromatic compounds;
- naphthenes and aromatics undergo dealkylation reactions on the side chains located on the (more stable) ring structures, leading to the formation of paraffins, olefins, further naphthenes and aromatics with shorter side chains. Naphthenes in turn can lead to aromatics by means of dehydrogenation reactions, aromatics that can undergo further condensation reactions thus resulting in the formation of asphaltenes and coke.

The mechanisms of reactions are given in §1.2. With regard to nonorganic compounds, it can be highlighted the influence of metals in promoting condensation reactions, thus the formation of coke.

1.2 Chemistry of thermal cracking

Thermal cracking reactions turn out to be innumerable and complex to describe. The reaction mechanism is weakly endothermic radical chain reactions. The alkyl radicals, formed by the homolytic breaking of the carbon-carbon bond (C-C), can follow two propagation routes: removal of

hydrogens from other molecules, leading to the formation of additional, larger radicals, until these are decomposed in a definite pattern, resulting in the continuous regeneration of smaller radicals that continue down the chain; or beta-scission, which results in the formation of double bonds as a result of the bonding of the radical obtained from homolytic cleavage and the carbon that forms the beta bond with the carbon that has undergone hydrogen loss. Altogether, such reactions have as their products shorter-chain paraffins than the starting paraffin and olefins.
Dehydrogenation reactions, given by the breaking of the carbon-hydrogen bond (C-H), are, on the other hand, thermodynamically disadvantaged with respect to the C-C bond cleavage reaction, since at higher enthalpy. In this case, the products are represented by olefins and aromatics.
The main reactions described by Nelson (1958, p.627) are given as examples On the experimental work of Hurd and Spence (1929) for the decomposition of butane:

$$CH_3 - CH_2 - CH_2 - CH_2 - CH_3 \rightarrow CH_4 + CH_3 - CH_2 = CH_2 \quad (1.1)$$

$$CH_3 - CH_2 - CH_2 - CH_2 - CH_3 \rightarrow CH_3 - CH_3 + CH_2 = CH_2 \quad (1.2)$$

The secondary reactions are isomerization reactions, which are disfavored because they have lower reaction rates than the other propagation reactions, and chain termination reactions by interaction between two radicals. The secondary reactions from which polymers are formed are given below:

$$CH_2 = CH_2 + CH_2 = CH_2 \rightarrow CH_3 - CH_2 - CH = CH_2 \quad (1.3)$$

$$CH_3 - CH_2 - CH = CH_2 + CH_2 = CH_2 \rightarrow CH_3 - CH_2 - CH_2 - CH_2 - CH = CH_2 \quad (1.4)$$

$$RCH = CH_2 + R'CH = CH_2 \rightarrow tar, olio, etc.. (polimeri) \quad (1.5)$$

In addition, side reactions of polymerization and condensation can occur as reported in equation (1.5), given by the recombination of hydrocarbons into more stable compounds of high molecular weight.
The distinction with respect to catalytic cracking processes (e.g., *fluid catalytic cracking – FCC*) lies in obtaining reaction products predominantly represented by short alkyl chains and olefins as opposed to products consisting of branched alkane chains (as it occurs in the FCC process). More generally, products obtained from thermal cracking reactions consist of gas, gasoline, and products having boiling points above that of gasoline but lower than the feed to the process (usually gas oil), unreacted

feed, products with higher boiling points than the feed (products from condensation and polymerization reactions), and coke.

1.2.1 Variables influencing the process

The main variables, which determine the reactions described in §1.2, thus the rate and distribution of the products are: temperature, pressure, residence time in the furnace coils where the reaction takes place, and the composition of the feedstock.

The following observations on the variables related to process chemistry can be summarized.

- Reaction rates decrease as conversion increases due to the co-presence of residues in chain-terminating reactions. The decrease in speed is proportional to the formation of the residue, the inhibition of which is greater for aromatics, while it is less for major fractions and finally to a lesser extent for saturated compounds.
- Temperature is related to product distribution through its effect on propagation reactions. Beta-scission reactions have a higher activation energy than other propagation reactions, so an increase in temperature causes shorter chain products and olefins to increase.
- Pressure turns out to be important in propagation reactions because an increase in it favors hydrogen removal, and termination reactions, while it disfavors beta-scission. Therefore, an increase in pressure causes the formation of saturated compounds and higher molecular weight compounds.
- Recycling the reaction product is less prone to reaction as it has shorter side chains and higher aromatic content than the fresh charge. It also causes dilution of the concentration of hydrogen donor compounds, leading to an increase in yields of lower molecular weight products with reduced product saturation. It is worth noting that, on the other hand, as conversion per step increases, there is the opposite effect from the effect caused by increasing the recycling ratio.

The design of the reacting zone and the control of the process variables allow for the possibility of optimizing yields to obtain the products of greatest interest.

1.3 Thermal cracking kinetics

At low conversions per step (20% to 25%), the cracking reactions are of the first order as suggested by Nelson (1958, p.650), the predominantly reactions are the main type of cracking reactions described in §1.2.

The kinetic constant of the process can thus be represented:

$$k = \frac{1}{t} \cdot \frac{\ln 1}{1 - X} \tag{1.1}$$

Where k [s^{-1}] represents the first-order kinetic constant, t [s] the residence time and X is the percentage of reactants converted over time t.

Additionally, the kinetic constant can be represented through the standard Arrhenius equation, so the equation for the kinetic constant can be written as follows:

$$k = k_0 \cdot e^{\frac{-E_a}{RT^2}} \tag{1.2}$$

Where k_o corresponds to the extrapolated kinetic constant at zero percent conversion, T $[K]$ to the absolute temperature, R $[J/mol\ K]$ is the universal gas constant, and E_a $[J/mol]$ is the activation energy. Some important observations can be summarized through the studies conducted by Sachanen and Tilicheyev (1927), Sachanen (1940), and Nelson (1958) related to the kinetics of process.

- The yield in light distillates increases as reaction time increases until it decreases due to the formation of coke and gas phase products. Similarly, there is an initial increase in the formation rates of cracking reaction products and a gradual decrease in the formation rate as the boiling point increases. This results from the fact that the light fractions obtained from thermal cracking are more thermally stable than those of higher molecular weight. As a result, gasoline formation occurs at the expense of the heavy fractions obtained in the early stages of thermal cracking. The close relationship between the cracking rate and the boiling range of the products is explained by the thermal stability of petroleum hydrocarbons, which, as molecular weight increases (thus heavier fractions) become less stable and undergo cracking more readily than lighter fractions. Within the same boiling range, the cracking rate depends on the chemical composition of the starting feed. Charges rich in aromatic compounds are more resistant to cracking because they are more stable, and have a lower cracking rate than paraffins. High molecular weight paraffinic chains and compounds decompose more easily than naphthenes. Therefore, the cracking rate is closely related to the percentage and molecular weight of the paraffins and paraffinic side chains in the feedstock being fed to the process.

  In general, it can be said that the shorter the reaction time and conversion, hydrocarbon decomposition will predominate, while for longer times and higher conversions, polymerization products (heavier products) will prevail.
- Temperature is the most important factor in cracking reactions; as shown in expression (1.2) it influences the rate of hydrocarbon decomposition reactions. The yield increases rapidly with increasing temperature, so commercially for the higher yields in light distillates it is preferred not to adopt long reaction times but to use high temperatures (Nelson, 1958, p. 649). It should be noted, however, that as the temperature increases, the rate of polymerization is relatively faster than at lower temperature conditions, further promoting rapid coke formation. The operating temperatures at which the process operates, based on the considerations mentioned above, range from 450°C to 495°C with residence times of about one minute.
- Pressure mainly affects polymerization and condensation reactions, in that, the kinetic constant of first-order reactions can be considered independent of pressure under conditions of low conversion per pass and moderate temperatures. In fact, however, given the conditions (in practical applications) of process temperature (450°C - 495°C), pressure plays an important role

due to the formation of a gas phase, which will be subject, under high-pressure conditions, to condensation and polymerization reactions due to the presence of olefins. Overall, at the end of the process, a gas phase with a high paraffinic content will be obtained, thus contributing to the increase in gasoline yield.

1.4 Product selectivity

The products of interest in the case of thermal cracking of gas oils are mainly gasoline and gas. Instead, the formation of high-molecular-weight compounds and the formation of coke along the walls of the cracking furnace coils is undesirable, causing the furnace run length to be shortened and the heat exchange to be reduced (i.e., reducing the conversion).

In relation to the need to obtain the two products of interest, based on the considerations outlined in §1.2 and §1.3, selectivity toward gasoline is negatively affected by consistent increases in temperature and residence time, as in the former case there is reduction of saturated compounds, in the latter there is progressive reduction of chains leading to lower molecular weight compounds; conversely, selectivity toward gas oil and gasoline is favored by increasing pressure.

Note that the effects reported are minor, and the variables affecting the process must be evaluated by considering the feedstock characteristics and the plant equipment itself.

1.5 Coke formation

Experimental observations reported in the literature, particularly by Reyniers, *et al* (1994), extensively define the complex mechanism of coke formation in the thermal cracking process. Only those elements that provide an understanding of the phenomenon from a general perspective, which is useful for the purpose of this paper, are reported in this section.

According to the study by Reyniers *et al* (1994), the mechanism of coke formation is given by the contribution of three mechanisms, of which the heterogeneous non-catalytic mechanism is considered to be the most important.

The structure of coke, represented by the deposition of graphitic layers containing sp^2 hybridized carbon atoms, can be attributed to the degradation of hydrocarbons to aromatic structures by the chemical reactions reported in §1.2. The generation of active sites on the surface of the coke (due to hydrogen abstraction) leads to the continuous growth of the aromatic structure. Such sites dependent on the composition of the liquid-gas phase at the interface with the coke, lead to the assertion that more reactive charges, thus generating more active radicals, are also those that lead to greater coke production. Consequently, the tendency to form coke increases as the severity of thermal cracking increases due to the radical mechanism and chemical stability.

The main components of the charge in relation to their influence on coke formation are briefly summarized:

- paraffins and naphthenes, low direct contribution
- unsaturated compounds, important precursors as they are very reactive
- aromatics, determine the structure of the coke

Thus, it is possible to construct a model of the coking for each precursor (molecule) that reacts with the radical active site present on the coke surface, leading to an increase in the coke layer with a contribution in terms of carbon atoms equal to that of the carbons that constitute the precursor, and regeneration of the active site.

It must be noted, however, that the set of reactions is broader, and each molecule can follow a different pathway. In particular, there is evidence of cross-linking of aromatic layers, causing the formation of cross-linked carbon layers that are extremely hard and difficult to remove during decoking (pigging) operations.

The relationship between the rate of coke formation and the increase in temperature is equal to that of the hydrocarbon decomposition reactions, thus being able to state that coke formation is inevitable, even if the process is carried out at lower temperatures, which, however, would require longer reaction times to obtain the desired products; in any case, the same amount of coke is obtained in proportion to the obtainable yield of product, since coke and product formation proceed in parallel. It should be pointed out that the rate of coke formation increases at higher temperatures.

As for the effect of pressure on coke formation, it can be considered partly negligible, although a positive effect should be expected since condensation reactions, leading to coke formation, are favored by pressure. Conversely, low pressure should be avoided as it causes vaporization of the liquid phase, leading to the rapid formation of coke. More generally, the greatest contribution to coke is made by the chemical composition of the feedstock to the process: aromatic compounds lead to greater coke production.

The coke, constitutes one of the most significant problems in the management of the thermal cracking process, since the formation of a layer of coke inside the tubes leads to the reduction of heat flow reaching the charge, causing lower conversion and at the same time to an increase in pressure drop, thus to lower residence times. There will be an increase in operating temperature and pressures, and ultimately a reduction in the run length of the thermal cracking furnace, hence to the shutdown of the plant in order to carry out furnace cleaning (decoking) when conditions have been reached such that temperatures are close to the maximum operating temperatures of the furnace tubes. In conclusion, the evolution of coke layer thickening over time can be observed by the increase in skin temperatures of the furnace coils.

Chapter 2

Description of the API refinery plant

API refinery is a refining plant, situated in Falconara Marittima (AN, Italy), that can be attributed to the hydroskimming-thermal-cracking type of refinery, i.e., it operates a crude oil processing cycle such as to increase the yield of light distillates (with boiling points no higher than 370°C), at the expense of heavy distillates. For this purpose, it uses a thermal cracking process for fractions distilled at 340°- 540°C, while for fractions with boiling temperatures above 425°C (residue) it uses a visbreaking process. The thermal cracking unit represents the most important part of the refinery as it allows to increase the total conversion of the refinery. The purpose of this chapter is to present thermal cracking unit of the API refinery by analyzing the process, the design and the control system.

2.1 Overview of API refinery thermal cracking plant

The thermal cracking plant at API's refinery operates according to the thermal cracking process described in Chapter 1 on a feed consisting of heavy distillates: heavy gas oil from topping (HGO), heavy gas oil from vacuum distillation (HVGO), heavy gas oil from visbreaking after atmospheric fractionation (HVBGO), light gas oil from vacuum distillation (LVGO), and heavy gas oil from visbreaking after vacuum fractionation (HGOVB), plus any additions given by cold feed to storage (TK-177), and heavy distillates sent to the unit under abnormal conditions (i.e., upset). The unit is part of a larger plant in which it is connected to the units: vacuum, visbreaking (VB), vacuum flash and high pressure thermal cracking (HPTC). The VB and HPTC units adopt the same principle of thermal decomposition of hydrocarbons, but under different conditions. In fact, the thermal cracking allows for the greater production of gas, LPG and gasoline compared to the other units (specifically compared to VB, which leads to the obtaining of bitumen and fuel oil with heavy distillate extraction). Because of this connection between units, it is necessary to manage thermal cracking from a global perspective that takes into account the fact that any disturbance or inconvenience on one unit affects the others.

The thermal cracking plant, the unit of which named Unit 1850, can be divided into the following sections for:

- feedstock reception
- furnace
- preflash column
- products

The process flow diagram (PFD) is reported in Fig. 2.1 for what concerns the furnace, with the relative process control system. In Fig. 2.2 the separation section is reported.

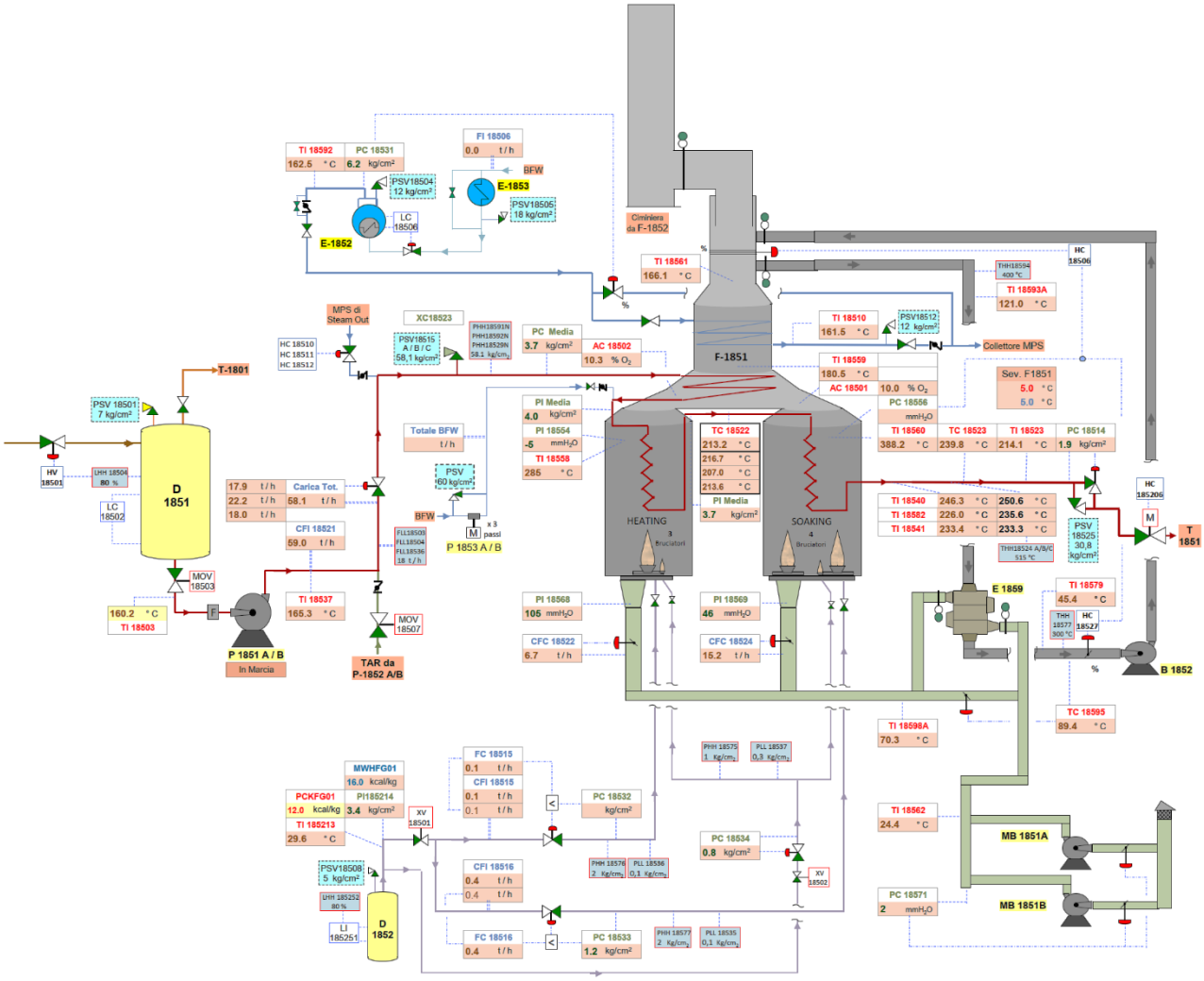

Figure 2.1 Process flow diagram of the thermal cracking furnace; the values reported should not be considered as the fixed and indicative values of the process, as they are variable according to process needs.

The flow diagram reported in Fig. 2.1 is briefly described for better understanding. The hot feed (288°C) is sent to the thermal cracking furnace named F-1851 where it reaches the reaction temperature (above 400°C). On leaving the furnace, products are sent to the preflash column (T-1851), whose corresponding separation section is reported in Fig. 2.2, where separation between the distillates produced, in the vapor phase, and residue (heavy unreacted product) takes place. Next, the distilled fractions are sent to the fractionation column T-1801. The residue is stripped with steam and then sent to the vacuum flash column to recover the distillates present in the TAR (i.e., heavy residue). The furnace F-1851 represents the most important element as the site of the thermal cracking reaction. Therefore, the control of the furnace is crucial, since taking into consideration the quality of the charge and the main operating variables of the process (furnace outlet temperature (FOT), flow rate, pressure), the severity (SEV) of the thermal cracking is determined, thus the degree of conversion (i.e., higher severity corresponds to higher conversion).

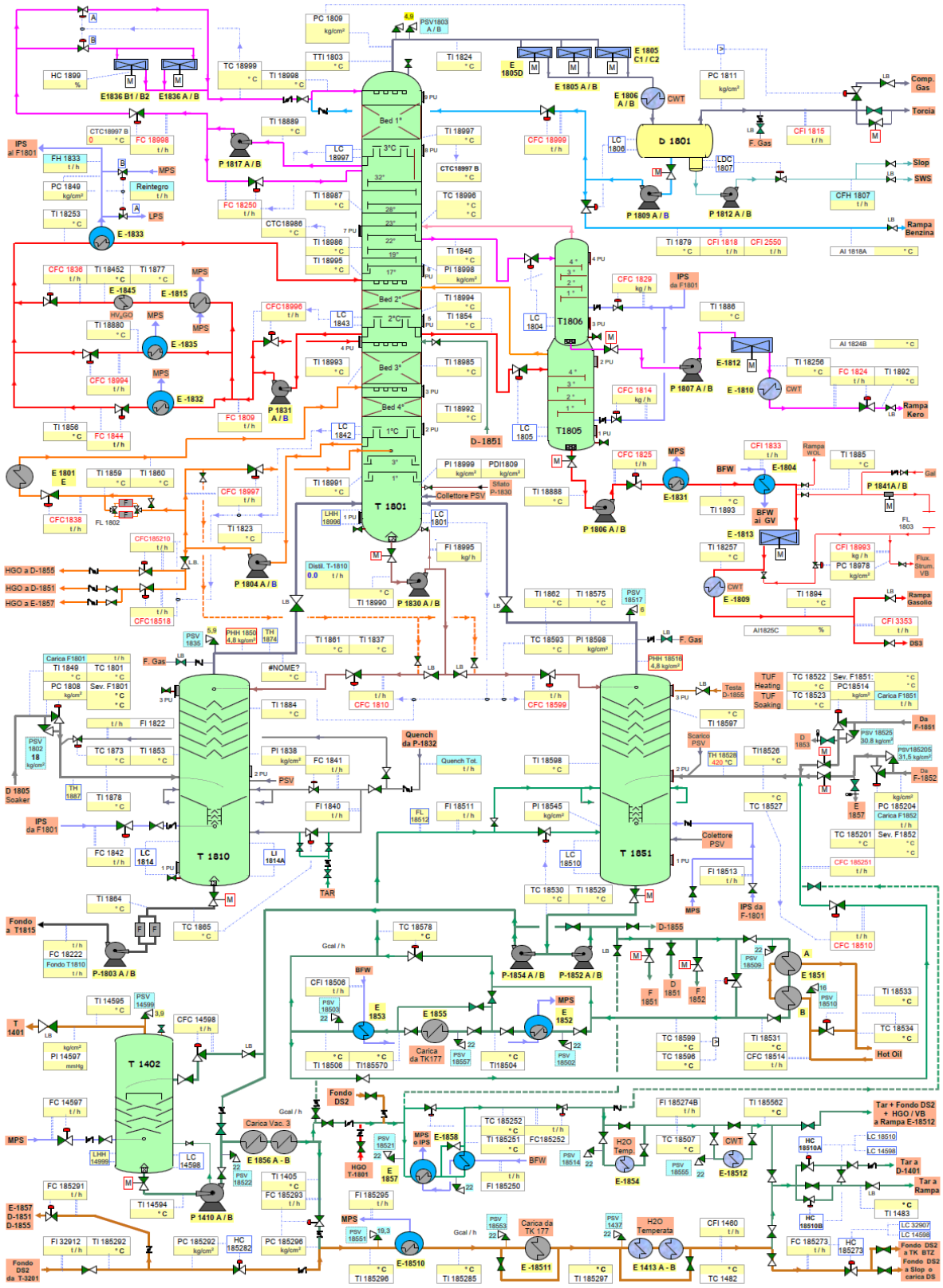

Figure 2.2 Process flow diagram of the separation section related to the thermal cracking unit.

2.2 Thermal cracking feedstock receiving

The feedstock to the plant consists of a set of fixed streams and variable streams based on operating conditions (different types of plant set-ups based on feedstock characteristics) and need with respect to abnormal conditions. The Table 2.1 summarizes the streams updated to the last running cycles and their flow rate indicators, taking into consideration that for some cases (HGO, LVGO) there is no direct flow rate indicator of the specific stream, but rather it is necessary to evaluate other variables to determine whether or not a current goes to the thermal cracking.

Table 2.1 *Thermal cracking feedstock composition.*

Feed	Tag	Flowrate controller	Presence in the inlet feed to the furnace
heavy gas oil from vacuum distillation	HVGO	FC1440	always
heavy gas oil from visbreaking after atmospheric fractionation	HVBGO	FC18205	always
heavy gas oil from visbreaking after vacuum fractionation	HGOVB	FC18518	always
cold feed to storage	TK-177	FC18509	always
desulfurization column residue	BOTTOM DS2	FC185291	always
light gas oil from vacuum distillation	LVGO	FC185209	presence if HDS2 unit is not running
heavy gas oil from topping	HGO	FC1058	presence if HDS2 unit is not running

Specifically, HGO and LVGO are fed to the thermal cracking when, respectively for the two streams, the HPTC and HDS2 (Hydro-DeSulphurization unit) units are not running, since the valves are not partialized.

The total charge at thermal cracking is indicated by flow controller FC18500.

The streams shown in Table 2.1 come together in a manifold on which the TAR recycle (used only during startup) also fits. Each incoming line to the manifold is equipped with a check valve. The charge is mixed in the charge accumulator D-1851, whose hold-up allows sufficient operational leeway in case of disruption. At maximum system capacity, the hold-up is seven minutes between LLL (lower liquid level) and HLL (higher liquid level). The bottom of the accumulator is connected to the P-1851 A/B feed pumps that feed the furnace, which require special attention given the high operating temperature (295°C). The two feed pump seals are of the double seal type in tandem with barrels, which are water-cooled, and each equipped with a high-level alarm, cumulated at the panel into a single alarm (XA-18511). It should be noted that the standby pump must be kept hot at all times by special by-pass of the discharge valve and its check valve; the suction valve must therefore be open to allow backward circulation. The discharge line to the furnace is equipped with both a low-pressure alarm PSL-18507 and low-flow alarm FAL-18521. There is also a temperature indicator of the inlet feed to the furnace, TI-18537.

2.2.1 Characterization of the feed

As can be seen in Table 2.1, the charge is mainly made up of heavy fractions, with the exception of LVGO, which is in fact a component to pay attention to given the higher amount of coke precursors it may contain within it. At the same time, it is necessary to consider the high variability of the cold feed (TK-177), which, being made up of storage gas oil also derived from possible different source crude oils, will exhibit different characteristics and composition. At the same time, it is necessary to point out that the composition of the feedstock will depend not only on the cuts (in the sense of petroleum products), but also on the crude. In fact, crude oils have different chemical compositions (paraffins, unsaturates, aromatics, naphthenes), which can considerably influence the behavior of the feedstock upon thermal heating. In the specific case of the API refinery, during a run cycle (run duration between two consecutive maintenances, usually equal to one year) several crudes may occur, thus making the management of the furnace complex, which will therefore have to adapt with different set-ups to the different conditions that may vary from time to time. In this sense, the characterization of the crude plays an important role in the choice of operating variables (i.e., furnace severity), allowing to avoid increased fouling. The API refinery uses four main parameters, given by laboratory analysis, to characterize the feedstock to the thermal cracking.

- Conradson carbon residue (CCR) is a measure of carbonaceous material left as a residue after a sample is subjected to a specific high-temperature pyrolysis process. It is used as an indicator of the carbon content and tendency to form carbonaceous deposits. The test involves heating a sample to a high temperature in the absence of air (under pyrolysis conditions) to simulate extreme heating conditions similar to what the material might experience during the thermal process. Therefore, it is an important parameter in assessing the thermal stability and carbon-forming tendencies of the feedstock. Higher values indicate a higher amount of carbonaceous material that could lead to fouling, coking, or carbon deposition.
- Percentage of light distillates (%380-) evaluated by ASTM D-1160, is used to evaluate the boiling range distribution of petroleum products and fractions. This method is specifically designed for samples that have an initial boiling point above 50°C and a final boiling point not exceeding 400°C. Therefore, it provides valuable information about the volatility and boiling range distribution of petroleum products. Percentage of light distillates (%380-) should be less than 5%. They present a negative effect on both conversion and running time. This is due to their passage into vapor phase within the furnace coils during heating, thus leading to reduced residence time, subtracting heat (thus higher heat load demand) increasing pressure drop and shifting yield to gas and gasoline (due to cracking of the light phase).
- UOP characterization factor (also reported as K-UOP) is a parameter that reflects the chemical nature of the crude oil and it is used to determine whether the crude oil is predominantly paraffinic or exhibit properties of a naphthenic or aromatic crude oil. It is defined by:

$$K = \frac{(T_B)^{\frac{1}{3}}}{d} \tag{2.1}$$

where T_B [°R] is the average boiling point and d is the specific gravity (at 60°/60°F). This factor has been shown to be additive on a weight basis. It was originally devised to show the thermal cracking characteristics of heavy oils; thus, highly paraffin oils have K in the range 12.5 to 13.0 and cyclic (naphthene) oils have K in the range 10.5 to 12.5 (Speight, 2006, p. 40). In addition, if the characterization factor is above 12, the liquid fuel or product might, because of its paraffinic nature, be expected to form waxy deposits during storage.

- Viscosity Gravity Constant (VGC) is a parameter used to provide an indication of the paraffinic character of the crude oil as a means of petroleum characterization rather than for petroleum classification. Specifically, is a useful function for the approximate characterization of the viscous fractions of petroleum (Coats and Hill, 1928, p. 641). The calculation can be performed from kinematic viscosity at 40°C and density at 15°C according to:

$$VGC = \frac{G - 0.0664 - 0.1154 \cdot \log(V - 5.5)}{0.90 - 0.109 \cdot \log(V - 5.5)} \tag{2.2}$$

where G [g/mL] correspond to the density at 15°C and V [mm^2/s] corresponds to the kinematic viscosity at 40°C. The calculation can also be carried out from other formulations (Saybolt seconds universal, or the relative density). The lower the index number, the more paraffinic the feedstock. Values near 0.8 indicate paraffinic character, while values close to 1.00 indicate an aromatic predominancy.

It has to be noticed that in terms of direct characterization of the feed that goes to the thermal cracking furnace, the VGC is the more appropriate parameter, since it is directly applied to the sample inlet feed to the furnace, instead the other parameters are performed on the crude oil.

2.3 Thermal cracking furnace F-1851

Thermal cracking furnace F-1851 is a three-step double vertical chamber furnace with a common convective section above. The combustion chamber is divided into two separate sections:

- heating - heating section equipped with 3 gas burners;
- soaking - radiant heating section equipped with 4 gas burners.

Each chamber has an independent setting, thus allowing for the best balance of the cracking reaction. The tubes are arranged perimetrically in a vertical position; in soaking part of each pass is also arranged in a central position exposed to the flame on two sides (double fired). The furnace has undergone several structural changes over time. The most important one is the addition of a third pass (B) posthumously compared to the first two pass (A and C); this also denotes some differences in terms of the performance of the individual pass. Specifically, pass B has a longer path in order to provide the charge with the same reaction volume as the other two steps; remembering that the reaction volume and flow rates at each pass determine the residence times, thus conditioning the severity of cracking. For sake of clarity, the exchange surfaces and treated volumes are reported in Table 2.2 for the heating zone.

Table 2.2 *Geometric characteristic of the thermal cracking heating zone.*

Passes	Heat exchange surface [m^2]	Volume [L]
A (1st)	379.2	2912
B (2nd)	252.8	2910
C (3rd)	379.2	2912

The soaking section is also characterized by a structural difference between the passes; the layout of the pipes exiting the process are similar for the 1st and 3rd passes, while the 2nd pass is slightly different. Overall, the soaking zone presents:

- heat exchange surface area of 711 m^2;
- overall volume 16616 L.

The design capacity of the furnace is 133333 kg/h. Combustion takes place with forced-draft air.

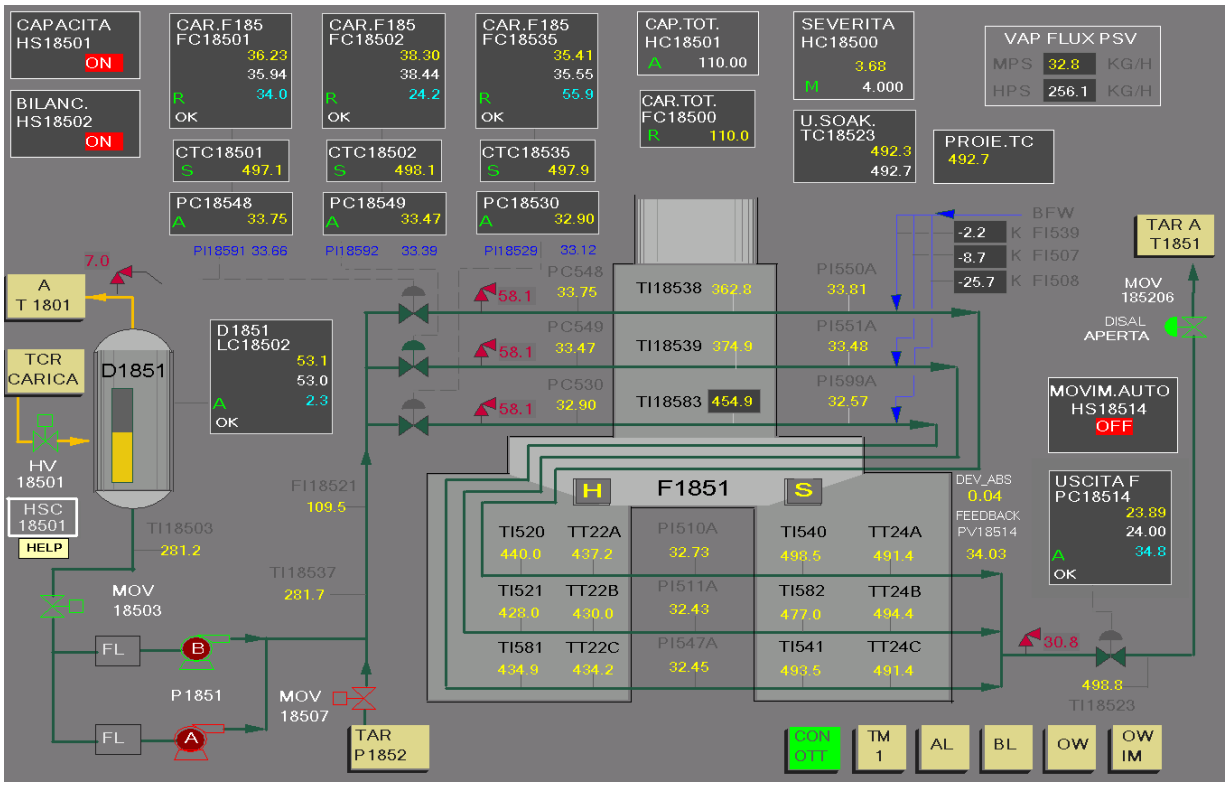

Figure 2.3 Graphic page of the distributed control system (DCS) of the thermal cracking furnace; pressure and temperature controls.

The flow rate of the feed to the furnace is regulated by acting on the flow rate controllers FC-18501, FC-18502, FC-18535 for the 1st, 2nd and 3rd passes, respectively, located at the inlet of the convective zone as it can be possible to be observed in the Fig. 2.3. The regulators receive the signal from the respective flow controllers that are in turn protected by the pressure control system in the various sections of the furnace. The gauge flange of each individual pass is equipped with dual transmitters: FT-18501, FT-18502 and FT-18535 for the 1st, 2nd and 3rd passes, respectively; in case of low flow

rate (equal to 18000kg/h) in each individual pass, as measured by the latter transmitters, the fuel blockage to the furnace is activated.

The convective inlet operating temperature is 295°C. The furnace is designed to release 42540 kW divided into 25800 kW in the heating zone and 16740 kW in the soaking zone, with an energy efficiency of 92%, with excess air at 10% equivalent to about 2.5% oxygen; the values are to be referred to a 100% load. Note, however, that the oxygen percentage is currently maintained at higher values (3.77%O_2) than the operational targets, resulting in a loss of efficiency.

The most important elements of the furnace include the metal temperature of the tubes (for both zones), which is 660°C, and the pressure drop ΔP, which at clean furnace and design charge correspond to 9.8 kg/cm^2.

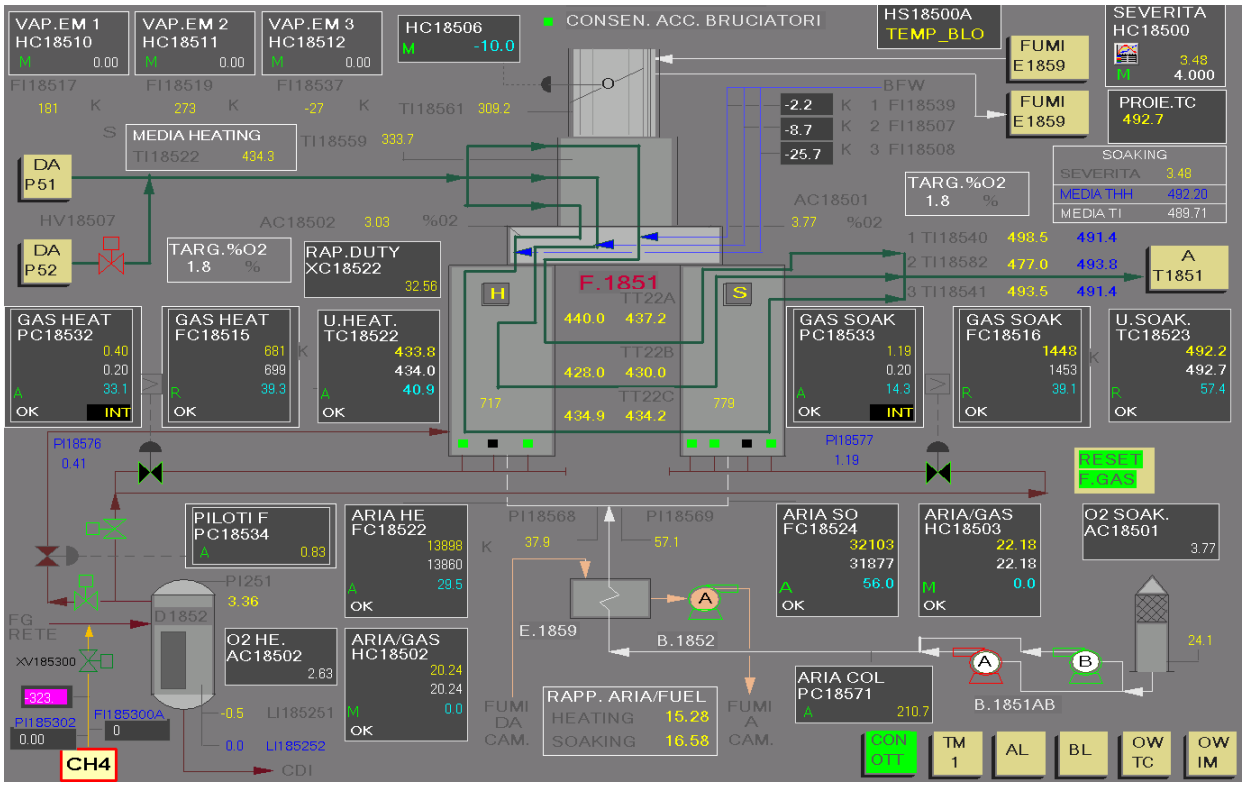

Figure 2.4 Overview by graphic page of the distributed control system (DCS) of the thermal cracking furnace F-1815.

An overview of the distributed control system (DCS) of the furnace is reported in Fig. 2.3 and Fig. 2.4.

2.3.1 Pressure and feed flow rate control system at the furnace

The F-1851 furnace consists of a convective section and two radiant sections in series, heating and soaking. The design pressures and temperatures for all of the three section are 58.8 barg and 660°C. The total feed to the furnace and especially the distribution of flows through the three passes depends on the degree of fouling of each pass. In the course of the operation, the coke formed as a result of cracking reactions is deposited on the tubes, reducing their diameters and thus their passage cross-sections. This results in increased velocities and pressure drops through the pass. The presence of the coke also reduces the ability of the individual passes to absorb heat, so more heat must be supplied

to the furnace to keep the exit temperature from the pass unchanged. This increases the radial flow further promoting coke formation and thus increasing the pressure drop in the furnace. The increase in pressure drop results, in practice, in the need to operate the furnace at higher pressures over the course of the run at the same total feed (progressive increase in convective inlet pressure until design constraints are reached, minus the margins on the safety valve trip).

The pressure control is realized on each pass by:

- a pressure relief valve (PSV) placed at the furnace inlet;
- three pressure controls (PIC) at the input of each section;
- a high pressure block (PSHH) arranged at the furnace inlet;

In case the pressure reaches the calibration threshold value, a solenoid valve (XY-18508, XY-18507, and XY-18503 for the 1st, 2nd and 3rd passes, respectively) intervenes and reduces the inlet flow to the three coils to 25% of the normal value. The same thresholds also act on the fuel gas valves that reduce fuel flow to the burners of the heating chamber and soaking chamber (FV-18515 and FV-18516) via manually reset solenoid valves (XY-18515 and XY-18516). This also partializes the amount of fuel gas so as to prevent an undesirable temperature rise at the coil. The tripping of the above valves is signaled by an audible/visual alarm at the panel. Pressure controls (PIC-18548, PIC-18549 and PIC-18530) are arranged at the inlet of each section. Each control is set at the maximum operating pressure of the section. The signal from the three pressure controls is cumulated through a "low-pass" (FY) device that acts on the flow controller (FC) of the pitch in case of pressure increase in each of the three sections.

The flow controllers of the three FC-18501/18502/18535 passes work exclusively in manual (MAN) or cascade (RSP, remote set point) position. Automatic mode is not allowed to ensure pressure control at all times (except when in MAN). If any one of the three controls reports a pressure value equal to its set, FY acts on the FC by reducing the flow rate to the step just enough to reduce the pressure below the set. The pressure controls for the convective inlet and their respective alarm values are shown in the Table 2.3.

Table 2.3 *Pressure control of the convective section of the thermal cracking.*

Passes	Tag	Alarm values [barg]
1st	PC-18548	53.7
2nd	PC-18549	53.7
3rd	PC-18530	53.7

The pressure gauges installed at the heating and soaking inlet for the control function have the sole function of locally reading the pressure at the inlet to each section of each step.

2.3.2 Convective section

The convective section consists of two zones: feed preheating, medium pressure (MP) steam overheating. The expected operating temperature at the outlet of the convective zone is 372°C.

Thermocouples TI-18538, TI-18539, and TI-18583 for 1st, 2nd and 3rd passes, respectively, indicate the temperature of the charge exiting the convective zone/heating inlet. At the outlet of the convective, after the thermocouples mentioned above, there is an injection of demineralized water (taken from the generator feed manifold) on each of the furnace passes using the P-1853A/B positive displacement pumps, driven by an electric motor. The pumps are 3, one for each pass. The water supply lines are each equipped with check valves. Injection of water to the furnace (0.25% weight on charge) is intended to limit coke formation for high CCR values in charge. If the feed quality is good, it is possible to remove the injection water to the furnace by monitoring the metal temperature trends and pressure drop across the furnace. If the charged flow rate is reduced to 60% of the design value, or if the CCR increases above 0.5, water must be fed back to the furnace, in an amount equal to 0.25% weight of the feed flow rate. Flow indicators FI-18508, FI-18507, and FI-18539, for the I°, II°, III° pass, respectively, allow control over the amount of water injected on each step of the furnace.
Steam produced in the plant (generator E-1852) is superheated in the furnace and then sent to the refinery MP steam network. The steam superheater coil is placed downstream convectively, in the direction of flue gas flow. The TI-18510 shows the temperature of steam leaving the superheater on the panel. The design steam flow rate is 7300 kg/h. The expected operating temperature at the inlet of the superheater is 183 °C; at the outlet of the superheater it is 278 °C. In case of low flue gas temperature, it is possible to partially by-pass the superheater by means of a disc valve placed so that TI-18511 can be seen locally indicating the steam temperature downstream of the by-pass line insertion. The steam thus superheated is sent into MP's network. The steam coil is designed for zero flow, but during decoking operations it must be protected with continuous steam flow. For this purpose, it is possible to feed the coil from the MP network and discharge the steam to the atmosphere in the safety zone.

2.3.3 Heating section

The temperature controller of the heating section TIC-18522 receives the signal from the three passes through TT-18522A/B/C, for the 1st, 2nd and 3rd passes, respectively. The controller, as the process variable to compare with the set-point, uses the average of the passes. The output signal of the controller acts on the combustion control system of the heating chamber. Each pass, exiting from the heating section has a thermocouple, TI-18520 for 1st, TI-18521 for 2nd, and TI-18581 for 3rd, which indicates the temperature of the charge in the individual coils on the panel. Local pressure gauges PI-18510B, PI-18511B, and PI-18547B, located on the 1st, 2nd, and 3rd steps, respectively, provide a local reading at the outlet of the heating section. Each coil also has three metal skin-temperature detectors (skin-point).

2.3.4 Soaking section

The charge exiting the heating section enters the temperature holding zone (soaking zone). The soaking section provides an operating output temperature of 500 °C. The temperature controller of the soaking zone TIC-18523, located at the furnace outlet, receives the signal from a single

thermocouple located on the furnace outlet manifold that collects the passes; the output signal from the controller acts on the soaking chamber combustion control system. Each pass, exiting the soaking section, has a thermocouple that indicates the temperature of the charge in the individual coils:

- TI-18540 for the 1st pass;
- TI-18582 for the 2nd pass;
- TI-18541 for the 3rd pass.

The furnace outlet passes are equipped with the TI-18524A/B/C for the I°, II° and III° pass, respectively, which supply the signal to the TSHH-18524 A/B/C ultra-high temperature block installed on the furnace outlet. When the threshold value is reached, the flow rate of fuel gas to the heating and soaking burners is reduced to a sustainable minimum; if the sensed temperature remains above the threshold value continuously for more than 60 seconds, the flow rate of fuel gas to the heating and soaking burners is reset to zero by closing the fuel valve to the burners (XY 18501) (leaving the pilots on).

Each coil also has eight metal skin temperature detectors (skin-point):

- TI-18588/549/550/604/551/605/612/552 for the 1st pass;
- TI-18553/589/590/601/548/602/611/591 for the 2nd pass;
- TI-185887/554/555/607/556/608/610/557 for the 3rd pass

coil skin temperatures are important indicators of coke formation along the pipe walls.

2.3.5 Burners

The heating chamber has three gas burners; the soaking chamber has four more gas burners. The burners are placed on the furnace slab and arranged upward. Pilots are of the aspirated type, which means that they are not affected by forced combustion air. This allows, in the event of a lack of the latter, not to send the pilots' circuit into lockout and thus allows the flushing phase of the combustion chamber to be omitted, which saves considerable time during the furnace emergency. Each pilot is equipped with a photocell, with flame signal indication and flame lamp present, on the front of the ignition panel. The flame detection system is active only when the furnace is turned on. In fact, the photocell, when the furnace is started, does not produce blockage but simply an acoustic signal of lack of flame. In case of an alarm, it is necessary to verify the actual lack of flame by proceeding to re-ignition if necessary. Each pilot is equipped with a blocking valve that intervenes, closing, in the washing phase, before ignition. This allows, at the end of the flushing phase, the actual pressurization of the pilot manifold to be detected.

2.3.5.1 Fuel gas and combustion air

The fuel gas to the two chambers comes from the D-1852 scrubber, which is equipped with a high level alarm LAH-18508. Any liquid hydrocarbon entrainment is routed to the flare manifold. In the case of overpressure (maneuvering error) of the D-1852, the PSV-18508 intervenes by discharging into the flare manifold. The calibration of the PSV-18508 is 6 kg/cm^2. In the case of low or high gas

pressure at the burners, blocks PSLL-18535 and PSHH-18576 for heating and PSLL-18536 and PSHH-18577 for soaking are activated, respectively, which, when the threshold value is reached, act on gas flow block valve XY-18501, located upstream of the corresponding sub-collectors, reducing the flow rate to the minimum sustainable level. If the detected pressure remains above the threshold value continuously for more than 30 s, the flow rate of fuel gas to the burners is reset by closing the valve itself (XY-18501). The pilot manifold receiving gas from D-1852 is maintained at the required value via PV-18534, which receives the signal from the respective controller. Again, low or high manifold pressure activates the PSLL-18537 and PSHH-18575 blocks, respectively; in both cases, the flow rate of fuel gas to the heating and soaking burners is reset to zero by closing the fuel valve at the burners (XY 18501); in addition, the flow rate of fuel gas to the pilots is also reset to zero (XY 18502). The pilots are fed from a single manifold. The flow rate of fuel gas to the burners in each section is indicated on the panel by FI-18515, heating, and FI-18516, soaking. Furnace lockout due to low gas pressure at the pilots operates only on the general valve and not on the individual lockout valves at each pilot.

Combustion air is supplied to the furnace by two blowers (B-1851A/B) both driven by an electric motor. The combustion air intake is provided with a metal grid filter common to the two blowers. To prevent ice formation during the winter period, a low-pressure steam coil (E-1860) sized to raise the air temperature from - 5°C to 15°C is installed. The heater is intended to provide maximum protection to the cast iron exchange surfaces of the air heater. The combustion air pressure regulator PC-18571 located on the supply line common to the two chambers receives the signal from the respective transmitter and sends the control signal to the manual stations HC-18571/A and HC-18571/B. The latter make it possible to act on the air control dampers located at the inlet to each blower: either automatically (the signal passes directly) or manually (in which case the opening must be set). The signal thus filtered moves the dampers via an air-driven servomechanism. This system also allows the blowers to be paralleled when they need to be interchanged (e.g. for maintenance). Alarm pressure switch PAL-18566, located on the common discharge line, sends the corresponding signal to the panel. The TI-18562 indicates to the panel the temperature of the air in the blower supply heater inlet (E-1859). The flue gas temperature at the E-1859 outlet is controlled by TC-18595, which acts on the air bypass damper to the E-1859. The ΔPI-18513, placed in the field, indicates the ΔP of air through the heater. On the E-1859 inlet flue gas duct, the TSHH-18593 high temperature block is installed to protect the heater from temperature rises above the mechanical design limit (400°C). TSHH-18596 and TSLL-18597 blocks are installed on the flue gas duct exiting E-1859. The TSHH-18596 trips in case of high flue gas temperature to protect the extractor (design temperature 300°C); the TSLL-18597 (with double alarm) in case of low flue gas temperature exiting E-1859. TSLL-18597 protects the heater from the possibility of corrosion due to acid condensation. On leaving the heater, air is sent through two separate ducts to the burners of the two radiant chambers. Air flow rates are controlled by dampers (FV-18522 and FV-18524 heating and soaking, respectively) operated by FC-18522 (heating) and FC-18525 (soaking) flow controllers based on the measurement made in the Venturi tubes and corrected for the actual air temperature at the burners. Transmitters FT-18523 (heating) and

FT-18525 (soaking), based on the measurement made in the Venturi tubes, send the flushing consent signal to the ignition logic if the flow rate is higher than the pre-set value. Combustion air regulation takes into account the priority of action with respect to fuel (smoke-less, anti-smoke device). Each change in heat load results in the change of only one variable at a time, and selectively, so as to prevent smoke formation. In practice, regulation is based on the ratio of combustion air to fuel. The TC-18522, placed at the heating zone output, sends a signal to the low-pass device FY-18515/B which in turn also receives the signal of the combustion air flow rate produced by FI-18522/B. The comparison generates a signal that becomes set-point for the gas flow controller FC-18515 acting on the heating zone controller FV-18515. The signal from TC-18522 is also sent to the other high-pass device FY-18515/A, which compares it with the signal sent from the gas transmitter FT-18515 to the burners. The comparison generates a signal that becomes set-point for the FC-18522 air controller at the heating chamber. The air/fuel ratio indicator FFI-18501 receives the signal from both the gas flow transmitter FT-18515 and the combustion air system and sends the corresponding alarm to the panel in case of low ratio. The above applies similarly to the regulation of the soaking chamber.

2.3.6 Flue gas

The expected flue gas outlet temperatures are 884°C, 800°C, and 344°C for the heating, soaking, and convective outlet (charge preheating and MP steam superheater) zones, respectively. Flue gas coming out of the convective zone recovery is sucked in by the flue gas extraction fan and sent to the air preheating system. Flue gas coming out of the air preheating system is again sent to the stack. The flue gas duct exiting each zone, upstream of the convective, is equipped with an analyzer, the AT-18502 for the heating zone and the AT-18501 for the other zone, respectively, which indicate the percentage of oxygen in the flue gas.

2.4 Separation section

The cracking reaction, started in the furnace is stopped by reducing pressure and temperature. To reduce the pressure, the PV-18514 reducer is used, which receives the signal from the corresponding controller. The pressure port of the controller is continuously flushed with steam to prevent clogging by coke. The calibrated orifice allows a constant flow rate of fluxing steam to be sent out. To reduce the temperature and stop the cracking reactions, an initial quench is made at a minimum distance from the pressure reducer. The quench flow rate is regulated by TC-18527 located downstream of the quench engagement point. The TC-18527 acts in cascade on the flow controller FC-18510, which receives the signal from its transmitter. The design column inlet temperature is 401°C and the quench flow rate is 70000 kg/h. The TSH-18528, placed on the column input current sends the corresponding alarm signal to the panel, highlighting a possible abnormality due to the absence of quench current. The quench is carried out with TAR coming out of the feedwater preheater E-1853, at a temperature of 200°C controlled by TC.

The preflash column T-1851 improves the separation between liquid and vapor phase, particularly by separating the residue from the distillates. The column is divided into three sections: flash, stripping, rectifying. The flash zone receives the F-1851 furnace effluent cooled by quenching. The TI-18526

indicates in-screen the column inlet temperature (over the TC-18527). PI-18545 indicates in the field the flash zone pressure. The flow rate is adjusted manually with a disc valve and indicated in the field by FI-18531. The stripping section consists of 6 diaphragm plates. The diaphragm plates are slanted, damless and undrilled. Underneath stripping plates is installed the corresponding steam distributor at MP. A controller-controlled additional quench, located at the column bottom line, TC-18530 (35818 kg/h), is used to further cool the TAR. The expected design temperature at the bottom outlet is 360°C. The TI-18529 indicates the relevant value on the panel. The column bottom level is regulated by the corresponding controller LC-18510. The grinding section consists of 6 diaphragm plates. Unlike those in the stripping zone, the diaphragm plates have a weir, saw-toothed, which acts as a weir and have a row of 13-mm holes at a minimum distance from the weir, in increasing numbers (40, 50, 60) toward the top plates (7/8, 9/10, 11/12 respectively). Above the last plate the blind tube distributor of the reflux is arranged. Part of the background product of the VB plant fractionation column (T-1801) is used as reflux. Column head temperature T-1851 (383 °C) is controlled by TC-18593 acting in cascade on FC-18599, which regulates the flow rate of head reflux (47998 kg/h); in the case of VB reaction stops a special selector switch allows the signal to be received from LC column bottom T-1801. The head temperature is also indicated by TI-18575. It is worth noting that there are no flow rate indicators at the preflash column outlet. The separated distillates in the preflash column are sent to the T-1801 fractionator, which also receives the feed from the T-1810 separation column from the VB unit. From the T-1801 the product distillates are obtained.

2.4.1 Separation products

The thermal cracking plant, as described in §2.4, does not allow qualitative evaluation of the desired products, i.e., light fractions, because their production is sent to the VB fractionation column (T-1801). Distillate production (yield) can only be evaluated quantitatively by difference with residue. At design conditions, a residue yield (370°C+) is expected to be:

- 38.62 % weight of the charge in the case of T-1402 inserted;
- 53.62 % weight of the charge in the case of T-1402 excluded.

For a more precise assessment of the yield, it is necessary to perform a plant test.

The main products of the reaction are gas and gasoline, while the secondary products are intermediate distillates, such as kerosene and light diesel, which have not undergone complete conversion to gasoline and gas.

2.5 Operating variables

The main operational variables that influence the thermal cracking process are temperature and reaction time on the furnace coils (both in the heating and soaking section), the latter related to charge flow rate. Pressure has influence in the process, but is not usually varied.

- Heating section outlet temperature influences the cracking reactions. The consequences of an increase in reaction temperature are increase in conversion, distillate and gas yields increase, increasing coke formation, decrease of the stability of the residue. The opposite occurs if the

reaction temperature decreases. The temperature is controlled at the outlet of the heating chamber (TC-18522).

- Soaking section outlet temperature greatly influences the cracking reactions, since this temperature is maintained at higher temperatures than the heating section. Same considerations of the heating section outlet temperature can be applied to the soaking section outlet temperature. The temperature control is carried out by means of the TC-18523.
- Furnace pressure increase leads to lower vaporization, increase of the residence time inside the furnace, increase of conversion. The operating outlet pressure is usually set at 23 kg/cm^2 but theoretically it can work at 25 kg/cm^2. However, furnace pressure conditions are affected by pressure drops, a consequence of both the accumulated coke and the quality of the charge (% light distillate input). The pressure of the furnace is controlled by PV-18514.
- Feed flow rate affects the reaction time. A decrease in flow rate, if not accompanied by changes in temperature and pressure, leads to an increase in both the residence time and conversion; the opposite occurs if the flow rate increases.

It is worth noting that the reported operating variables directly determine the severity of the furnace, which can be directly controlled, thus acting on the above variables. It should be noted that the iso-severity curve underlying the algorithm that controls the FOT in relation to plant capacity was created to ensure, with respect to changes in flow rate (i.e., residence time), the same 16%wt conversion level at given temperature. The operating limits are defined by the iso-severity curve, which determines the FOT corresponding to zero severity as capacity varies. The characteristics of the iso-severity curve are as follows:

- a base severity of 0°C corresponds to a FOT of 500°*C* for 133 t/h charge and POF of 18 barg;
- a change in FOT of +/- 0.2°C should be matched by a change in charge of +/- 1 t/h;
- relative to changes in FOT versus changes in pressure, +/- 1.4°C is considered for each +/- 1 barg change in pressure.

It should be noticed that the management of the operating variables depends on the skin temperature trends of the furnace coils, as the control of the running length depends on the maximum temperature that can be reached by design by the coils.

2.6 Evaluation of furnace performance

The coke formation during the process operation holds a significant importance. As described from a chemical point of view in §1.5, the coke formation refers to the formation and deposition of a coke layer on the inner surface of furnace tubes. Due to the heat transfer occurring from the tube to the product, the tube's temperature is higher than that of the product itself. The product's thin boundary layer closest to the tube experiences an extended residence time and elevated temperature, leading to excessive cracking and, consequently, coke production. As a result, despite having a well-designed furnace, some degree of coke formation and deposition within the furnace tubes becomes inevitable. The coke layer will build up slowly and eventually the feed pump capacity may be insufficient to overcome the excessive pressure drop across the furnace coils (recalling the fact that the pressure of

the furnace cannot be greater than 25 barg). But even more important is the overheating of the tubes, which becomes the primary constraint on plant operation due to the substantial heat resistance caused by the presence of the coke layer. Beyond the maximum structural skin temperature of the coils (680°C), the furnace must be shut down, and cleaning operation (decoking) should be carried out.
Despite having a well-designed furnace and implementing the meticulous operation outlined in the preceding sections, coke deposition in the furnace tubes remains inevitable. As a result, it is crucial to conduct regular monitoring of the furnace's performance. This monitoring serves a dual purpose: first, to identify any potential issues that may arise, and second, to track the coking rate of the furnace. By doing so, it becomes possible to predict when the furnace will require decoking, ensuring efficient maintenance and operation. The furnace performance can be assessed by means of:

- skin temperatures, of which the values are indicated by means of thermocouples along the tubes as reported in §2.3.4., and which increases along the run because of coke formation;
- pressure drop ΔP of the furnace, evaluated as the difference between the pressure at inlet of the convective section and the furnace outlet pressure (FOP), increases as coke formation increases;
- fuel gas consumption (of both heating and soaking sections), since it tends to increase along the run because of coke formation;
- furnace efficiency is not directly related to the coke formation but instead by various factors, including design, insulation, combustion efficiency (air-fuel ratio, excess of air). Improving furnace efficiency is essential for reducing energy consumption, lowering operating costs, and minimizing environmental impact.

Chapter 3

Design of an advanced control system

As described in Chapter 2 the importance of controlling the thermal cracking furnace plays a crucial role in order to increase the performance of the furnace (§2.6). The application of Advanced Process Control (APC) system, particularly considering the application based on Model Predictive Control (MPC), can lead to stabilize the operations in order to achieve the set-goals, allowing to increase the profitability of the process. The purpose of the project is the realization of an advanced control system on the F-1815 furnace of the thermal cracking unit of the API refinery in Ancona, with the aim of maximizing distillate yield and controlling furnace fouling, thus defining two objectives in the short and long term respectively. The intention of this chapter is to provide an overview on the advanced control systems, and to define the steps in the realization of an advanced control application referred to the specific case by combining the theoretical aspects on which this control methodology is based with the more practical ones that are of interest mainly during the phase of use of industrial packages, in the present case by using the Aspen DMC3™ (DMC3) package provided by Aspen Technology, with whom the present project is under development, and for what concerns the long-term model the use of MATLAB. The sources from which this chapter is drawn are derived from the practical work carried out during the activity of this thesis and from information and contribution provided by both API refinery and AspenTechnology.

3.1 APC overview

Advanced control technologies are located in a high layer of the control pyramid Fig.3.1.

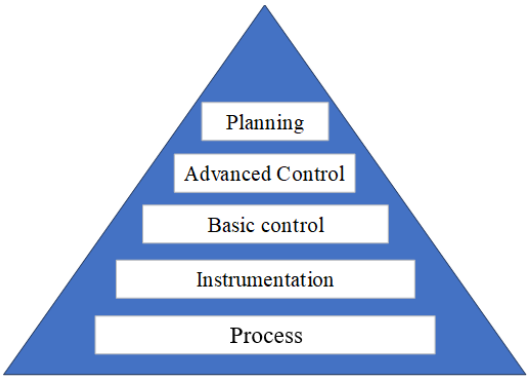

Figure 3.1 General representation of the control pyramid.

- The controlled technology represents the basic process with which the technologies implemented in the upper layers interact.

- The instrumentation layer gathers all sensors and actuators that are installed in the process under control.
- In the basic control layer are the controllers that guarantee the basic functionality, reliability, and safety of the controlled process. All standard control architectures that are regularly operated by operators (e.g. PID control loops) are placed in this layer.
- Advanced control applications are managed in the advanced control layer. The technologies implemented in this layer are responsible for optimizing the entire process. Optimization takes place through the "intelligent" coordination of the controllers implemented in the lower layer. Generally, the applications implemented in this layer have a shorter sampling time than the controllers used in the lower layer.
- The planning layer gathers all the higher-level supervisions that are generally managed by plant managers. The main purpose of these supervisions is to plan production and dictate objectives to the levels below.

The focus of this work will be on the advanced control layer. Specifically, in the design of an APC for the thermal cracking furnace F-1815.

3.1.1 APC in the industrial world

One of the main objectives of advanced control projects in industry is to stabilize process operations and then achieve quantifiable goals in economic terms. It is precisely the economic benefits that result from the introduction of an APC application that make it possible to assess the convenience of using these highly innovative technologies in numerous sectors.

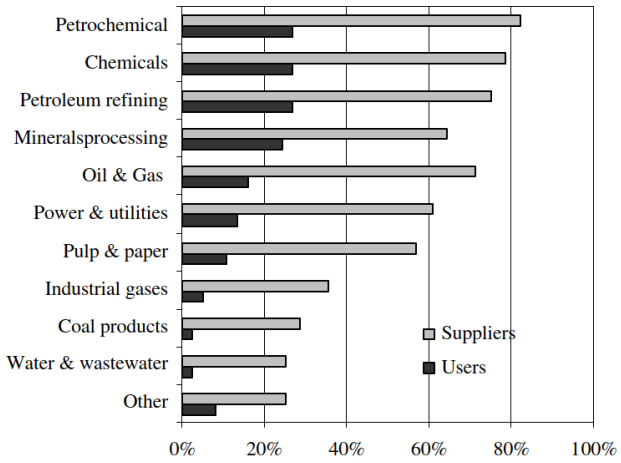

Figure 3.2 Ranking of industrial sectors where most APC applications are used as reported by Bauer and Craig (2008).

In the past, several studies have been conducted to identify the industrial sectors in which APC applications are proposed by the various suppliers and where they are actually used. One interesting survey proposed by Bauer and Craig (2008) reports the results in Fig. 3.2, showing the extent of use in the petroleum refining process.

Among the most widely used APC applications are based on model predictive control (MPC). The reasons for the success of MPC-based applications lie in the fact that predictive control is a family of methods that offer the possibility of:

- explicitly including constraints on state, input, output, as well as logical relations in the formulation of the control problem;
- controlling systems with hundreds of manipulated and controlled variables;
- formulating the control problem as an optimization problem, in which even very different (even conflicting) objectives can be considered;
- using very simple models derived from experimental tests (impulse and step responses);
- using, on the contrary, more sophisticated, non-linear models (e.g. derived from system physics), with continuous and integer variables.

In the present work, use was made of the package provided by AspenTech, DMC3, and as it will be discussed in Chapter 4, apart from the models developed for the control system also a statistical dynamic model has been designed in order to be implemented in the APC system.

3.1.2 Benefits of APC

Generally, implementing an APC application leads to the increase of the profitability of a process by affecting the following five areas:

- maximizes the input charge to the process and seeks to maximize the highest yield products contained in the charge;
- minimizes the consumption of utilities used in the process, where the highest consumption comes from the use of fuels, steam, cooling water and electricity;
- forces the process by moving it to a point of operation where it is the most economically efficient;
- reduces the variation in product quality by approaching the process constraints in which productivity is highest;
- responds quickly and automatically to specification changes or process disturbances, effectively reducing the transients in which process margins are reduced.

Of course, these results could be achieved by the skill of the operators who monitor the process on a daily basis. But, given the amount of equipment and units that an operator very often has to monitor, he/she is not always able to manually steer the plant to the most economically efficient working points. And it is not necessarily the case that in all situations operators are able to keep track of all the interactions that the various processes exhibit. The consequence is that, in the vast majority of cases, operators run the plants in such a way as to ensure process safety while neglecting the economic benefits of optimized operation. For this reason, the presence of APC applications could be extremely advantageous both in facilitating the operators' task during normal process operation and in obtaining economic benefits on a continuous basis over time.

3.2 Mathematical formulation of MPC

The greatest success of MPC applications is because they allow for a systematic and standardized approach to multivariable process control problems with constraints. MPCs base their control paradigm on the process model they use to predict future process behavior. The prediction is used to compute the optimal control action. Fig. 3.3 shows the mechanism employed within the control algorithm.

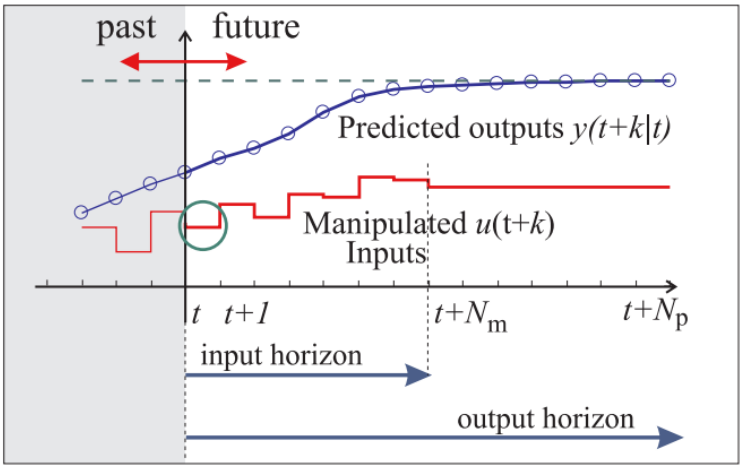

Figure 3.3 MPC control strategy. Source: Bemporad, Morari (1999).

In the basic formulation of an MPC it is assumed a linear model of the process, a quadratic cost function and the definitions of constraints in the form of linear inequalities. The definition of the cost function J involves penalizing the predicted controlled variables $\hat{y}(k+i|k)$, i.e. predicted variable of the output y at horizon $k+i$ at instant k, against an imposed trajectory $r(k+i|k)$ and the manipulated variables $\hat{u}(k+i|k)$ and/or their variation $\Delta\hat{u}(k+i|k)$. In detail, the cost function can be expressed in the following general form:

$$J(k) = \sum_{i=H_w}^{H_p} \|\hat{y}(k+1|k) - r(k+1|k)\|^2_{Q(i)} + \sum_{i=0}^{H_u-1} \|\Delta\hat{u}(k+1|k)\|^2_{R(i)} \tag{3.1}$$

where, the parameter H_p is referred to as the prediction horizon whose starting point is H_w. Choosing to set $H_w > 1$ allows to avoid using the cost function during undesirable transient conditions of the process (non-minimum phase systems or delays). The H_u parameter is referred to as the control horizon (prediction horizon). Of course, it is assumed that $H_u \leq H_p$ since the prediction is based on past measurements of the inputs and outputs. The two different formulations above refer to the fact that in some cases it is preferable to penalize variations in the manipulated variables ($\Delta\hat{u}$) in other cases it is preferable to penalize the manipulated variables directly (u). Nothing prohibits setting up a functional that simultaneously penalizes the manipulated variables and their variations. The weight matrices **Q** and **R** represent tuning parameters that allow the controlled and manipulated variables (or their variation) to be penalized appropriately. In addition to the definition of the cost function,

constraints can be defined on the controlled variables and the manipulated variables (or their variation). Constraints are defined in the form of linear inequalities in the following standard form:

$$E\ vec(\Delta\hat{u}(k|k), \dots, \Delta\hat{u}(k + H_u - 1|k) \leq vec(0) \tag{3.2}$$

$$F\ vec(\hat{u}(k|k), \dots, \hat{u}(k + H_u - 1|k, 1) \leq vec(0) \tag{3.3}$$

$$G\ vec(\hat{y}(k + H_w|k), \dots, \hat{y}(k + H_p|k, 1) \leq vec(0) \tag{3.4}$$

where, E, F and G are matrices of appropriate size and *vec(0)* denotes a column vector in which every element is equal to zero. Of course, it is always possible to fall back to the standard form for defining constraints.

3.3 Dynamic matrix control (DMC)

In this work, the model predictive control strategy addressed corresponds to a dynamic matrix control (DMC), applied through the Aspen DMC3™ (DMC3) package provided by AspenTech. This control technique uses a matrix (a set of models), i.e. a set of relationships between process variables, used to estimate the behavior of the plant in the near future (predictive control) by considering the effect of all variables (multivariable). In order to bring the plant into the most cost-effective region while respecting the constraints imposed on the variables (constrained control), the DMC controller solves an optimization problem for each cycle, considering material and energy flows, plant costs and constraints. Consequently, the DMC controller is model-based, multivariable, constrained, predictive and operates as a supervisor, manipulating basic controllers (PIDs).

A DMC controller differs significantly from a standard PID controller. Typically, a standard PID controller has only one controlled variable (CV) and one manipulated variable (MV). A multivariable controller has two or more controlled and/or manipulated variables. Furthermore, one MV can be moved to control more than one CV and one CV can be controlled by more than one MV. Standard PID controllers are based on feedback from the process. Thus, for example for a flow controller, the valve position is only changed when the current flow value (process value, PV) deviates from the desired flow value (set-point, SP). No other information is available to determine the valve position. Multivariable controllers use empirical (model-based) models, i.e. derived from the observation of plant behavior by means of step tests, which represent the dynamic relationship between a CV and one or more MVs. This relationship not only describes the magnitude of the effect on the CV of a move on a MV, but also describes the variation of the same effect over time. A model-based controller uses these relationships to predict the future behavior of the unit. Based on this prediction, the DMC controller can calculate a set of moves to drive the process in the desired operating region.

3.3.1 Definitions in APC application

To understand how the system work a description of the key terms used within the DMC is necessary.

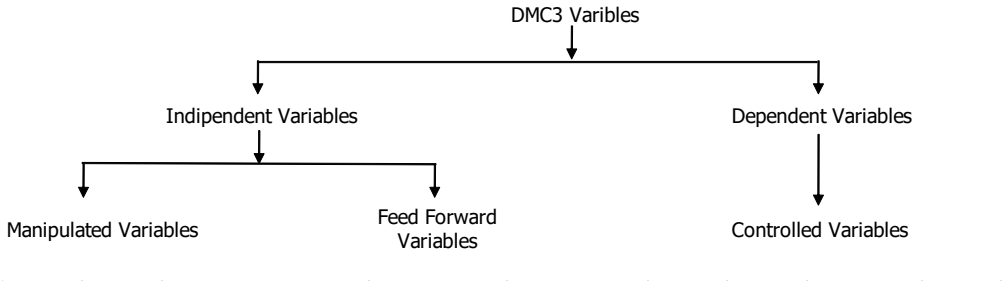

Figure 3.4 Variables definitions in the DMC framework.

- A manipulated variable (MV) represents a "knob" that can be used to control and/or direct the process. Typically, manipulated variables are the setpoints of existing PID controllers or the outputs (initial value problem IVP or output OP) of manually operated valves or controllers. For example, charge, temperature and pressure controllers can be manipulated variables. The DMC controller will move the setpoints of the basic loops and/or their IVPs/OPs in the same way an operator would in order to meet set control objectives. These variables are often referred to as independent variables because they can be varied independently of other setpoints and/or OPs in the process.
- A feedforward variable (FF) impacts the process, but cannot be varied by the DMC controller. A typical feedforward variable is room temperature, which affects many process variables but cannot be manipulated by the DMC. The controller can only observe changes in temperature and make appropriate adjustments in other manipulated variables to correct the expected disturbance. These variables, like MVs, are also independent variables since they do not depend on other setpoints and/or IVPs in the process.
- A controlled variable (CV) is one that varies in response to changes in a manipulated variable or feedforward. Product compositions are examples of controlled variables. These variables are often referred to as dependent variables because their value depends on the value of other variables in the process. It is not possible to change the value of a dependent variable directly. To change a dependent variable requires one or more manipulated variables that have an effect on it.
- The time to steady-state is the time interval for a change in a manipulation to completely exhaust its effect on a dependent variable.
- The steady state target (SS-target) is a value calculated at each controller run (once per minute) for each manipulated and controlled variable. This value is chosen to drive the plant in a high economic profit region while meeting all process constraints. The controller will move the MVs to ensure that each CV reaches its target.
- A controller execution loop for PID controllers that perform basic control typically execute their control action once a second or even every 0.5 s. The DMC controller, on the other hand, has an execution cycle that is usually 60 s. Between executions, the controller is idle and any change, or

disturbance on the plant, or change in control strategy, is not acknowledged until the next execution.

- A model represents the pattern between a manipulated and a controlled variable, it is the effect on the manipulated variable. Models are built during step tests and are derived from direct observation of plant behavior (that is why they are called empirical).
- In the DMC controller it is possible to configure some variables as "critical." This does not mean that the controller will pay special attention to managing or controlling these variables, but simply that the controller cannot be activated when these variables are unavailable (because they are disabled by the operator, or because it is in BAD measurement on the DCS). If the controller is originally in service and a critical variable becomes unavailable, the controller will automatically shut down.

3.3.2 DMC controls

A multivariable controller has two or more variables controlled and/or manipulated. The input to a multivariable controller can be any variable having a target value or acceptable range. There is no 1:1 linkage between a controlled and a manipulated as in the case of PID to DCS controllers. Multiple manipulated variables are linked to multiple controlled variables by the presence of patterns. A pattern is a dynamic relationship between a controlled variable and a manipulated variable. It not only describes the magnitude of the effect of the manipulated variable on the controlled variable, but also how the effect develops over time. There are several mathematical methods used to describe a dynamic process model, however, the simplest and easiest to understand is the "step-response" model.

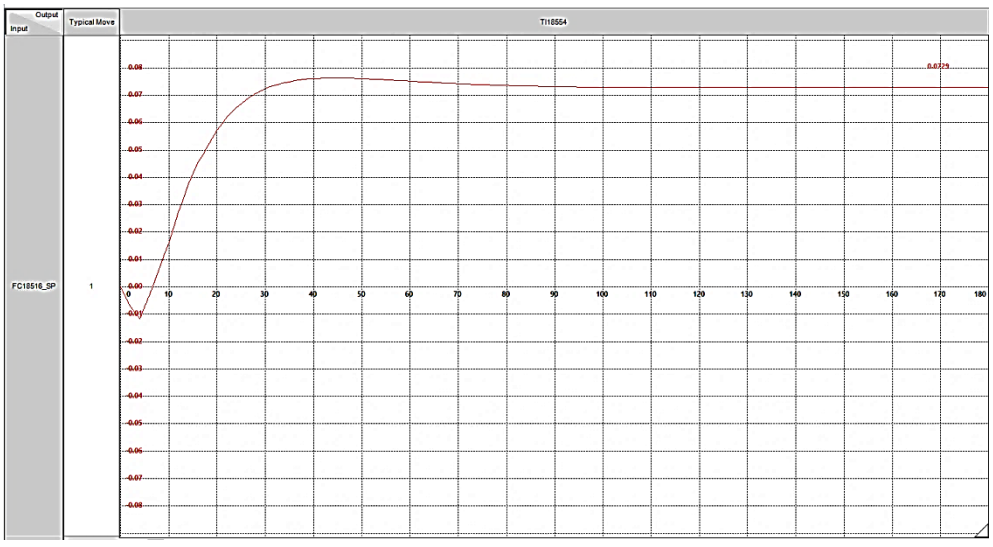

Figure 3.5 Model between TI18554 (skin temperature) and FC18516 (fuel gas flowrate soaking).

A "step-response" model describes the expected response for a controlled variable following a step change in the manipulated variable. Analysis of the data collected during plant testing is used to derive the dynamic model (a time-dependent model) of the process, an example can be seen in Fig.3.5.

During testing, each of the MVs is moved in order to test its effect on each CV that is affected. A model-based controller uses an array of these models to predict the future behavior of the unit. This allows the controller to calculate a plan of future moves, for each manipulated variable, that will keep the controlled variables within their acceptable range. Thus, a predictive controller rejects disturbances faster than a simple PID loop, as shown in Fig.3.6.

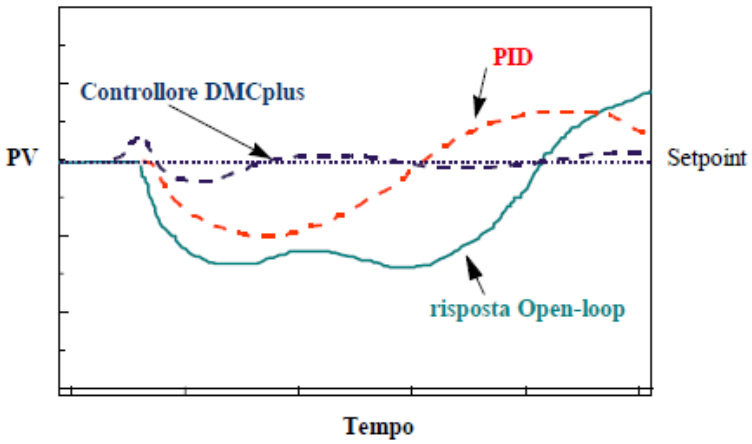

Figure 3.6 Typical responses of a DMC and a PID controllers. Source: API, AspenTech.

Each time the controller runs, the prediction of future plant behavior is updated using current information. This ensures consistency between the prediction of the DMC and the current behavior of the process.

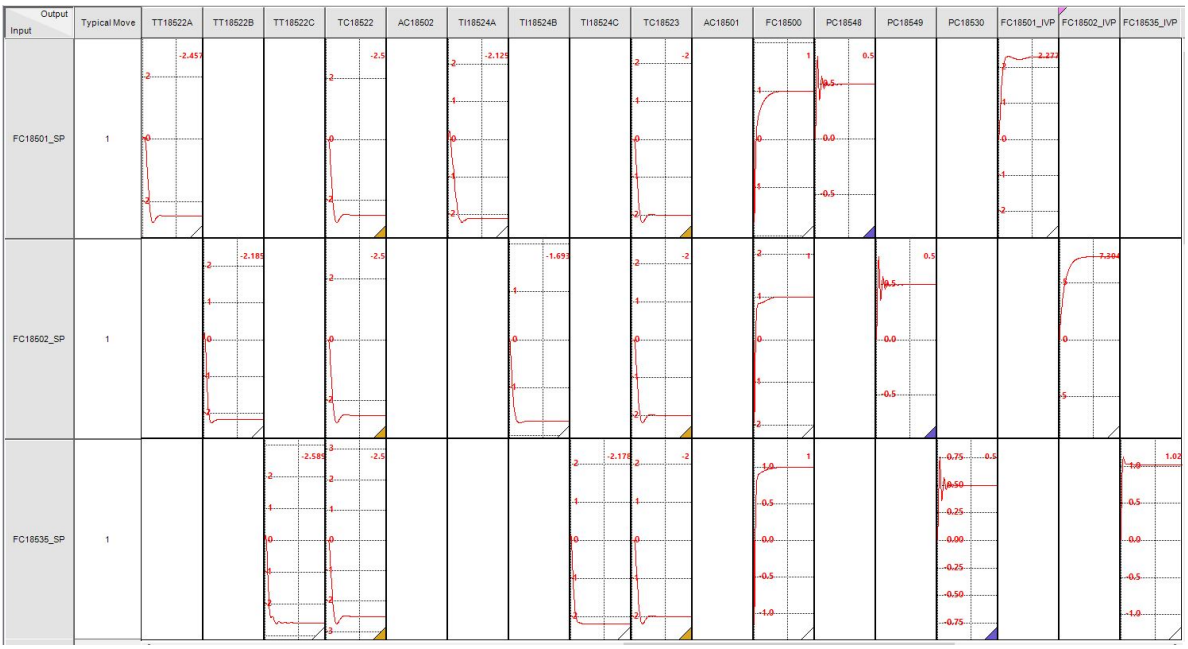

Figure 3.7 Example of dynamic model matrix used by DMC3 system.

An example of the matrix of the models used by the DMC system is reported in Fig. 3.7, specifically it represents a portion of the control matrix of the thermal cracking furnace that has been built; here

in Fig. 3.6 are reported only 3 MVs and 17 CVs, but in fact there are 7 MVs, 2 DVs and 52 CVs, which are listed in §3.4.2. A detailed discussion of the models will be provided in Chapter 5.
It has to be noticed that constrained controllers have to be often used to be sure that the process remains confined within desired limits. A constrained controller is defined as a controller that can keep the controlled variables within a specific range of values. Limits are chosen in relation to process conditions or plant constraints. There are three types of limits: operational limits, engineering limits and validity limits.

- Operating limits are those within which the DMC can move and are set by the operator; note well that the range of operating limits is within and not beyond the engineering limits.
- Engineering limits are those within which operational limits can be set and are set by the control engineer. Note that the engineering limits can be set within and not beyond the value of the validity limits. These limits can be possibly changed only in the engineering key in the computer where the DMC controller performs its calculations or directly by DCS.
- Validity limits are those within which engineering limits can be set and are usually established based on the instrument's measurement range. If a variable is within its validity limits, its value is recognized as "GOOD." Conversely, if it exceeds its validity limits, its signal is automatically recognized as "BAD".

Given a certain set of constraints, there is more than one set-up of the plant that meets them. The controller, within the constraints set, will guide the plant into the set-up that is economically best. It is therefore clear that by varying the limits of the controller's variables, the plant's point of economic optimum will also vary.

3.4 Development steps

The procedure applied for the development of the APC follows the usual standard procedure proposed by the American Petroleum Institute, largely employed by all major producers of MPC applications. The steps are articulated as follows:

- definition of the objectives of the work, which consist of definition of project scope and KPIs, benefit study, definition and installation of hardware and software;
- preliminary project, gathering information at the plant (P&IDs, PFDs, interviews, historical operation data), defining baselines for comparison, identifying key constraints (draft MVs/CVs matrix);
- preliminary tests, which consists of implementation of communication interface, start of data collection, survey on instrumentation and basic control, preliminary steps on the plant;
- plant test, excitation of all MVs within allowable limits agreed with the plant, initiation of the pattern identification procedure and review of the MV/CV matrix;
- final project, identification and validation of mathematical models between MVs and CVs, APC controller simulation and off-line tuning, production of preliminary documentation;
- start-up, online downloading of APC controller, commissioning and fine-tuning, documentation;
- performance evaluation, monitoring and any controller adjustments, operator training.

It has to be noticed that at the present moment this work has been delivered the project has arrived to the final project stage, which has to be completed, therefore, only brief remarks will be made about the final stages of the implementation of the APC (final design, start-up and performance evaluation).

3.4.1 Objectives

The main objectives of the work are two:

- maximizing the conversion (i.e. increase of the yields in distillates) in the short-term by considering the maximum operating temperature that can be reached daily. As described in Chapter 1, an increase in temperature (combined with the control of the other variables, i.e. increase the severity of the process) will lead to an increase of the conversion;
- control of the fouling (coke) in the long-term due to the increase of the severity of the process to increase the conversion, which lead to the coke deposition on the coils surface as described in §1.5, thus limiting the run length of the furnace, which has to be avoided since it's required to reach a specific target day of end of run at specific conditions. In particular, plant shutdown occurs after a run length of one year circa ideally, and obligatorily when the limit operating temperature of the furnace coils 660 °C (skin temperature) is reached. Therefore, the goal is to reach the set run end by reaching the maximum operating temperature of the furnace, e.g. around 330 days of run with a skin temperature of 660 °C in the last days.

Along with those objectives there are the benefits that the advanced control system can provide as mentioned in §3.1.2, which are related to the increase of the efficiency of the furnace thanks to the multivariable control system. Some of those objectives are:

- minimizing the O_2% to the stack in order to balance the combustion mixture to the heating section (AC18502) and soaking (AC18501) of the furnace F-1851, thus increasing the efficiency.
- balancing the feed-flowrate of the passes (FC-18501, FC-18502, FC-18535) to the furnace F-1815, in order to increase the overall conversion (avoiding under-cracking and/or over-cracking between passes) and increase the efficiency of the furnace.
- minimizing the consumption of fuel gas to the heating (FC-18515) and soaking (FC-18516) section of the furnace F-1851, in order to increase the efficiency of the furnace and reduce the related cost of fuel gas.
- avoiding under-cracking and protecting from over-cracking, controlling upset conditions when it is possible, stabilizing downstream fractionation operations.

All objectives must be considered from an overall perspective respecting safety, environmental and process constraints.

3.4.2 Preliminary project

In this phase all documents and information on the process have been collected along with the process data of the current and last few years. This procedure allows to have a better understanding of possibility to accomplish the set objectives of the APC application. In fact, the data acquired and the information gathered make it possible to identify exactly the economic goals that the APC will have to pursue and, more importantly, allow the constraints that will limit the region of operation of the

advanced controller to be defined. It is of crucial importance to define only those constraints that will actually have to limit the APC at the stage of finding an economic optimum because the inclusion of inconsistent constraints could be detrimental to the success of the APC. In particular, in this stage it has been enlightened that the APC is limited to the F-1851 furnace unit only, and does not have the whole thermal cracking unit to be covered, since has described in §2.4 the separation section is not equipped with sufficient control system that can provide a useful application to the optimization system, even for the estimation of the yields which cannot be performed automatically (§2.4.1).
Also in this stage, all issues related to basic process control were investigated, as it is necessary that the architecture of the basic control does not interfere with the operation of the APC application during its operation. That is why all architectures that do not allow direct manipulation of a control loop (e.g., cascade control) or that introduce nonlinearities (e.g., override control, spilt range control, nonlinear level control) will have to be readjusted. It is obvious that all controllers that will be under APC will have to be configured to accept the control mode via a supervisor when APC is activated. In addition, it is necessary to engineer a logic to handle the loops manipulated by the APC during the on/off phases of the APC to avoid causing undesirable behaviors to the process; the goal is to make the on/off transitions in the absence of bumps on the process.
Another important activity to be conducted at this stage is the evaluation of the performance in terms of tuning of the loops belonging to the basic control; therefore, at this stage it was necessary to carry out a loop tuning activity aimed at stabilizing/improving the performance of the basic loops in such a way as to ensure that the APC will efficiently use the MV that it will use to govern the entire process.
Another issue that has been enlightened in this stage is the distorted historical data for those data collected in feedback loops, since the physical effects of the process variables it is distorted by the feedback control, specifically on the variables TSHH (high temperature control at the outlet of each section of the furnace) and furnace outlet pressure (FOP), which are affected by the feedback control on furnace outlet temperature (FOT), i.e. in order for the set FOT to be maintained the variables are offset against each other, thus not allowing for reliable correlation. As an example, increasing TSHH heating results in decreasing soaking's skin temperatures, this occurs due to the feedback control reducing the amount of fuel gas at soaking to reestablish the same FOT.

Table 3.1 MVs of the APC system.

Number	Variable type	Tag	Description	Unit of measurement
1	MV	FC18501_SP	feed-flowrate 1st pass	ton/h
2	MV	FC18502_SP	feed-flowrate 2nd pass	ton/h
3	MV	FC18535_SP	feed-flowrate 3rd pass	ton/h
4	MV	FC18515_SP	fuel gas flowrate heating	kg/h
5	MV	FC18522_SP	air flowrate heating	kg/h
6	MV	FC18516_SP	fuel gas flowrate soaking	kg/h
7	MV	FC18524_SP	air flowrate soaking	kg/h

Table 3.2 DVs of the APC system.

Number	Variable type	Tag	Description	Unit of measurement
1	DV	PC18514_SP	furnace outlet pressure	kg/cm^2
2	DV	TI18537	feedstock temperature	°C

Table 3.3 CVs of the APC system.

Number	Variable type	Tag	Description	Unit of measurement
1	CV	TI18587	skin temperature 1st pass	°C
2	CV	TI18554	skin temperature 1st pass	°C
3	CV	TI18555	skin temperature 1st pass	°C
4	CV	TI185607	skin temperature 1st pass	°C
5	CV	TI18556	skin temperature 1st pass	°C
6	CV	TI185608	skin temperature 1st pass	°C
7	CV	TI185610	skin temperature 1st pass	°C
8	CV	TI18557	skin temperature 1st pass	°C
9	CV	TI18553	skin temperature 2nd pass	°C
10	CV	TI18589	skin temperature 2nd pass	°C
11	CV	TI18590	skin temperature 2nd pass	°C
12	CV	TI185601	skin temperature 2nd pass	°C
13	CV	TI18548	skin temperature 2nd pass	°C
14	CV	TI185602	skin temperature 2nd pass	°C
15	CV	TI185611	skin temperature 2nd pass	°C
16	CV	TI18591	skin temperature 2nd pass	°C
17	CV	TI18588	skin temperature 3rd pass	°C
18	CV	TI18549	skin temperature 3rd pass	°C
19	CV	TI18550	skin temperature 3rd pass	°C
20	CV	TI185604	skin temperature 3rd pass	°C
21	CV	TI18551	skin temperature 3rd pass	°C
22	CV	TI185605	skin temperature 3rd pass	°C
23	CV	TI185612	skin temperature 3rd pass	°C
24	CV	TI18552	skin temperature 3rd pass	°C
25	CV	TT18522A	TSHH outlet heating 1st pass	°C
26	CV	TT18522B	TSHH outlet heating 2nd pass	°C
27	CV	TT18522C	TSHH outlet heating 3rd pass	°C
28	CV	TC18522	furnace outlet temperature	°C
29	CV	AC18502	oxygen smoke heating	%
30	CV	TI18524A	TSHH outlet soaking 1st pass	°C
31	CV	TI18524B	TSHH outlet soaking 2nd pass	°C
32	CV	TI18524C	TSHH outlet soaking 3rd pass	°C

33	CV	TC18523	furnace outlet temperature	°C
34	CV	AC18501	oxygen smoke soaking	%
35	CV	FC18500	total feed-flowrate to the furnace	t/h
36	CV	PC18548	inlet pressure convective section 1st pass	kg/cm^2
37	CV	PC18549	inlet pressure convective section 2nd pass	kg/cm^2
38	CV	PC18530	inlet pressure convective section 3rd pass	kg/cm^2
39	CV	FC18501_IVP	feed-flowrate 1st pass	t/h
40	CV	FC18502_IVP	feed-flowrate 2nd pass	t/h
41	CV	FC18535_IVP	feed-flowrate 3rd pass	t/h
42	CV	FC18515_IVP	fuel gas flow-rate heating	kg/h
43	CV	FC18516_IVP	fuel gas flow-rate soaking	kg/h
44	CV	DT1_HEAT	ΔT 1st pass heating	°C
45	CV	DT2_HEAT	ΔT 2nd pass heating	°C
46	CV	DT3_HEAT	ΔT 3rd pass heating	°C
47	CV	DT1_SOAK	ΔT 1st pass soaking	°C
48	CV	DT2_SOAK	ΔT 2nd pass soaking	°C
49	CV	DT3_SOAK	ΔT 3rd pass soaking	°C
50	CV	DF1	ΔF 1st pass	t/h
51	CV	DF2	ΔF 2nd pass	t/h
52	CV	DF3	ΔF 3rd pass	t/h

In this stage all the MVs, DVs and CVs has been defined as reported in Tab. 3.1, Tab. 3.2, Tab. 3.3. As it can be observed, the IVP variables of the flowrates have been selected as CVs in order to control the behavior of the valve, preventing it from going into saturation. The air flowrates to the two chambers of the furnace has been considered as MVs in order to control the oxygen composition at the stacks along with the combustion. Calculated variables has also been included as CVs.

3.4.2.1 Calculated variables

To balance the three passes of the furnace, some variables has been constructed (from variable number 44 to variable 52 of the listed control variables in Tab. 3.3) in order to guarantee the same degree of heating to each pass, avoiding the under-cracking or the over-cracking of one pass with respect to the other. The following describes in detail all the controlled variables whose value is the result of a calculation:

- DT1_HEAT, DT2_HEAT, DT3_HEAT, DT1_SOAK, DT2_SOAK, DT3_SOAK calculated variables ensure the same temperature to each pass of each section of the furnace. In a general form it is expressed as

$$DTn\_SECTION = T_{section}^{out} - \left(\frac{\sum_{n=1}^{3} T_n^{out}}{3}\right) \tag{3.5}$$

The *DT* [°C] is the difference between the outlet temperature of the specific section (heating or soaking) and the outlet mean temperature given by each single pass *n* out of the furnace (note that it is not the FOT).

- DF1, DF2, DF3 calculate variables ensure the same amount of flowrate to each pass

$$DFn = F_n - \left(\frac{\sum_{n=1}^{3} F_n^{out}}{3}\right) \tag{3.6}$$

The *DF* [*t/h*] is the difference between the outlet flowrate of the specific pass *n* and the outlet mean flowrate given by each single pass *n*.

3.4.3 Preliminary test

There are numerous activities to be performed during this phase of the project. The main ones concern the perturbation of the most critical variables to anticipate the conditions that will occur during the plant step test, the installation and verification of the proper functioning of the installed software, the implementation of the benefits that can be obtained from the APC, the verification of the objectives to be pursued by the APC, the refinement of the purpose of the APC and, finally, the design of the APC control matrix on which the automated step test procedure will be based.

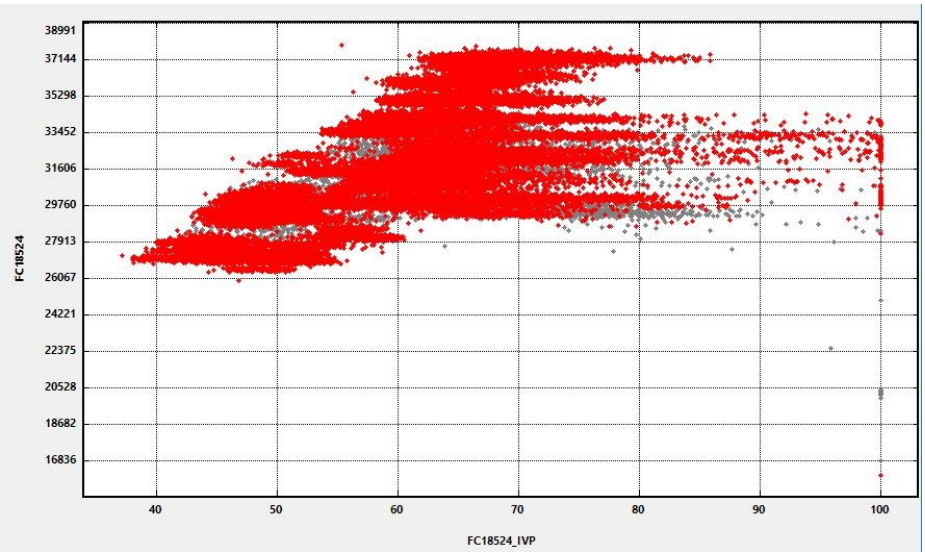

Figure 3.8 FC18524 PV vs OP, sticky valve behavior.

During this phase it is also important to investigate the configuration of the basic control system to analyze some important properties of the measuring instruments, actuators and control loops used for basic process control.

- For measuring instruments it is necessary to assess whether the measurement range is adequate for monitoring operations; a range that deviates greatly from normal plant operation greatly reduces the resolution of the measurement.
- Actuators must ensure stable and robust process regulation; in most cases regulation is carried out through control valves that may exhibit cycling or sticking phenomena.

- Control loops need to be configured in such a way that they can be easily managed by the APC. It is necessary to consider whether some typical configurations (e.g., cascade control) should be revised considering their use in the APC. Of course, it is necessary to remove all advanced control structures, other than the APC being designed, that manipulate the same loops that will be handled by the APC.

As an example, during this phase the behavior of two sticky valves, specifically related to the control of air flow rates to the burners of the two heating and soaking chambers, FC18522 and FC18524, respectively, has been detected as it can be seen in Fig. 3.8 for the FC18524.

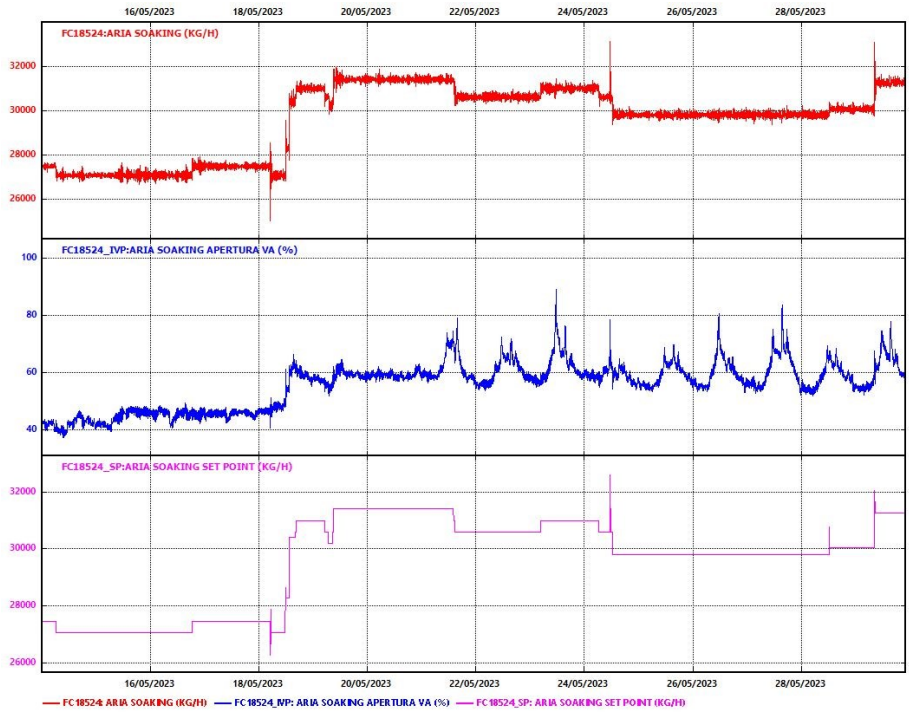

Figure 3.9 FC18524 sticky valve comparison of PV, IVP, SP.

More precisely, has it is shown in Fig. 3.9, the valve position (IVP, blue line) tends to make rapid adjustments, but the process variable (PV, red line) does not respond as expected. Thus, the two controllers were tuned to see if there were any issues related to this, but despite this, the problem does not seem to be related to the tuning of the controller, but rather could be due to the valve positioner. In such cases, the plant operator needs to be notified so that the necessary maintenance can be performed in the next shutdown. It should be noted that a difficulty in controlling the air flow rate to the burners, can lead to poor control of combustion, thus the skin temperatures of the furnace coils, and thus on the process temperature, thus causing over-cracking or under-cracking conditions.

Another fundamental activity at this stage is the preparation of a tag list necessary for the collection of implantation data. It is clear that the proper functioning of any data collection mechanism must be thoroughly tested to avoid losing data from the implantation step test, which, of all the activities presented, is the most substantial in terms of execution time.

A "raw" control model of the APC is also developed at this stage; there are several ways to create a raw model, some of them consist of:

- using an existing model, perhaps employed in similar processes, and adjust it for the process under consideration;
- using a dynamic simulator to create data in simulation and identify such data;
- creating first-order models with lag (of course overestimating gains, time constants, and lags increases confidence in manipulating process variables);
- perform 2-4 moves for each variable manipulated in the process and model the data collected after this test.

The magnitude of the moves during plant pre-step/step testing, whether manual or automatic, is to perform a move "as large as possible" i.e., to ensure that through that move it is possible to correctly estimate the gain of the process by noting an actual change in the most critical controlled variables. The problem that is possible to encounter is not seeing any change in the most critical CVs; in that case it may be necessary to increase the magnitude of the move, filter the CV measurement (if it is particularly noisy) or check for instrument malfunctions. Once the correct amplitude of the move has been identified archive this amplitude and set it as the typical amplitude of the move. Proceed with this procedure with all other MVs. Of course, avoid changing the mode of operation of loops not affected by the current move; all controllers should be in the mode they will be in during normal APC operation. In the specific case, a seed-model (as it is called in DMC3^{TM}) has been created by means of the step-test performed on the MVs listed in Tab. 3.1; the related gain matrix will be reported and commented in §4.1.1.

3.4.4 Plant step-test

The plant step test activity is the most critical activity in the process because it disrupts the process under consideration. This activity must be fully shared by the personnel of the plant being optimized and must be constantly monitored by the executing team of the APC application. During the execution of the step test the available data collected are used to refine the raw model developed during the previous steps and at the same time the step test phase is refined, if available, by using cross correlation tools to verify that correlated moves are being performed (of course in the automated multiple step test this has already been verified during the step test design). Three types of step-tests are possible, among them in the specific case under consideration only the manual step-test has been applied to perform this phase of plant step-testing.

- Manual step-test, the duration of this type of test is given by

$$8.10 \cdot (N_{MV} + N_{CV}) \cdot t_{ss} \tag{3.7}$$

where, N_{CV} and N_{MV} represents the number of CVs and MVs respectively, and t_{ss} [s] represents the time to steady state. Note that 15-20 moves are performed for each independent variable (MV, DV) and to perform the moves individually for each independent variable avoiding correlation between different moves. The moves should be executed with different waiting times between

one move and the next covering the different times to steady-state. In this way the average waiting time should be half of the time to steady-state, the shorter moves help to identify the dynamics of the process while the longer moves allow to identify steady state gains. In the case where the time to steady-state is not well identified, longer moves than the estimated time should be performed. As usual, the magnitude of the move should be such as to visualize a change in the most critical CVs. A standard suggestion is that the signal-to-noise ratio of the most critical CVs should be 6:1. Whenever possible, overlapping moves between different variables is avoided even though it very often happens, due to process requirements, that some variable has to be adjusted; if the number of moves is large this generally does not create major problems.

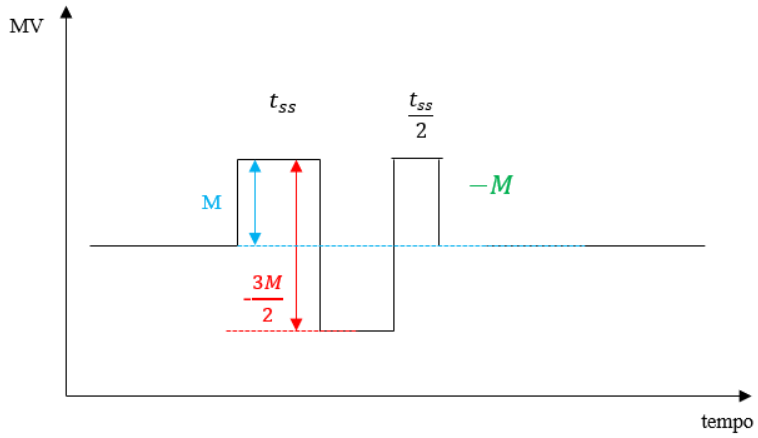

Figure 3.10 Step-test pattern adopted in the specific case.

The step-test pattern adopted in the specific case is represented in Fig. 3.10, where M [*unit of measure of the MV*] represents the magnitude of the amplitude of the perturbation in the MV, the value of which has been determined depending on the degree of influence on the CVs, in order to appreciate a significant change in the CV. The time to steady-state t_{ss} after two steps it has also been considered to be moved up to the point where the variable reaches only half of the time to steady-state, that is done in order to observe the dynamic behavior of the model.

- Automated single step, is a test that involves using a raw model of the process to generate a pattern of moves to be applied to each MV individually. Essentially, this testing mode reproduces manual step testing by adding the additional potential of software for generating and monitoring moves and protecting imposed constraints. During the generation of moves and the acquisition of the first useful data, it is desirable to refine the initial raw pattern to produce moves increasingly suitable for the process.
- Automated multiple step test, this step test has the same characteristics as the single automated step test with the added potential that all MVs are moved simultaneously for almost the entire duration of the step test. It is clear that this type of testing is conducted only in the presence of a reliable model and especially by trained personnel since it is very difficult to visualize and understand the effects on a single CV as a result of the moves of one or more MVs. Of course, the time taken to perform this task is reduced in the presence of an automated multiple step test.

Generally if a typical manual step test takes 4 weeks of time, an automated single step test takes 3 weeks while an automated multiple step test takes 1 week. An additional benefit of automated step testing (both single and multiple) comes from the ability to employ people on the project team in activities other than step testing.

In conclusion, the step test activity ends when additional information cannot be derived from the data to enrich the internal models of the APC application.

It should be noted that the use of the automated step test functions, which within AspenTech DMC3 system are defined through the calibrate feature, can also be used during running operation of the APC. The purpose is to refine the models of the dynamic matrix with an automated update, such functionality will be exploited to update both short- and long-term models implemented in the APC system, the possible application will be further discussed in Chapter 4.

3.4.5 Final project

In this step, all data generated during the previous step are reviewed in order to exclude from the final modeling all data generated under anomalous process conditions. Based on the remaining available data further refinement of the models and critical analysis of the identified links are performed. Of course, it is advisable to perform this activity in collaboration with the process engineers and some of the operators whose experience gained in the plants is an invaluable support.

At this stage, in order to get an offline indication of the characteristics of the APC application, that is, to determine how good the models are for control, it is necessary to design operational scenarios on which to test the application offline and obtain indications of:

- achievement of optimal targets at permanent regime;
- verification of the feasibility of CV control solutions;
- dynamic performance on CV control;
- performance of MVs in achieving CV targets and economic targets.

To resolve any issues that emerge in the points just listed or simply to increase application performance, the actions to be taken involve adjusting tuning parameters. Each platform that runs APC applications has a well-defined set of parameters that must be set to meet certain performance goals. It can be mentioned at this stage that, in order to make the APC application lead the plant to an economically favorable permanent operating point while avoiding exceeding the imposed constraints, appropriate weights can be specified to the MVs and CVs. In addition, in the case of an infeasible solution, it is possible to specify which and how some secondary constraints (soft constraints) can be sacrificed; other tuning parameters deal with adjusting the application to make the process response to typical disturbances change or give more importance to keeping some CVs at target than others. It is clear that at this stage the application is finalized and must be ready for online commissioning.

3.4.6 Start-up

At this stage the APC application will be commissioned and the process will begin to be governed to achieve the imposed objectives. Prior to commissioning, it is necessary to perform training to the operators who will be the main actors to use the application. For commissioning, there are

standardized procedures called SIT (Site Interface Test) that allow in-depth testing of the proper functioning of the application, especially in terms of communication and management (power on and off). Once the SIT phase is completed, one can proceed to online commissioning of the entire application. The advice is to initially keep tuning and limit settings conservatively to avoid overstressing the process. If provided for by the software being used, the advice is to activate the application in the prediction mode without performing the control actions; in this way it is possible to check the reliability of the identified models and possibly refine before the process checks some bindings. After accepting the performance in terms of prediction, it is possible to switch to the control mode. A good method is to proceed in SISO (Single Input Single Output) mode or, at most, MISO (Multi Input Single Output) mode with the following criterion:

- force the chosen CV to its current value (i.e., enter the maximum and minimum limits close to the current value of the measurement);
- carefully set the maximum and minimum limits of the MVs so that there is a safe operating range where each individual MV can move;
- move a limit of the CV being tested, leaving the other CVs disabled, and check the behavior of the MVs that will move to bring the CV back within range;
- if the behavior is not satisfactory, act on the tuning parameters and check the dynamic behavior again;
- repeat this test for all CVs in the project.

Eventually all variables will be in control and adjustments to the APC application as a result of the presence of the disturbances identified in the previous steps can also be observed.

3.4.7 Performance evaluation

Once the commissioning phase is over, after verifying that the application consistently meets the specifications given prior to the design phase, it is possible to begin the activity of collecting the information necessary to assess the actual benefits derived from the completed project. It is clear that maintaining the benefits requires ongoing activity aimed at constantly indicating the correct economic information (cost of raw materials, product prices) and possibly at adjusting some of the model parameters as a result of some change in the process being controlled. It is clear that all this will be tied to two fundamental aspects: keeping the application running and updating the application when necessary. The first requirement necessitates the coexistence of several aspects: proper functionality of plant equipment, smooth operation of the basic control system, and assistance from operators and process engineers. The second requirement necessitates that, as announced earlier, the enhancement of the products being considered within the application is constantly updated with respect to the target (this aspect could greatly affect the application's strategy of finding the optimum). In addition, necessary adjustments must be made to ensure reliability of the models used.

3.5 How DMC works

Each DMC controller performs calculations at fixed intervals, typically every minute. Part of these calculations are the following operations:

- read the current process values for all variables included in the controller;
- build a prediction of future behavior;
- calculate the steady-state target, i.e. the movement that the manipulated variables must make in order to satisfy all the constraints and reach a situation of economic optimum;
- determine a sequence of future moves to guide the manipulated variables to their stationary target, minimizing the error on the controlled variables.

In addition, in the present case, the implementation of a dual-horizon optimizer was considered with the objective of providing the daily optimal target and such that the end-of-run target for the long run is achieved. In the following section, the discussion is limited to the operation mode of a DMC system with reference to the AspenTech DMC3 system. The models, their operating principle and the architecture of the control system, will be discussed in Chapter 4.

3.5.1 Calculation of predictions

The DMC controller uses all available models to predict the future evolution of the plant, based on the changes that occurred on MV and FF during the previous steady-state time.

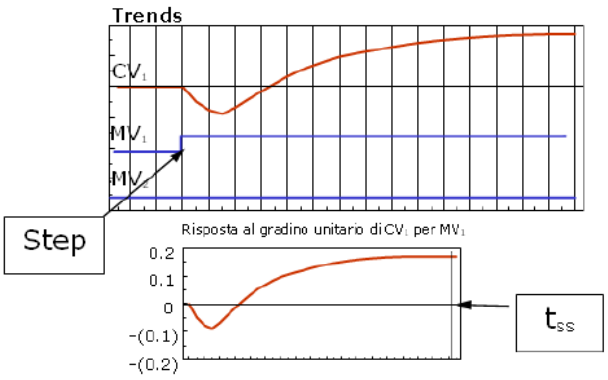

Figure 3.11 Example of a model between a MV and a CV. Source: API-AspenTech.

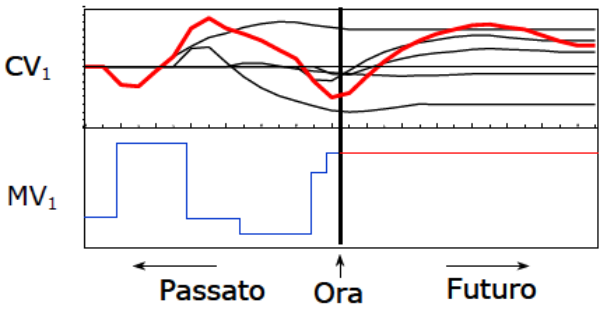

Figure 3.12 Dynamic prediction of the CV_1. Source: API-AspenTech.

The ability to predict the behavior of the CVs makes it possible to implement all necessary measures to prevent violations on the set limits. Suppose the model of CV_1 with MV_1 is as represented in Fig.3.12. In this way, future CV behavior will remain as close as possible to the calculated target steady-state.

3.5.2 Calculation of the moves

As already explained in §3.5.1, the DMC will decide future moves on the MVs so as to obtain, for each CV, the curve that most closely approximates the mirror image trend of the open-loop prediction, as shown in Fig. 3.11. At each execution, the DMC compares the current value of each controlled variable with its prediction made at the previous cycle so that any unmeasured disturbances are taken into account. Based on this comparison, the controller recalculates all future moves on the MVs to update the predictions and align them with the current process trend. Future moves extend approximately one-half of the controller's steady-state time. The path of future moves chosen by the controller to reach the steady-state target of each MV follows the path of economic optimum.

3.6 CV ranking

Considering the multivariable control system, the DMC controller divides all CVs into ranks so as to control all the most important CVs and neglect the least important ones when it proves impossible to find a solution that satisfies all the constraints. In DMC3 the valid ranks for CVs are between 1 and 9999. The lower the rank, the more important the variable. For example, the percentage of oxygen to the flue gas is more important than the furnace outlet temperature. This means, that if the aim is to optimize the furnace outlet temperature (TC18522) by increase the heat provided by the flames, thus by decreasing the air flow rate FC18522 and FC18524, and this will lead to lower the oxygen percentage (AC18501, AC18502), the controller will tend to increase the oxygen percentage to flue gas (by increasing the air flow rate FC18522, FC18524), even if this results in a reduction in FOT. Namely, the minimum oxygen percentage (AC18501, AC18502) is considered more important than the FOT.

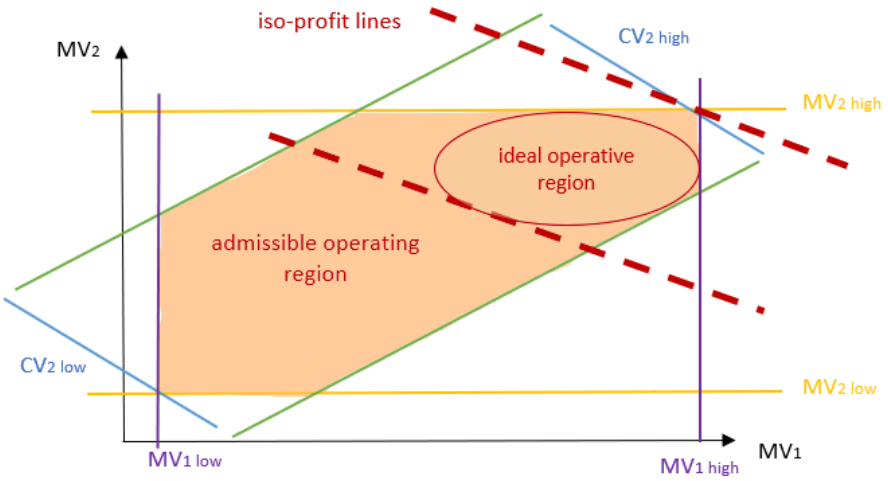

Figure 3.13 Optimal operative region defined in the APC. Source: API.

The combination of all the limits, on the manipulated and the controlled, will identify a whole series of possible set-ups, within which the controller must guide the system. The final set-up is determined based on economic considerations: each manipulated is assigned a cost, and the displacement that minimizes the total cost tells the DMC3 which direction it should take. In this way, the operational region of the DMC will tend to shift toward a point of economic optimum, as shown in Fig. 3.13.

Table 3.4 Preliminary suggestion of ranks for the controlled variables.

Number	Tag	Description	Low limit	High limit
1	TI18587	skin temperature 1st pass	none	20
2	TI18554	skin temperature 1st pass	none	20
3	TI18555	skin temperature 1st pass	none	20
4	TI185607	skin temperature 1st pass	none	20
5	TI18556	skin temperature 1st pass	none	20
6	TI185608	skin temperature 1st pass	none	20
7	TI185610	skin temperature 1st pass	none	20
8	TI18557	skin temperature 1st pass	none	20
9	TI18553	skin temperature 2nd pass	none	20
10	TI18589	skin temperature 2nd pass	none	20
11	TI18590	skin temperature 2nd pass	none	20
12	TI185601	skin temperature 2nd pass	none	20
13	TI18548	skin temperature 2nd pass	none	20
14	TI185602	skin temperature 2nd pass	none	20
15	TI185611	skin temperature 2nd pass	none	20
16	TI18591	skin temperature 2nd pass	none	20
17	TI18588	skin temperature 3rd pass	none	20
18	TI18549	skin temperature 3rd pass	none	20
19	TI18550	skin temperature 3rd pass	none	20
20	TI185604	skin temperature 3rd pass	none	20
21	TI18551	skin temperature 3rd pass	none	20
22	TI185605	skin temperature 3rd pass	none	20
23	TI185612	skin temperature 3rd pass	none	20
24	TI18552	skin temperature 3rd pass	none	20
25	TT18522A	TSHH outlet heating 1st pass	40	40
26	TT18522B	TSHH outlet heating 2nd pass	40	40
27	TT18522C	TSHH outlet heating 3rd pass	40	40
28	TC18522	furnace outlet temperature	30	30
29	AC18502	oxygen smoke heating	10	40
30	TI18524A	TSHH outlet soaking 1st pass	40	40
31	TI18524B	TSHH outlet soaking 2nd pass	40	40
32	TI18524C	TSHH outlet soaking 3rd pass	40	40
33	TC18523	furnace outlet temperature	30	30
34	AC18501	oxygen smoke soaking	10	40
35	FC18500	total feed-flowrate to the furnace	30	30
36	PC18548	inlet pressure convective section 1st pass	none	10
37	PC18549	inlet pressure convective section 2nd pass	none	10

38	PC18530	inlet pressure convective section 3rd pass	none	10
39	FC18501_IVP	feed-flowrate 1st pass	10	10
40	FC18502_IVP	feed-flowrate 2nd pass	10	10
41	FC18535_IVP	feed-flowrate 3rd pass	10	10
42	FC18515_IVP	fuel gas flow-rate heating	10	10
43	FC18516_IVP	fuel gas flow-rate soaking	10	10
44	DT1_HEAT	ΔT 1st pass heating	50	50
45	DT2_HEAT	ΔT 2nd pass heating	50	50
46	DT3_HEAT	ΔT 3rd pass heating	50	50
47	DT1_SOAK	ΔT 1st pass soaking	40	40
48	DT2_SOAK	ΔT 2nd pass soaking	40	40
49	DT3_SOAK	ΔT 3rd pass soaking	40	40
50	DF1	ΔF 1st pass	40	40
51	DF2	ΔF 2nd pass	40	40
52	DF3	ΔF 3rd pass	40	40

The operator limits on the manipulated variables are never violated: the controller determines the value to be associated with these variables and always keeps it within the limits. The controller will also try to stay within the operational constraints of the controlled variables but, as noted, some of them may not be kept within the limits depending on the operating conditions of the plant. In this case, the controller will have to decide which variables are to be kept within the constraints (high priority) and which are to be released (low priority). The ranks of the controlled variables defined for the seed-model of the APC are shown in the Tab. 3.4, pointing out that they do not represent the final value, as they will need to be reviewed before commissioning. As can be seen from Tab. 3.4, the lowest rank, thus the highest importance, is that of the oxygen percentage in the fuel to stack of both section of the furnace, heating and soaking, respectively AC18502 and AC18501, also the fuel gas flow rate valves (FC18515_IVP, FC18516_IVP) and feed flowrate valves to each pass (FC18501_IVP, FC18502_IVP, FC18535_IVP) represent a major constraint. In the first case it is important to keep the lower limit under tight control because of the environmental aspect and efficiency of combustion. In case of the valves their priority is higher as they represent physical and inviolable limits of control systems, and it is therefore necessary to ensure that they are always in a valid operating range and do not reach saturation, consequently losing control capability. It follows the high limit set on the skin temperatures because of structural failure that may occur, but before that also because it is unwanted to have over-cracking conditions that can lead to an excessive production of coke that can cause the shortening of the run length, which means economic loss.

Chapter 4

Modeling

Given the objectives of the APC of maximizing yields while meeting environmental, process and safety constraints in the short term, and at the same time considering the long-term objectives of controlling furnace fouling due to coke deposition in order to reach the goal of the set end of run under the given conditions (i.e. final skin temperatures), it is necessary in the design of the APC system to integrate models that enable the achievement of those objectives. Specifically, in addition to building models for the controller, which allow for predictive control to be achieved, a statistical model has been designed to forecast the fouling during the run length taking into account the operating conditions, variability of the feedstock to the thermal cracking unit and past behavior, with the final objective to determine the residual run length. The purpose of this chapter is to describe the models developed and their advantages, highlighting the enhancement of the APC system.

4.1 Short-term horizon models

The experimental step-testing phase described in Chapter 3, aims to gather the information necessary to describe the dynamics of the process and its disturbances. This information is then transformed into mathematical models of the process and disturbance through appropriate identification algorithms. Three of the dynamic models are given as examples in order to describe the MV-CV relationship obtained from the step-tests.

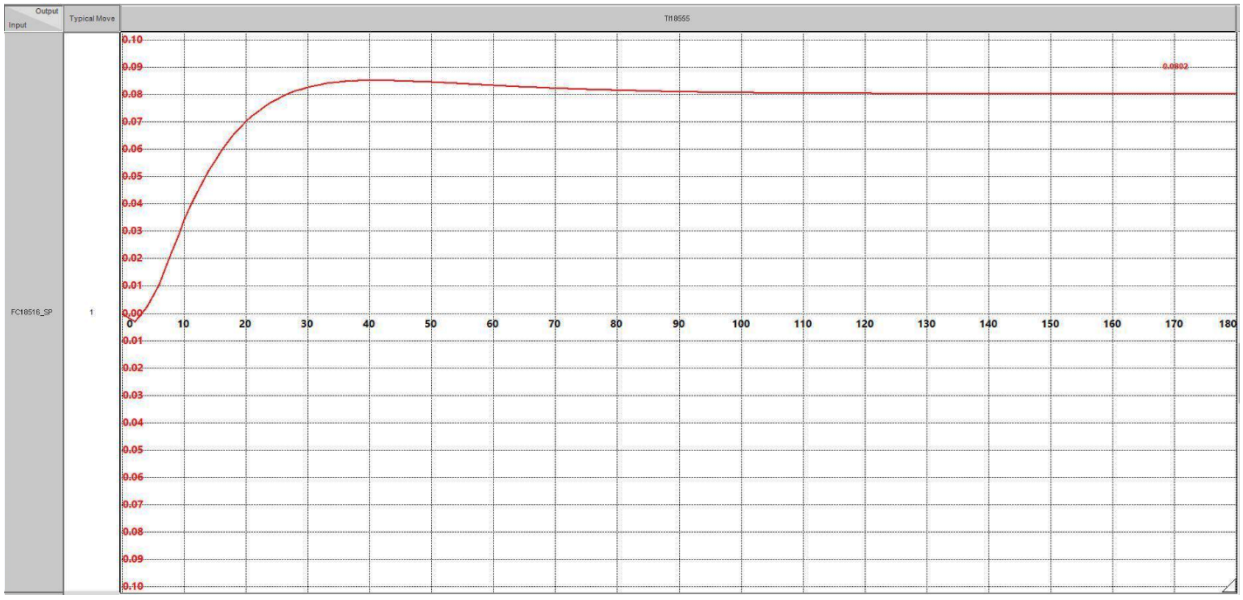

Figure 4.1 Model between fuel gas flow rate of the soaking (FC18516_SP) and the skin temperature of the first pass of the soaking (TI18555).

The effect of the fuel gas flow rate of the soaking (MV, FC18516_SP) on the skin temperature of the 1st pass (CV, TI18555), which is equivalent for all the skin temperatures of each pass, is illustrated in Fig 4.1. The model found appears to be a non-minimum phase model, as shown by the change of sign in the early samples. A good design rule is to eliminate those early samples and insert a delay time in their place, in order not to have initial controller moves of the opposite sign to those needed for steady-state to be reached.

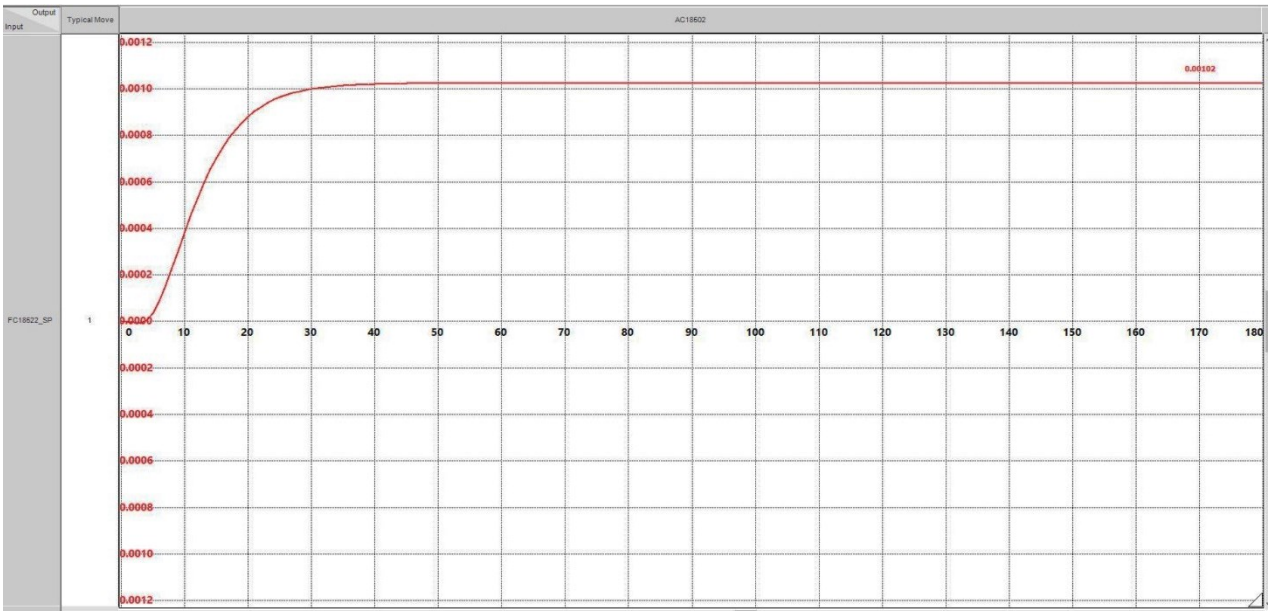

Figure 4.2 Model between the air flowrate in the heating (FC18522_SP) and the oxygen concentration in the flue gas to stack of the heating (AC18502).

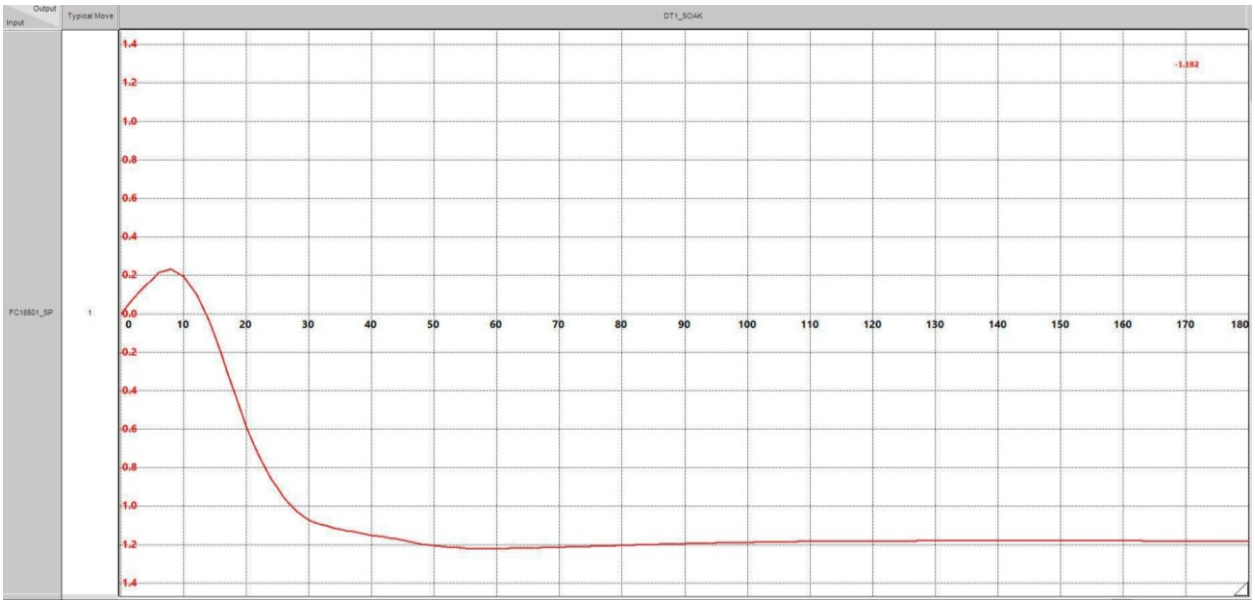

Figure 4.3 Model between feed-flowrate of the first pass (FC18501_SP) and the calculated variable DT1_SOAK used to balance the passes in terms of outlet temperature.

Another important model to highlight is the one representing the relationship between the air flowrate (MV, FC18522_SP) and the oxygen composition (CV, AC18502) in the flue to stack, which is reported in Fig. 4.2. In this case the model corresponds to a first order plus dead time with a steady-

state gain equal to 0.00102°*C/kg/h*, which is reasonable since the order of magnitude of the air flow rate is 10,000 *kg/h*. The behavior is similar for both the soaking and heating section. The model reported in Fig. 4.3 is related to the balance of the passes by means of the calculated variable DT1_SOAK (CV) described in §3.4.2.1. The model shows an inverse response of the system, which can be the result of two first order opposite processes, where for a step input, the first process with a direct response dominates, thus leading to an increase in the outlet temperature of one pass (in this case the 1st pass FC18501) with respect to the other two as there is an increase in the flow rate in the single pass (in this case the 1st pass FC18501_SP), which process could be justified by the increase of the heat transfer because of the increase of turbulence; after this initial phase, the second process with an inverse response will dominate in the steady-state, leading to a decrease of the outlet temperature of the pass in which the increase of flow rate occurred because of the decreased residence time. In this case, it may make sense not to simplify the model by eliminating the inverse response part, because it will be probably needed to control first with one sign and then with the opposite. The importance of those models is related to the capability of the controller to use them to predict the future behavior as described in §3.2.2.

4.1.1 Matrix of models

The model matrix is the main key on which controller operation is based. It sets the basis for the controller's ability to predict future plant behavior and avoid any constraints. In Fig. 4.4 the gain matrix produced in the seed-model is reported, which provides a simple view of the models configured. The model matrix consists of a sparse (i.e., not all full) matrix of patterns among the dependent and independent variables. Not all independent variables (MV, FFWV) have a pattern with all dependent variables, but many independent variables may have a pattern with the same dependent variable (the matrix is precisely sparse). Ultimately, the presence (or absence) of a model combined with ranking determines which particular MV of the controller will be moved to keep a particular CV in control. As an example, it is possible to observe from the matrix in Fig. 4.4, that there is no model between TI18537 (inlet temperature of the feed to the furnace) and any other variable except for the TC18522 (outlet temperature of the heating section). The matrix shows that if the controller has to control a particular CV, then only MVs where there is a pattern (+ or -) can be moved. For example, to control the skin temperatures of the coils in the soaking section, the controller may use only the flow rate of the respective pass and the fuel gas flow rate of the soaking section. The gain matrix also shows that there is an interaction in the process and that MV influences more than a single CV. As an example, if it is necessary to decrease the percentage of oxygen in the flue gas of the soaking chamber (AC18501), there will be an increase of air flow rate (FC18524_SP) and a decrease of the fuel gas flow rate (FC18516_SP) in the soaking chamber. It should also be noted, that the variables PC18514_SP and TI18537, furnace outlet pressure and furnace inlet charge temperature respectively, have been introduced as feed-forward disturbance variables (FFWDVs), as it is intended in the former case to provide to the operator the possibility to control the variable to cope with pressure drops, thus determining residence times, while in the latter case variable TI18537 allows reducing or increasing

the heat to be supplied in the different sections of the furnace to reach the imposed target by increasing the efficiency of the furnace.

MV \ CV	FC18501_SP	FC18502_SP	FC18535_SP	FC18515_SP	FC18522_SP	FC18516_SP	FC18524_SP	PC18514_SP	TI18537
DF3	-	-	+						
DF2	-	+	-						
DF1	+	-	-						
DT3_SOAK	+	+	-						
DT2_SOAK	+	-	+						
DT1_SOAK	-	+	+						
DT3_HEAT	+	+	-						
DT2_HEAT	+	-	+						
DT1_HEAT	-	+	+						
FC18516_IVP				+		+			
FC18515_IVP									
FC18535_IVP			+					+	
FC18502_IVP		+						+	
FC18501_IVP	+							+	
PC18530			+					+	
PC18549		+						+	
PC18548	+							+	
FC18500	+	+	+						
AC18501						-	+		
TC18523	-	-	-			+			
TI18524C			-			+			
TI18524B		-				+			
TI18524A	-					+			
AC18502				-	+				
TC18522	-	-	-	+					+
TT18522C			-	+					
TT18522B		-		+					
TT18522A	-			+					
TI18552			-			+			
TI185612			-			+			
TI185605			-			+			
TI18551			-			+			
TI185604			-			+			
TI18550			-			+			
TI18549			-			+			
TI18588			-			+			
TI18591		-				+			
TI185611		-				+			
TI185602		-				+			
TI18548		-				+			
TI185601		-				+			
TI18590		-				+			
TI18589		-				+			
TI18553		-				+			
TI18557	-					+			
TI185610	-					+			
TI185608	-					+			
TI18556	-					+			
TI185607	-					+			
TI18555	-					+			
TI18554	-					+			
TI18587	-					+			

Figure 4.4 Seed model gain matrix where positive (blue) and negative (red) gains are highlighted.

4.2 Long-term horizon models

Due to the nature of the objectives set for the APC system reported in §3.4.1, it appears necessary to design a model to predict the fouling trend of the furnace coils, so that a plan can be defined for the entire running period that will allow the daily target of operating conditions to be followed in order to achieve the set goals. Because of this, a preliminary analysis to understand the coking phenomenon

described in §1.5 has been made, ending up to the conclusion that an evaluation of the coke evolution can be made by means of the indicators reported in the performance evaluation described in §2.6. At the same time, an investigation of the current F-1851 furnace management system has been carried out, for which the process conditions (more generally, the severity of the furnace) is set based on the following variables:

- feedstock (crude oil processed by the plant and feed to the furnace) characterization;
- feedstock flowrate;
- skin temperature of the furnace coils;
- pressure drops ΔP of the furnace.

Of particular note is the use of furnace coil skin temperatures, which are the main indicators of coke development, since as mentioned in §1.5, an increase in coke formation will cause the coke layer on the furnace coils to grow, resulting in resistance to heat transfer. Consequently, in order to maintain furnace exit conditions at values that guarantee the production of distillates, it is necessary to increase the skin temperature of the tubes. In conclusion, the evolution of coke layer thickening over time can be observed by the increase in furnace coils skin temperatures related to the soaking section of the furnace, since it is the main section where the temperatures are greater than the value (450°C) of the heating section (which cannot go over that temperature), thus the coke formation is a major concern in the soaking chamber. As an example of this evaluation, the skin temperatures of the 2022 year of run length are showed in Fig. 4.5.

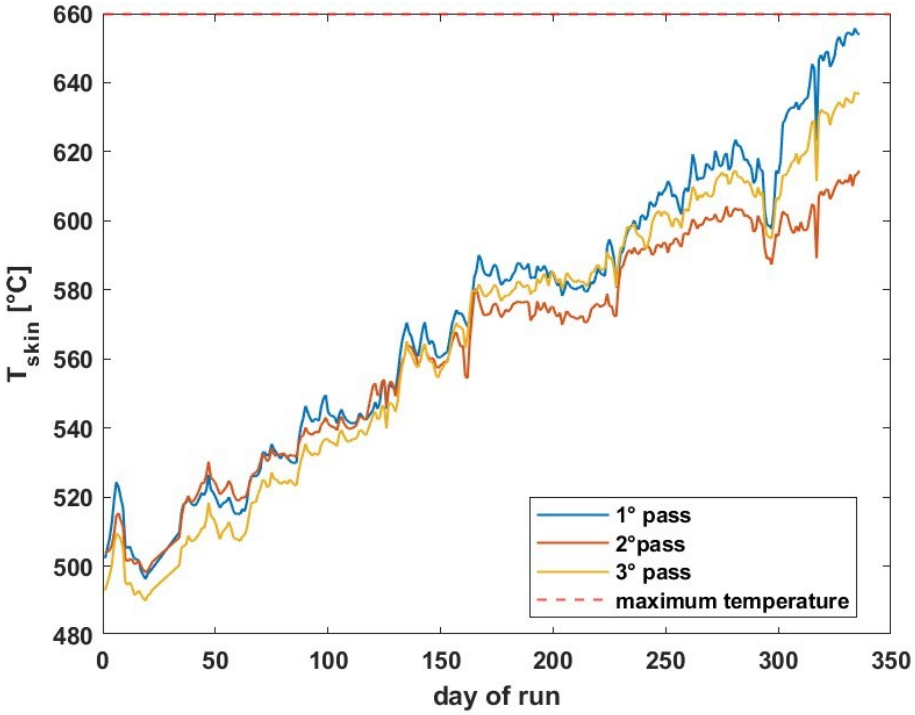

Figure 4.5 Skin temperature profile of each pass of the F-1851 furnace on 2022 run length.

As it is possible to observe from the Fig. 4.5, since up to now the approach is mainly based on the observation of the above mentioned performance parameters without a precise system that evaluates the daily targets in line with the short-term and long-term objectives, this leads to a conservative approach at the beginning of the run cycle to avoid increased carbon deposition on the tubes, thus not

achieving high yields (due to low charge conversion); also in case the processed crude oil presents more tendency to coke, the operator acts with manual preventive actions, i.e. reducing or increasing the severity, as long as these conditions are identified before the disturbance propagates. Such an approach makes it possible, with the exception of significant upsets, to arrive at the programmed end of the run, but it inevitably leads to suboptimal management of the furnace, with consequent loss of distillate yield, and in extraordinary cases to the reduction of the run cycle. It is therefore of primary importance to implement an advanced control system such as to maximize yields and control fouling throughout the run cycle, leading to considerable economic implications. The proposed method of evaluation of the fouling through skin temperatures of coils of the furnace, is largely accepted has an evaluation method to assess the coke development as it is discussed in §4.2.1.
We conclude that the fouling prediction model should be such that it provides the daily prediction of the furnace skin temperatures, so as to provide the prediction of the residual furnace run to understand how much margin is possible for the next optimization step (which will be described in Chapter 5).

4.2.1 Basis for construction

The model related to the skin temperatures is an approach largely accepted and even to the present day through the consultancy provided by Baker Hughes (BH) to the refinery. In fact, BH provides periodically (under request) an evaluation of the residual run length of the furnace F-1851 by considering a statistical approach using a static model based on current operative conditions.
A preliminary assessment was made through the consulting support of BH of possible strategies for approaching the model development, evaluating possible alternatives to the problem.

- Statistical-engineering model based on the analysis of plant data on the previous running cycles of the F-1851 furnace. It provides a series of advantages such as easiness of application and implementation, approach also proven by BH regarding the static model (not the time series model §4.2.3), reliable in that even a linear model approach does not have a large deviation from reality. It has also the potential to implement more features in order to get more details of the system under investigation, thus increasing the complexity of the model over time and by need by keeping the possibility to build the model progressively without a direct implementation of a complex model which requires more time to be validated and to be understood.
- Hybrid model based on both data analysis and kinetics of cracking reactions. The main issues of this type of approach are related to the frequent change in feedstock which is processed by the furnace. Note that the development of all or even part of the kinetics of the reactions involved in the process, would be long and laborious, possibly requiring years of research; suffice it to say that for a kinetic model of cracking reactions, such as the one developed in COILSIM1D by the AVGI research group at the University of Ghent in Belgium, involves even more than 300'000 reactions. In this specific case, the development will be supported by providing the kinetic of the reactions by AspenTech, but with the approximation to the reactions occurring in a VisBreaking unit, which equally undergoes a thermal cracking process but it is still an approximation of the process.

- Process simulator such as Aspen HYSYS or use of computational fluid dynamics approach. The issue is mainly related to the complexity and the time required for the development of project.

Given the advantages and time constraints for project development, it was decided to adopt a model based on statistic approach, the development of which is to be considered under the responsibility of API refinery with final validation of the model by AspenTech.

4.2.1.1 Data processing and analysis

The data collected and analyzed were only related to the unit of interest of the application, which is the furnace F-1851 for the reasons explained in §3.4.2. The data has been collected from IP.21 (process data storage system) on two run cycles, with analysis on 2022 and 2021, on daily sampling data on an hourly basis (e.g. 02/02/2022 00:01:00) and on a daily basis. This data collection was analyzed by using MATLAB and two data analysis software: Minitab®, PDS® (software provided at the API refinery). The analysis was mainly focused on evaluating the variables to be introduced within the model by assessing those with the greatest impact on the response variable represented by the skin temperatures of the furnace coils. It is good to point out that the choice of variables is not only to be referred to the highest correlation found, but also to the knowledge of the process itself.

For clarity, the steps of the analysis are briefly summarized:

- data cleaning based on removal of missing data (e.g. due to digital system crashes), removal of outliers generated by fluctuations in instrument measurements or oscillations due to upsets (which should not be considered);
- checking the distribution of the data so as to describe the variables and identify any outliers by choosing the most representative dataset;
- preliminary graphical analysis of scatterplots between the variable under consideration versus the response variable in order to hypothesize the correlation (whether positive or negative, whether linear or nonlinear);
- correlation analysis such as Pearson correlation (pairs) and VIP (variable importance in projection) analysis.

Since there is a large number of skin temperatures indicators (TI), which represent the response variables, and each one of them can have different values along the run length because of their position (proximity to the inlet or the outlet of the furnace) and the manual regulation of the air on field, it has been decided to take as reference (as it is done in practice) only one or two skin temperatures indicators per pass. Among the preliminary analyses, it has been compared for each step which skin temperature has higher average value for each run cycle. From the analysis done on two run cycles (2021, 2022) the same results were observed obtaining that the TI with higher average values are TI18555, TI18548 and TI185604 respectively for the 1st, 2nd and 3rd pass (for a more broad evaluation even other TI has been checked). Also for what concerns the construction of the models only few skin temperatures indicators has been considered. It has to be noticed that it is better to develop different models for each one of the passes since there is a structural difference as mentioned in §2.3.

The overall results of the analysis lead to the conclusion that the most important variables related to the skin temperatures, thus that affect the coke formation are the same as the ones defined in §2.6:

- feed flowrate to the single pass, FC18501, FC18502, FC18535;
- inlet pressure to the furnace (convective section), PC18548, PC18549, PC18530, or more in general the pressure drops (ΔP) of the furnace;
- fuel gas flowrate to the soaking section, FC18516.

It is also worth noting that the choice of the variables has been also related to the need to untie the variables from the feedback control that led to distorting the result of the analysis with respect to the interaction between the dependent and independent variable, as it has been said in §3.4.2. Such remark has to be considered in order to decouple the model from the actual feedback control system, since it can provide mathematical relationships that are not consistent with the physical meaning, thus deviating the future control system that has to be implemented (e.g. signs of the variables could be inverted). In addition, it should be noticed that these variables were introduced along with others given by the need to make the model more robust in both the static and time series models, as it will be discussed in the next paragraphs.

4.2.2 Static model

An approach considered in the development of the model, in order to get a first analysis of feasibility and profitability of the project, has been the design of a static model. In particular, a static model that predicts the skin temperatures over the days of run of the furnace (soaking section), providing the residual run length at the set operative conditions, following the same approach considered by Baker Hughes. The construction of the model has been made by using PLS (Partial Least Squares) linear regression considering the dependent variables described in §4.2.1.1, but in order to provide the increase in time of the coking, i.e. relate the response variable to time, a dummy variable called *days* has been constructed. The structure of the model, which provides the specific skin temperature of the related pass (1st, 2nd or 3rd) is the one of a linear model which is represented as follows:

$$T_{skin} = c + c_1 \cdot days + c_2 \cdot FF_{pass} + c_3 \cdot FG_{soaking} + c_4 \cdot P_{conv}^{in} \tag{4.1}$$

where c corresponds to a constant parameter, the c_1, c_2, c_3 represent the coefficients of the variables *days*, the feed-flowrate to the single pass FF_{pass} [*ton/h*], the fuel gas flowrate to the soaking section $FG_{soaking}$ [*ton/h*] and the inlet pressure to the convective section P_{conv}^{in} [kg/cm^2]. As an example of the accuracy of the model and in accordance with the way it will work, it has been simulated to construct the model on 2022 year of run length based only on 160 days of run, thus observing the accuracy on the remaining days of run (end of run set at 338 days). The coefficient of determination of the purposed model corresponds to 97.8%, overall the model can be considered to be statistically significant (also diagnostic tests are met). As it can be observed in Fig. 4.6 the result is relatively good considering that the set value of the dependent variable is the mean of the operative condition of 2022, leading to a mean absolute percentage error (MAPE) equal to 1.22% for the 2022 run length. The last days of run, namely from 300 days of run, the discrepancy increases since, as it can be seen,

the skin temperature is lower than the ideal condition at the end of run (nearly 660°C), which means a loss on conversion, therefore in the last days of run the operating condition has been changed (increasing the severity of the furnace) to reach the target, for this reason it cannot be considered a completely reliable comparison in the last period between model response and real data.

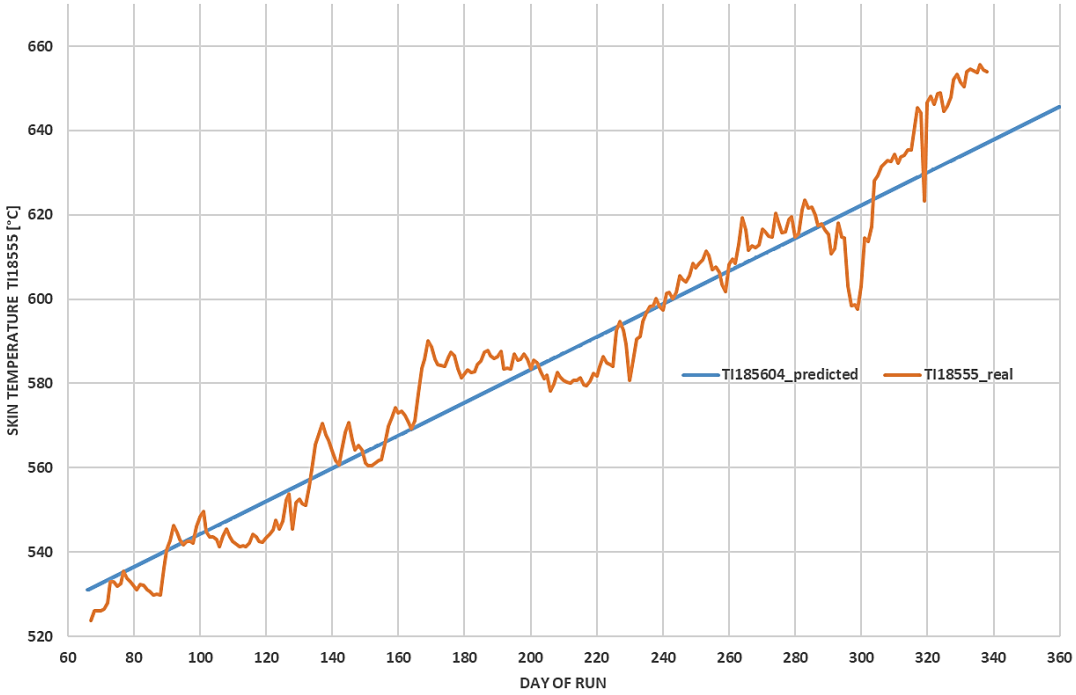

Figure 4.6 Regression model built on data 160 days of run length of 2022, providing the residual run length. Coefficient of determination of 97.4%. MAPE equal to 1.22%.

It should be noticed that the model is static since the dependent variables does not change over time, more generally it assumes that the relationship between variables and the parameters of the model remain constant and do not vary with time. Therefore, such type of model can be considered to be good only in case the process is relatively stable and do not change significantly over time, which in the specific case can be considered as that only for short periods of time since the feed flowrate change depending on the plant program of work and so the other variables such as the fuel gas, which changes along the run length to provide the required heat. It can be observed from Fig. 4.6 that the margin of increase in skin temperatures it could have been higher with respect to the occurred one because, if the end-of-run ideal condition (338-day end at 660°C) is considered, a much greater increase in temperatures along time could have been reached, avoiding a sharp increase in the last period of the run, which causes problems with cross-linking of the coke such that coil cleaning (pigging) operations are made difficult as described in §1.5. This margin of increase can be exploited to consider optimization of the model, thus providing a daily set-point to target the desired end of run at set conditions, this discussion will be further explored in Chapter 5.

4.2.2.1 DCS implementation

If some approximation is considered such as the process is considered to be stable, unaffected by the type of raw material being processed, and the coking formation is assumed linear, then it can be considered to apply the static type model as described in §4.2.2 by ensuring that there is a constant update, daily or periodically according to significant changes, of the dependent variables of the model.

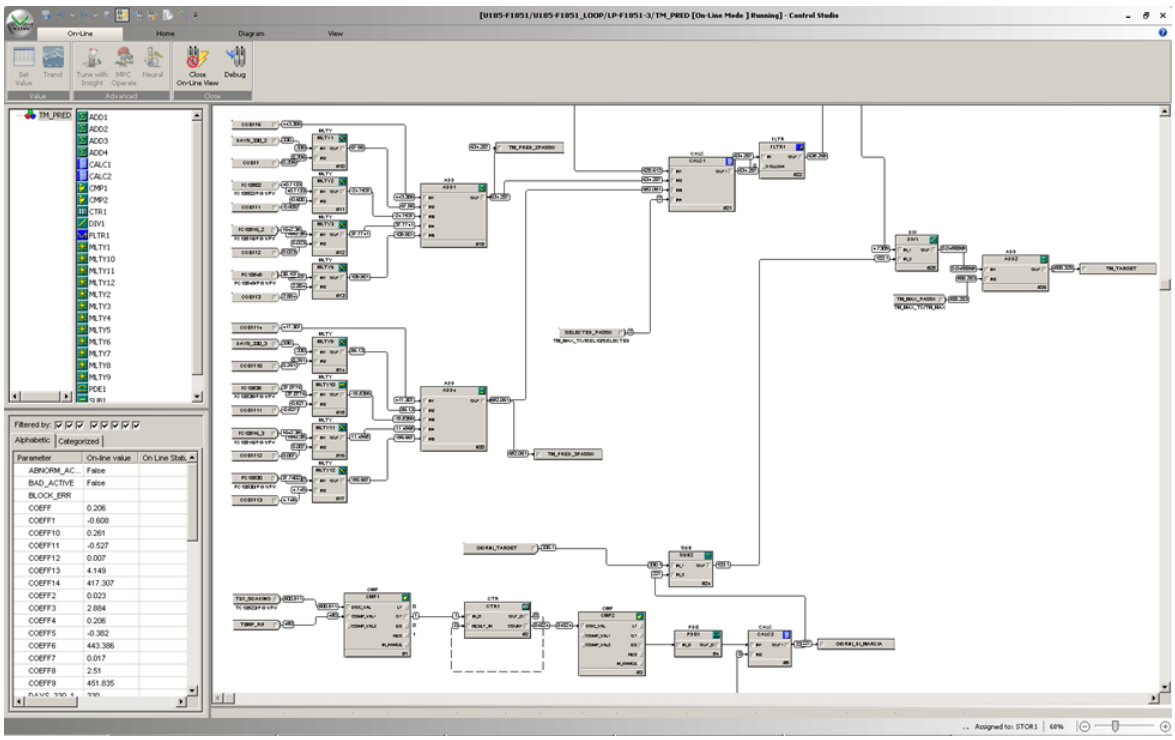

Figure 4.7 Overview of the logical blocks of the DCS implementation of the static model for the prediction of the residual run length of the thermal cracking furnace.

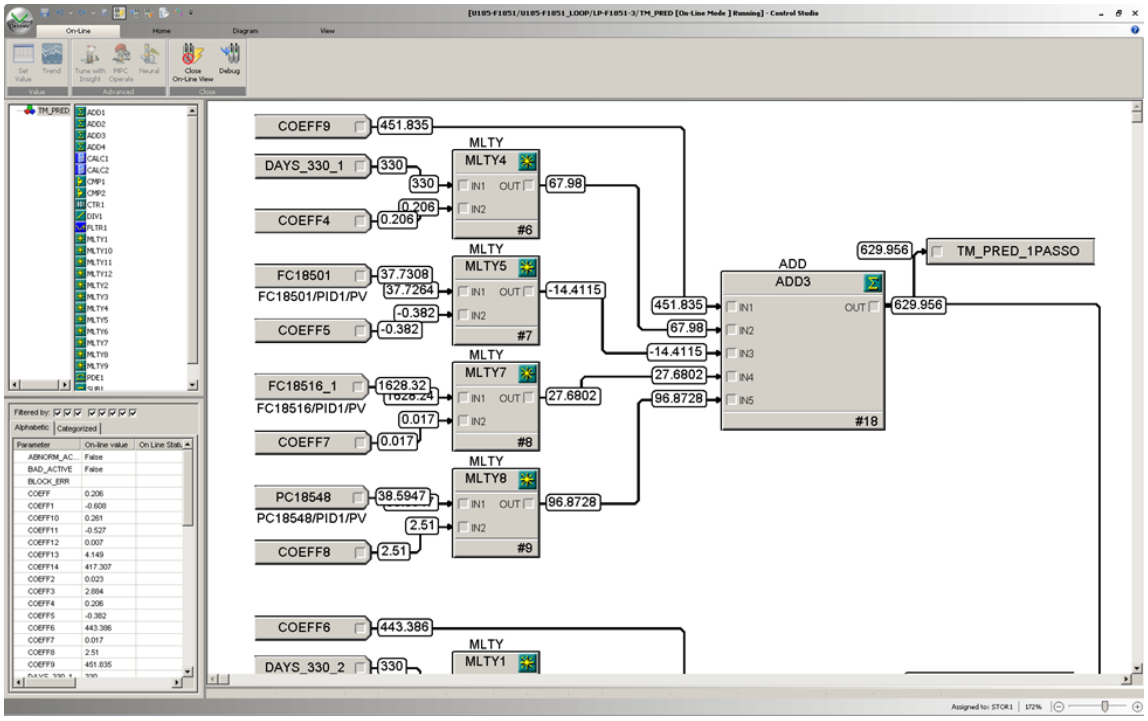

Figure 4.8 DCS logical blocks representing the first pass estimation of the predicted skin temperature of the thermal cracking furnace by static predictive model.

In this sense, the possibility of introducing the static model within the DCS system by means of the construction with logic blocks as reported in Fig. 4.7 has been done thanks to the simplicity of the model, which allows for the constant updating (according to specifications) of the variables by means of their online sampling. As a result, an update of the prediction on the end of run will be achieved according to the conditions under which it is operating. Since there is a structural difference between the three passes it is necessary to consider the implementation of the respective equation, as reported in Fig 4.8 for the first pass, by means of logical blocks it is possible to provide the output variable "TM_PRED_PASSO" (predicted value of the skin temperature) for each pass, then it is necessary to compare the results of each prediction in order to choose the one which provides the highest value as it is desired to keep track of the highest temperature.

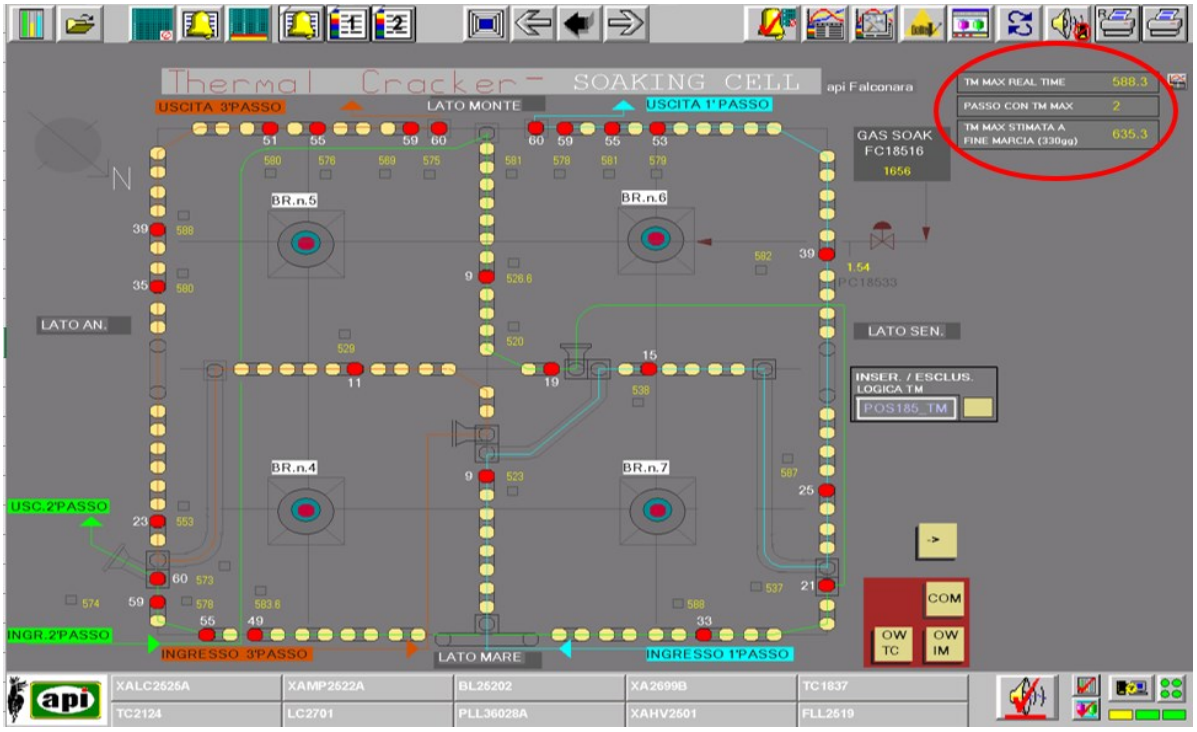

Figure 4.9 Display on DCS operator graphic of the end of run predicted skin temperature of the thermal cracking.

The final output of the described logic is the end of run predicted skin temperature, therefore it does not provide the set-point, instead it provides an estimation that can be displayed in the DCS operator graphic page as shown (highlighted in red) in Fig. 4.9. Such implementation could be a preliminary approach to the problem of fouling control in case of a base-layer control, thus providing the possibility to the operator to move the process towards the set end of run by having an estimation of the possible final condition of the skin temperature at the current condition. As it is possible to observe from Fig. 4.10, obtained by plotting the new created variable in the DCS, the predicted value of the end of run of the skin temperature changes along time depending on the conditions, allowing to obtain useful information to understand the effect of the actual operating condition on the end of run. If the variable reports a high temperature prediction, as can be seen in the initial part of the plot (end of August) where the temperature was above the expected end-of-run target (660°C), it is possible to

consider a reduction in the severity of the process by bringing it in an operative region where there is a sufficient margin for reaching the end-of-run safely.

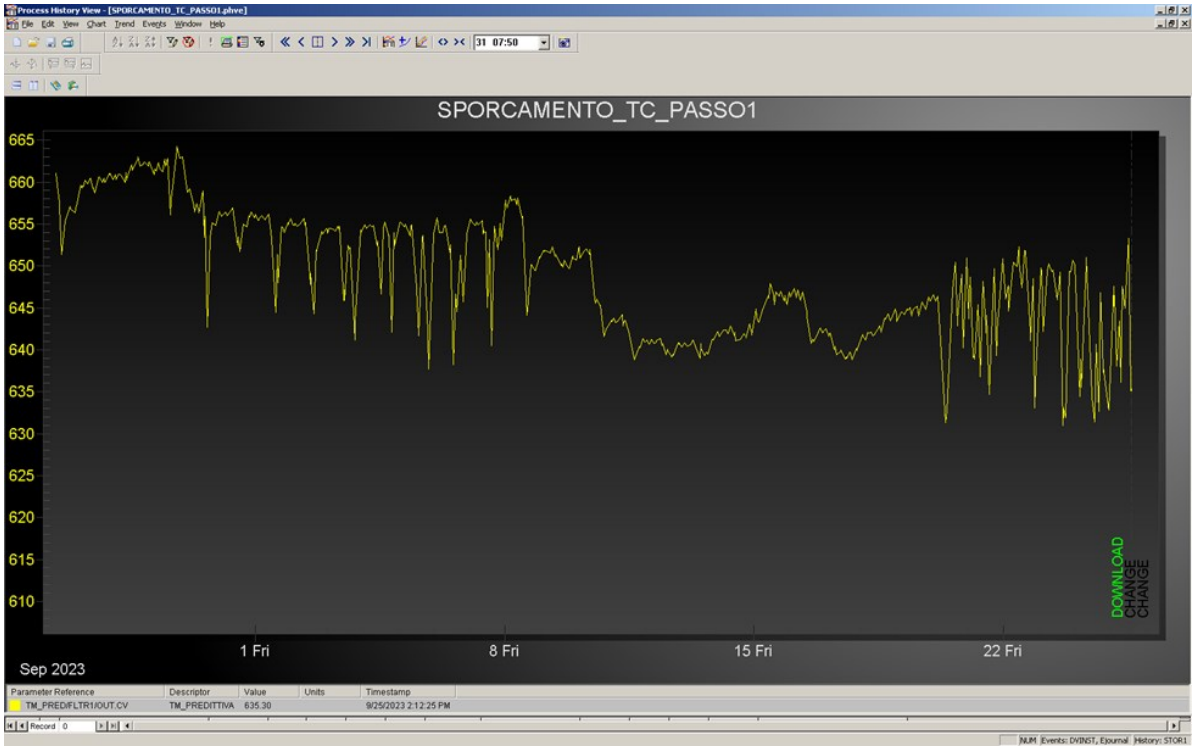

Figure 4.10 Process history view of the new created variable which provides the predicted final temperature of the skin temperature of the thermal cracking furnace at the end of run.

4.2.2.2 Critical aspects and benefits of a static model

The usage of a static model allows to simplify the application of the model for the APC system, and as seen in §4.2.2.1 it can be already implemented and provide reasonable good results with a low error (around 1.5% mean average percentage error). On the other hand, we should consider the limitations of this type of model:

- feedstock quality is not accounted for, therefore the model can be considered to be reasonably reliable only if the crude processed is the same along the run, and if it is, it has to be considered that the crude oil characteristics change even in the same type of oil;
- frequent update of the model as long as data are collected along the run length;
- transient periods cannot be considered as well as upset conditions, because the model does not account for abnormal condition by construction of the model itself, in fact it assumed that the model can be used only if the process is stable;

Overall, since the major disadvantage is represented by the lack of description of the feedstock quality inside the model, it results to be not so useful in this specific case since the crude oil processed by the API refinery is usually changed frequently along a run length.

4.2.3 Time series models overview

In order to capture the complexity of the system under consideration, which are not covered by the static model in §4.2.2, and given the characteristics of the process, it has been decided to adopt a time

series model. In order to provide a broader understanding to this class of models, an introduction is briefly presented through the description provided in Box, Jenkins (2015).

A time series consists of a sequence of observations recorded over time. Various fields, including economics, business, engineering, natural sciences like meteorology, and social sciences, are rich with examples of time series data. One inherent characteristic of time series data is the typical interdependence between adjacent observations. Understanding this dependency within time series observations holds significant practical importance. Time series analysis focuses on methods for examining this interdependence, necessitating the creation of stochastic and dynamic models for time series data and their application in various domains. Utilizing available observations from a time series at time t to forecast its future value at $t+l$ serves as a foundation for several purposes, including economic and business planning, production planning, inventory and production control, and industrial process optimization as in the case under study. Assuming that observations are collected at fixed evenly spaced intervals in time. For instance, using the example provided by Box, Jenkins (2015, p.2) in a sales forecasting scenario, current month sales z_t and previous month's sales $z_t - 1$, $z_t - 2$, $z_t - 3$, and so on, could be used to predict sales for future lead times $l = 1, 2, 3, \ldots, 12$ months ahead. Let $\hat{z}_t(l)$ represent the forecast made at time t for sales z_{t+l} in the future, at lead time l. The function $\hat{z}_t(l)$, which furnishes forecasts at time t for all subsequent lead times, based on information from the current and past values z_t, $z_t - 1$, $z_t - 2$, $z_t - 3$, up to time t, is referred to as the forecast function at time t. Our primary aim is to derive a forecast function that minimizes the mean squared deviations $z_{t+l} - \hat{z}_t(l)$ between actual and forecasted values for each lead time l.

A significant category of stochastic models used to describe time series, which has garnered considerable attention, consists of what are known as stationary models. Stationary models assume that the process remains in a statistical equilibrium state, characterized by unchanging probabilistic properties over time. Specifically, these properties involve variations around a constant mean level and a constant variance. Nevertheless, the realm of forecasting holds paramount importance in fields like industry, where many time series are often better suited for representation as nonstationary. In particular, they may lack a consistent mean level over time. It is not surprising that in some applications involving exponentially weighted moving averages can be demonstrated to be suitable for a specific type of nonstationary process. While these methods may not be universally effective for all the time series, the fact that they often yield the appropriate type of forecast function provides insights into the potential utility of nonstationary models for such problems. The stochastic model for which the exponentially weighted moving average forecast minimizes the mean square error belongs to a class of nonstationary processes known as autoregressive integrated moving average (ARIMA) processes. This broad category of processes encompasses both stationary and nonstationary models, adequately representing many practical time series encountered in real-world applications. Nevertheless, these series might still display consistent patterns over time. Specifically, while the baseline level around which fluctuations occur could vary at different points in time, the overall behavior of the series, accounting for these variations in level, may exhibit similarity over time. Following the construction proposed by Box, Jenkins (2015), such consistent behavior can often be

modeled using a generalized autoregressive operator $\varphi(B)$. Within this model, one or more of the solutions to the polynomial $\varphi(B)$ (i.e. the roots of the equation $\varphi(B)$=0) are situated on the unit circle. Especially, when there are d unit roots and all the remaining roots exist beyond the unit circle, it is possible to express the operator $\varphi(B)$ as

$$\varphi(B) = \phi(B)(1-B)^d \tag{4.2}$$

where $\phi(B) = 1 - \phi_1 B - \cdots - \phi_p B^p$ is the autoregressive operator of order p with ϕ_p parameters to be estimated, B is the backward shift operator, which is defined as $B^m z_t = z_{t-m}$, where z_t is the time series at time t, and d is the order of the integrating part.
Thus, the model form that represents homogenous nonstationary behavior is represented by

$$\varphi(B)z_t = \phi(B)(1-B)^d z_t = \vartheta(B)a_t \tag{4.3}$$

where $\vartheta(B) = 1 - \vartheta_1 B - \cdots - \vartheta_q B^q$ is the moving average operator of order q with $\vartheta_q$unknown parameters, and a_t is a sequence of random drawings (called shocks) from a fixed distribution, usually assumed normal and having mean zero and variance. Therefore, the equation can be written as

$$\phi(B)\omega_t = \vartheta(B)a_t \tag{4.4}$$

where,

$$\omega_t = (1-B)^d z_t = \nabla^d z_t \tag{4.5}$$

where ∇ is the backward difference operator defined as $\nabla = (1 - \mathrm{B})$, therefore providing the relationship $\nabla z_t = z_t - z_{t-1} = (1 - \mathrm{B})z_t$.
Consequently, consistent nonstationary patterns can occasionally be portrayed using a model that necessitates making the d^{th} difference of the process stationary. In real-world scenarios, d typically assumes values of 0, 1, or, at most, 2, where d equal to 0 signifies stationary behavior. The process defined is called autoregressive integrated moving average process of order (p, d, q), or abbreviated as ARIMA(p, d, q). Where the order is related on how the process is defined considering it written as

$$\omega_t = \phi_1\omega_{t-1} + \cdots + \phi_p\omega_{t-p} + a_t - \vartheta_1 a_{t-1} - \cdots - \vartheta_p a_{t-p} \tag{4.6}$$

where ω_t is defined as in Eq. 4.2. Note that the general ARIMA process can be also generated by summing the ARMA process $\omega_t d$ times if it is considered the inverse of the Eq. 4.5.
An extension of the ARIMA models are the ARIMAX, that allow for the additional inclusion into ARIMA models of exogenous variables (also called covariates or external regressors). Those external variables are included in because of their influence on the time series, thus their impact on the

forecast. The ARIMAX model identified, the equation and forecast are reported and discussed in a more operative approach in §4.2.4 and §4.2.4.1.

4.2.4 Time series model

The necessity to cover the critical aspects highlighted in the static model §4.2.2.2, and the need to decouple the variables behavior due to the feedback control loop from the mathematical relationships, and the purpose to design an APC which could be as autonomous and reliable as possible, led to the development of a time series model. The time series model designed has been considered as a linear model composed of two parts:

- black-box part of the model, which represents the static behavior; it has been built by means of the variables that are directly related to the coke formation (i.e. higher correlated to the skin temperatures) using the steady-state gain coefficients obtained from the plant step-tests, as the coefficients of the linear relationships between the variables and the response variable represented by the skin temperature; those variables are the feed flowrate to the single pass FF_i and the fuel gas flowrate of the soaking $FG_{soaking}$ section of the furnace;
- time-series part of the model, which represent the time-dependency; it is an ARIMAX model that describes the remaining part of the real variable (skin temperature) which is not described by the black-box part of the model, considering to be function of feedstock quality parameter (*VGC*) and the pressure drops (ΔP).

Thus, the time series model can be represented by means of the following expression:

$$T_{skin} = K_1 FF_i + K_2 FG_{soaking} + e(t) \tag{4.7}$$

where the predicted value of the skin temperature T_{skin} [°*C*] is given as the combination of a static part, which is represented by the first two terms, respectively the feed-flowrate to the single pass *i* treated daily on an hour base FF_i [*ton/h*] and the fuel gas to the soaking section $FG_{soaking}$ [*ton/h*] both multiplied for the specific steady-state gain K_1 [°*C/ton/h*] and K_2 [°*C/ton/h*] obtained from the step-tests; and the $e(t)$ term which represents the time series part of the predictive model that has been developed using an ARIMAX model on the error of the prediction which is not described by the static part. In order to define it, it is necessary to define the error of the prediction as follows:

$$e(t) = T_{skin} - K_1 \cdot FF_i + K_2 \cdot FG_{soaking} = f(VGC, \Delta P) \tag{4.8}$$

where *e(t)* [°*C*] represents the real error given as difference between the real value of the skin temperature T_{skin} [°*C*] and the static part of the predictive model which is function of the feed-flowrate and the fuel gas flowrate. It is assumed that the modelling error depends on the *VGC* and ΔP [kg/cm^2], thus embedding on the time series part the characteristic related to the quality of the feedstock to the thermal cracking (since the *VGC* is directly analyzed on the feed to the thermal unit) and the operative condition through the pressure drops. As a compromise between simplicity and goodness of fit the

purposed ARIMAX model considered has been the ARX, which is an autoregressive with exogenous inputs model, of which the structure can be presented as:

$$e(t) = \beta_1 \cdot VGC + \beta_2 \cdot \Delta P + \varepsilon_t + \varphi \cdot e_{t-1} \tag{4.9}$$

where $e(t)$ [°*C*] represents the estimated error of modelling that should be summed to the static part of the model (black-box part), and β_1, β_2 are the coefficients of the exogenous variables *VGC* and *ΔP* [*kg/cm²*], while ε_t represents the residual error, φ the autoregressive coefficient which is multiplied for the predicted error at the previous step e_{t-1} .
The overall time series model can be represented by the following equation:

$$T_{skin} = K_1 FF_i + K_2 FG_{soaking} + \beta_1 \cdot VGC + \beta_2 \cdot \Delta P + \varepsilon_t + \varphi \cdot e_{t-1} \tag{4.10}$$

which ultimately leads to obtain the predicted values of the skin temperature of the furnace coils.
It should be noticed that in order to make a forecast of the futures values of the skin temperature it is necessary to provide to the model the future values of the variables over time, in the specific case:

- the feed flowrate FF_i can be provided by the scheduled annual program, which is also refined on a monthly base;
- the fuel gas to the soaking $FG_{soaking}$ is retrieved from the specific consumption of the furnace by considering the following relationship

$$FG_{soaking} = SC \cdot \frac{FOE}{LHV} \cdot FF_{tot} \tag{4.11}$$

  where *SC* [ton_{FOE}/ton_{FFtot}] corresponds to the specific consumption of the furnace, the *FOE* [$kcal/kg_{FOE}$] is the fuel oil equivalent, the LHV [$kcal/kg_{FG}$] is the lower heating value of the fuel gas, which assumed to be mainly composed of methane and FF_{tot} [*ton/h*] is the total amount of feed flowrate to the furnace;
- the *VGC* is related to the characteristic of the feedstock which has to be processed, therefore it is related to the scheduling of the refinery in terms of crude oil to process, which usually can be known relatively in advance;
- the *ΔP* can be considered to be linearized since it presents typically a linear increase in time.

Another consideration has to be made in order to use the model. The coefficients of the static part of the model can be considered equal for every run length, with possibility of slight variations, for which a solution is presented in §4.2.3.2, while with regard to the time series part, it is good to consider to identify the coefficients of the model with the current run data since they vary for each run, since they are related to the processed crude and the pressure drops that will be different. To provide an evaluation of the goodness of the time series model, the result of the model prediction at day different days of the 2022 run length year, based on coefficients of the model retrieved with the available data time to time has been carried out in MATLAB and it is reported in Fig. 4.11, but it is worth nothing

that the model is updated day by day as data are made available, therefore the result is provided by simulating the model in time.

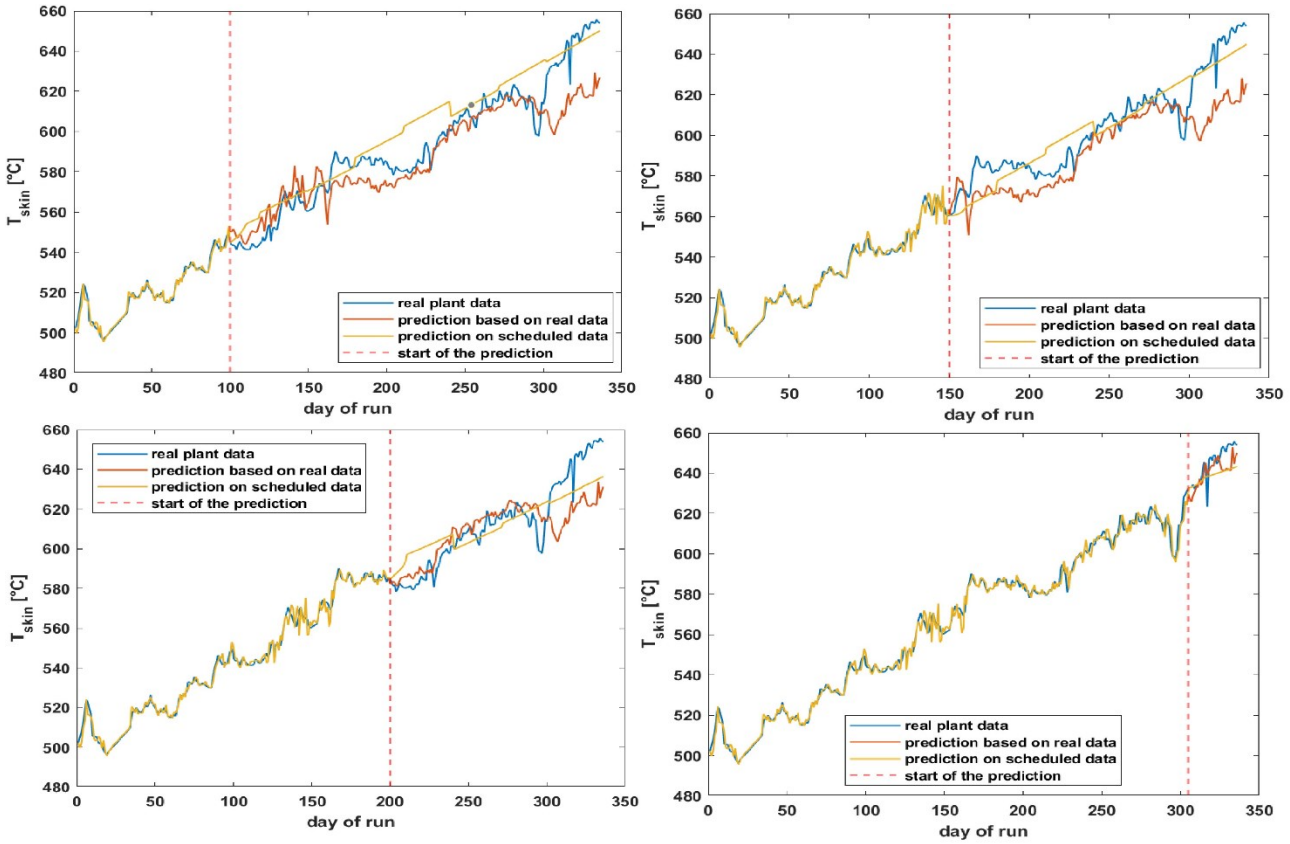

Figure 4.11 Time series model prediction provided at day 100 – 150 – 200 - 305 of run length. It should be noticed that the prediction would be updated day by day, e.g. day 101 provides different results. The prediction is related to the skin temperature of the thermal cracking based on real plant data (orange data) and prediction on scheduled data (yellow curve) compared to real plant data (blue curve).

To do so, it is necessary that the coefficients of the time series part are updated as it would happen in reality. Therefore, it has been considered to apply a variable change of the coefficients of the time series part of the model along the run length.

- For the first 100 days of run length the coefficients that should be used are the ones of the previous year, for example for the 2022 run length the coefficients of the 2021 run length could be used.
- After collecting the data up to 100 days of run length the coefficients could be updated with the current run length, for example with the coefficients obtained from the model identification for the 100 days of data available in the 2022 run length.

After collecting a sufficient amount of data up to a certain time, for example up to 200 days of run length, the coefficients could be updated for the last time, in order to provide an increased accuracy for the end of run. The result of such construction is reported in Fig. 4.12. It is possible to observe that the results is quite accurate, following the real plant data (blue curve) of the skin temperature. The strategy used for the time series model lead to an increasing of the accuracy of the model prediction time to time as it is possible to observe from the evolution of the mean absolute percentage error (MAPE) considering a running simulation.

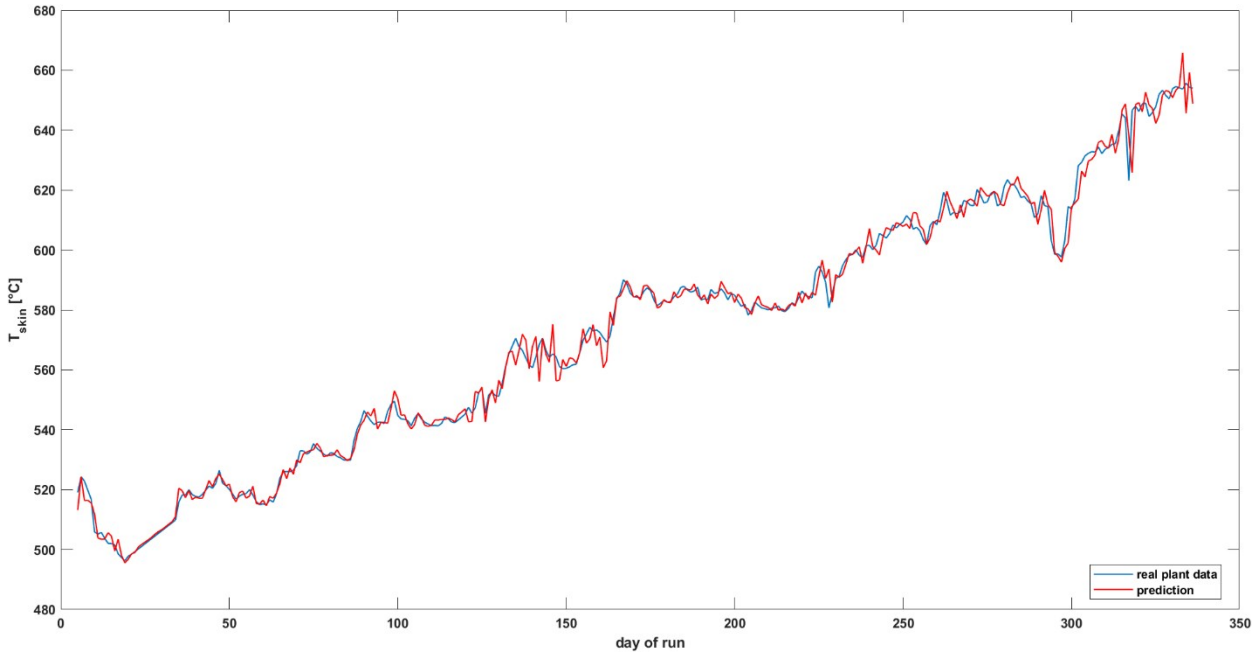

Figure 4.12 Simulated time evolution of the predictive model using different coefficients of the time series part of the model, namely for 100 days of run length the 2021 coefficients, from 100 days up to 200 days the 2022 coefficients retrieved from 100 days of run length data are used, then from 200 days of run the coefficients obtained from 200 days of data on 2022 run length.

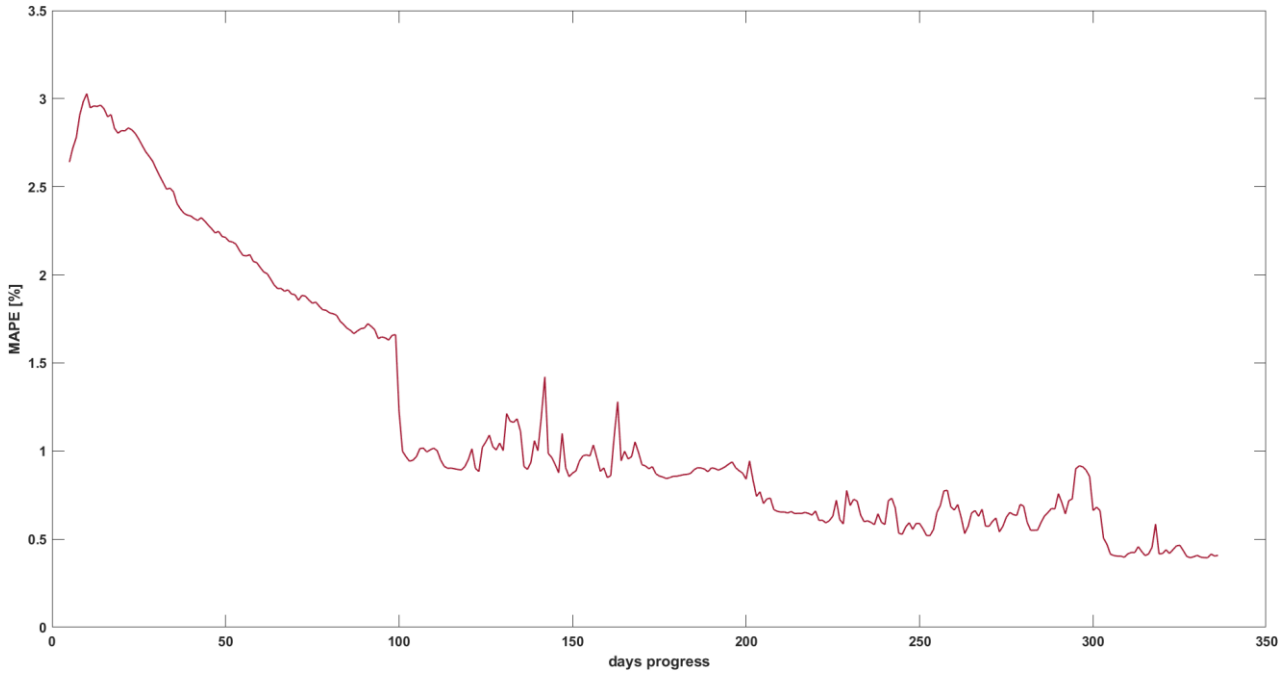

Figure 4.13 Mean absolute percentage error (MAPE) evolution as long as the simulation progress over the running period of run length of the furnace for the year 2022 by using a time series model where the coefficients for the time series part of the model are updated along the run.

As it can be observed in Fig. 4.13 the error starts from a 3% ca. in the first days of run and tends to decrease over time reaching a minimum of 0.41 % of error in the end of run. Therefore, it can be concluded that the model is sufficiently reliable and useful in order to provide the residual run length

of the thermal cracking furnace, thus an optimizer can be defined in order to determine the optimal value of the skin temperatures to reach the desired end of run as it will be discussed in Chapter 5.

4.2.4.1 Construction of the time series part of the model

The construction of the time series part of the skin temperature prediction model of the soaking zone of the thermal cracking furnace is here reported for explanatory purposes.

To define the ARIMAX model, the stationary condition is necessary in order to perform the pattern identification analysis. The stationary can be checked either visually or by applying the Augmented-Dickey-Fuller test. Note that data were analyzed when there was availability of *VGC* parameter and when it was possible its reconstruction by means of other parameters that are related to it as reported in §2.2.1, while avoiding the transient period (e.g. 50 days of run, where stability of operations was not continuous) of the plant.

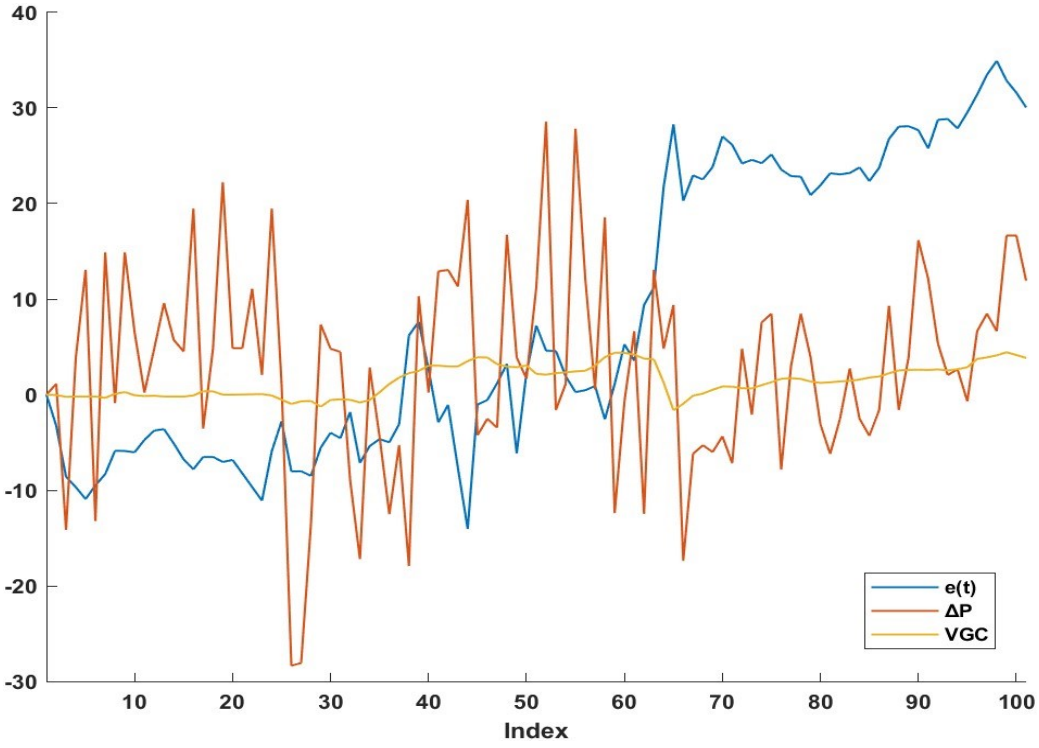

Figure 4.14 Profile of the *ΔP* (orange curve), *VGC* (yellow curve) and the error given as difference between the real value of the skin temperature and the predicted value of the skin temperature by means of the black-box part of the model (blue curve).

As it is possible to observe in Fig. 4.14, the data related to the error of the prediction *e(t)*, are not completely de-trended, thus a differentiation needs to be applied to obtain the stationarity of the series. Then, it is possible to proceed with autocorrelation analyses (total and partial) for the dependent variable *e(t)*, observing the possible presence of a lag in both the autocorrelation function (ACF) and partial autocorrelation function (PACF) for the dependent variable, demonstrating the correlation existing between the observation at a given instant with the observation at the previous instant. Data were included considering the standard deviation to be +/- 3σ.

Considering the need to use a model that is as accurate and simple in structure as possible to facilitate its subsequent implementation, following comparison on the goodness of fitting among the various

model forms analyzed, an ARX-type form was chosen for the time series on modeling error, which in a general form can be represented as:

$$(1 - \varphi_1 \cdot L) \cdot y_t = \beta_1 \cdot X_1 + \beta_2 \cdot X_2 + \varepsilon_t \quad (4.12)$$

where the y_t is the dependent variable (i.e., $e(t)$), and X_1, X_2 the exogenous variables, while the φ_1 represents the autoregressive coefficient which is multiplied by the lag term L, it is also considered the residual error ε_t. Note that, if not de-trended, it is not necessary to introduce the integration term because the exogenous variable ΔP serves the purpose (it contains the information needed to define the trend). The identified model was compared with other alternative models taking into consideration fitting and statistical tests, in particular, evaluating the Akaike Information Criterion (AIC) or Bayesian Information Criterion (BIC). To validate the time series model some analysis should be performed.

- For the analysis of the residuals, the plot of the residuals is analyzed by defining no patterns or trends. The Ljung-Box statistical test (or the Durbin-Watson) is also performed, with a p-value result of 0.2089, therefore there is no evidence of autocorrelation in the residuals, thus there is a good fitting of the model. The Ljung-Box test is a statistical test used to assess the presence of autocorrelation in the residuals of a time series model. The test assesses whether the autocorrelation coefficients of the residuals are significantly different from zero.
- To test the normality hypothesis, the distribution of residuals is analyzed by Q-Q plot (quantile-quantile) or use of the histogram plot, and possibly by applying the Shapiro-Wilke statistical test (or Kolmogorov-Smirnov).
- Engle's ARCH test can be used to test hypotheses of homoscedasticity. Engle's ARCH test examines whether there is a significant relationship between squared residuals (squared errors) and lagged squared residuals. The test helps determine if there is evidence of heteroscedasticity in the residuals, indicating that the variance of the errors is not constant over time. The result of the test is found to be above the significant level set (i.e. 0.05), thus rejecting the null hypothesis by being able to say that there is no evidence of heteroscedasticity in the residuals. Note that it is possible to apply other tests such as the White-test or the Breusch-Pagan test, which were not applied in this case since the analysis performed turns out to be sufficient.

Overall, all diagnostic tests indicate that the ARX model passed the necessary checks and the model fit is considered good: the model fit is adequate, the assumptions underlying the ARIMAX model (such as linearity, stationarity, and independence of residuals, are reasonably satisfied), the coefficients estimated are reliable, and the model can provide accurate predictions for future observations of the dependent variable given the values of the exogenous variables. It is important to note that passing diagnostic tests and obtaining a good model fit are encouraging, but do not guarantee the accuracy or reliability of the model in all scenarios. It is important to be cautious and consider the limitations of the ARIMAX model and the specific context of the data. In addition, continuous

monitoring and updating of model performance as new data become available are essential to ensure its continued validity. Periodic evaluation of the model's predictive accuracy and reassessment of its assumptions and fit will help maintain the reliability of the ARIMAX analysis. Because of the above observation, it has also been exploited, considering the ARX model, further identification by means of system identification methods (available in MATLAB as additional toolbox called System Identification Toolbox), in order to exploit a future possibility to identify directly the model by means of the MPC software that allows to identify models, such as the one provided by AspenTech (DMC3), which allows also a better identification of the coefficients of the model. The model with estimated one-step prediction is shown in Fig. 4.15., and in Fig. 4.16 the representation of the simulated model in free evolution without real data.

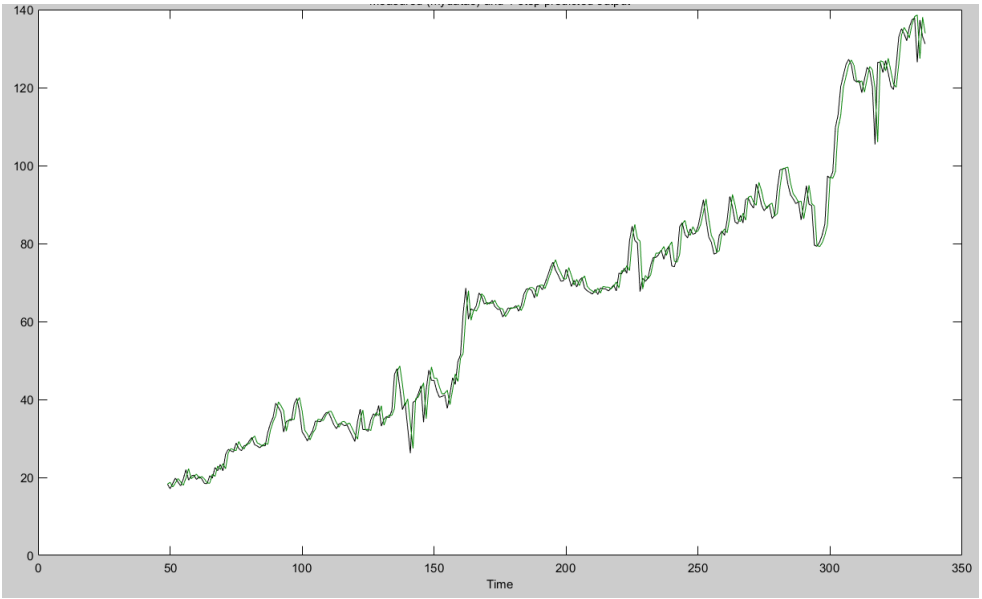

Figure 4.15 System identification plot of the measured (black curve) and 1-step predicted output (green curve) of the modelling error.

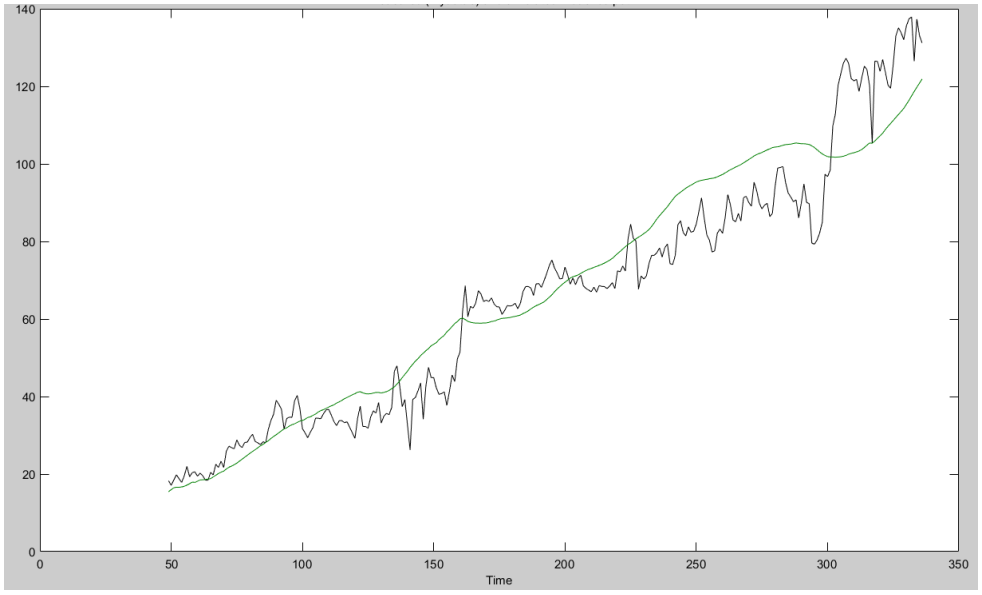

Figure 4.16 System identification plot of the measured (black curve) and simulated model output (green curve) of the modelling error.

Note that, the order of magnitude of the output value (identified dependent variable, in this case corresponding to the modeling error), corresponds to a difference given as difference from the real value and the prediction given by the black-box part, therefore it will then need to be added in the construction of the overall model to the stationary part (black-box).
The procedure described needs to be reproduced for each pass, so the shape of the model on the time series is assumed to be the same, thus needing only analysis of the coefficients.

4.2.4.2 Time series model considerations and advantages

The development of the time series model has led to solve the criticalities of the static model, specifically the feedstock characteristics and time evolution. The overall advantages are:

- including exogenous variables, such as the *VGC* which allows to account for the variability in crude, and the ΔP in order to account for the current and past operating conditions;
- controlling time delays by incorporating past events on current observations thanks to the autoregressive part of the model;
- modeling complex relationships between exogenous and response variables through the autoregressive, integral and moving average components of the model;
- managing autocorrelation (and seasonality);
- automatic update of the coefficient of the stationary part of the model (black-box) by means of the AspenTech DMC3's calibrate function, and eventual possibility of coefficients identification by means of already built in functionality in the same software where the APC application has been configured, giving the possibility of fully automated application.

In any case, at the actual state of the system some considerations are necessary. In particular, the necessity to collect data along the current run length, thus to update the model coefficients over time in order to increase the accuracy of the model. Another issue is related to the necessity to have the future values of the variables in order to provide the forecast, therefore it is of major importance to use data as much accurate as possible.

4.3 System architecture

To get an idea of the possible system architecture, since up to the moment this work has been delivered it has not been completed the implementation of the APC system, it is reported a simplified block diagram in Fig.4.17. The flow of information can be interpreted as follows:

- data of the CVs, MVs and DVs are collected from plant through the DCS with a very short time sampling (e.g. seconds);
- data relative to the CVs and DVs are sent to the APC short term models which evaluates the moves to be performed in the short term in order to bring the process in the optimal operating region and check the validity of the data within the set constraints;
- information between the two models are exchanged in order to provide from the short-term model to the long-term model the value of the maximum skin temperature T_{skin}^{max}, which has the aim to determined which pass should be predicted (i.e. to choose the respective time series model), and also it provides the updated coefficients by means of the calibrate function of the DMC3 software;

from the long-term model to the short-term model the value of the daily target of the skin temperature is provided, thus defining the set-point for the APC;

- the long-term model itself receives two external input, the scheduled data and the target of the end of run (T_{skin} , day of end of run), and consist of two parts, one of model prediction of the residual run length and one of long-term optimization which provides a single output, which is the daily skin temperature;
- the final output of the APC is represented by the final moves performed by MVs.

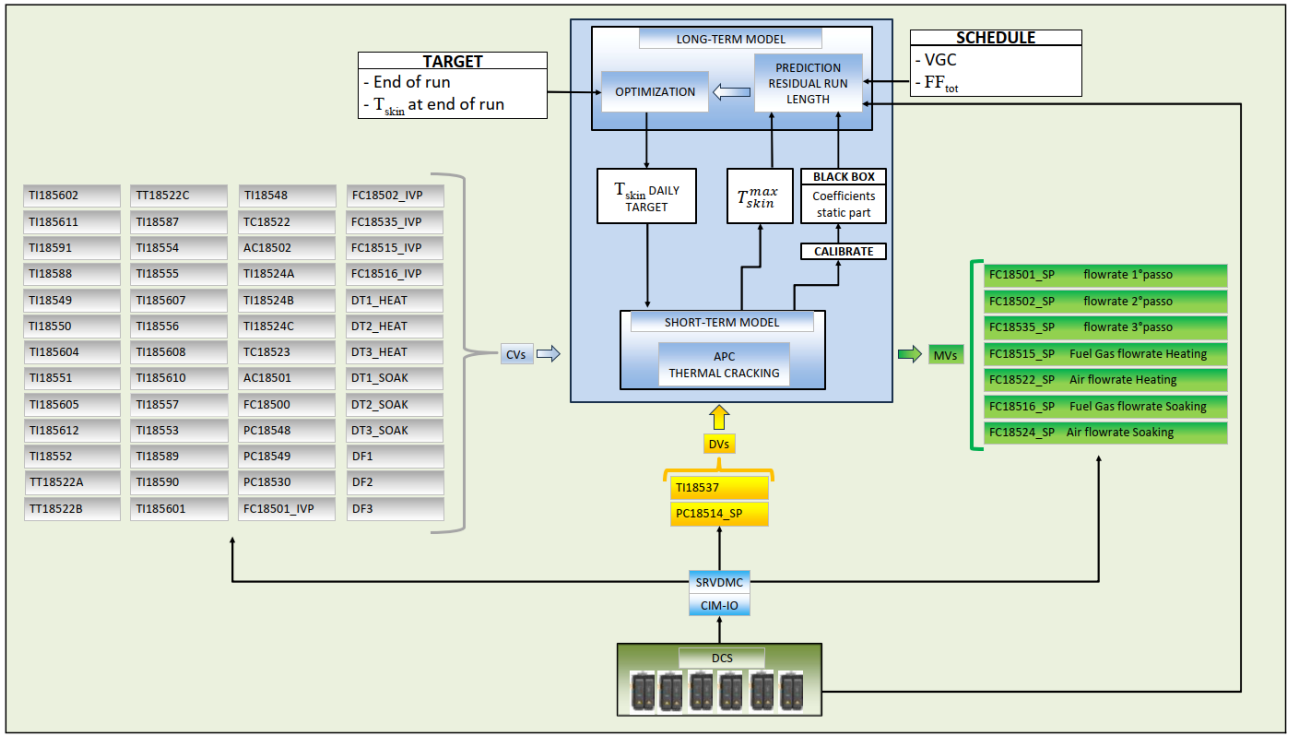

Figure 4.17 Block-diagram representation of the system architecture of the APC of the thermal cracking furnace.

The described architecture allows to understand that the APC is composed by a double horizon subsystems which communicates and interact with each other and with the basic-control layer (DCS), and above all it decides the control strategy depending on the external target provided by the plant decision makers.

Chapter 5

Optimization

The objective of the project is based on two-horizon optimization: short-term optimization of the yields and the efficiency of the furnace, and long-term optimization of fouling control. The predictive models developed allow us to understand the future behavior of the process, but in order to reach the set objectives, it is necessary to implement a dual-horizon optimizer that defines the target on a daily basis consistent with the long-term horizon, providing the set-point to the controller, which drives the system toward the optimal operating conditions. The need to define a control system that is reliable, efficient, and safe leads to constructing an optimizer that meets those requirements, in addition to the necessity of it being built into the APC system. The purpose of this chapter is to describe the functionality of the short-term optimization and the construction of the long-term optimizer, concluding with the benefits provided by the optimization in terms of yield and economic benefits, which allows for an evaluation of the potential applicability of the proposed APC.

5.1 Short-term optimization

Short-term optimization is related to the capability of the APC to reach an optimum of the operating region of the plant through the set constraints and ranking on the MVs and CVs as defined in §3.7.

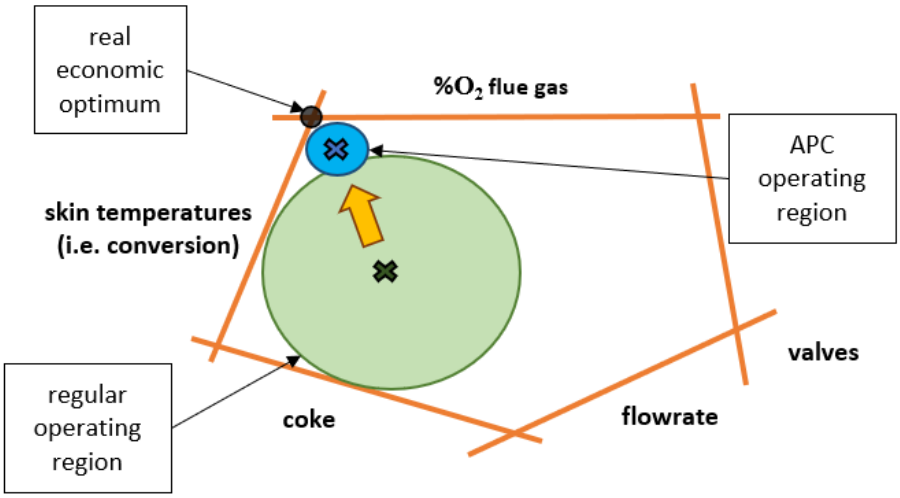

Figure 5.1 Steady-state optimization in short-term horizon.

The optimum is often economic, making it more intuitively understandable, as is the case here. As shown in Fig. 5.1, the short-term optimization is represented by the region where the skin temperatures of the furnace coils are at a maximum and the $\%O_2$ in the flue gas to the stack is minimized. In the first case, it is related to maximizing the conversion to increase the yield, but this

also corresponds to an increase in coke formation, which is one of the long-term process limitations (§5.2). In the second case, it corresponds to a decrease in furnace consumption, resulting in increased efficiency. Overall, short-term optimization involves a daily evaluation of the most economically feasible operational region. However, it is important to consider that the operational region of the APC (as shown in blue in Fig. 5.1) can change based on the constraints set for the CV ranking, as discussed in §3.7. It must also account for the need to stay within upper limits for the oxygen percentage in the flue gas. This objective could be disrupted, for example, by fluctuations in the fuel gas composition. Furthermore, it is essential to have control over the process while keeping the valves outside of the saturation condition.

It should be noted that the accuracy of predictive models defined in the APC matrix and the predictive model for fouling are crucial for short-term optimization. These two optimizers work simultaneously, causing changes in the operational region from time to time, as described in the system architecture in §4.2.

5.2 Long-term optimization

Long-term optimization is grounded in the results of predictive modeling of fouling, as described in the time series model in §4.2.3. Specifically, once the overall estimate of the residual run length at the current operating conditions is obtained, it becomes necessary to determine the required skin temperature value that needs to be maintained throughout the run length in order to achieve the set objective of reaching a specific final skin temperature on a given day of the run.

To do this, we need to make some preliminary considerations regarding the nature of the optimization, which can be summarized as follows:

- there should be no "jumps" between the on/off of the optimizer. For example, avoiding rapid temperature changes, such as going from 560°C to 620°C in a short period (e.g., within 1 day of the run);
- consider a gradual increase until the target is reached. This approach helps to prevent issues related to coke cross-linking formation or unexpected upsets;
- take into account the possibility of errors and assess a margin concerning the end run relative to the set target. It is also be possible to introduce a margin of uncertainty (e.g., -2%), which can vary (e.g., 3% for the first 100 days of the run, then 2% for the remaining days), on the set point. This approach allows for the inclusion of prediction errors;
- the optimization process should be easy to implement, easily understandable, and not resource-intensive.

In order to meet those conditions, the proposed optimization is based on evaluating the margin between the target skin temperature at the end of the run (typically 660°C) and the predicted skin temperature at the end of the run, thus defining a delta as follows:

$$\Delta T_{skin\ end\ of\ run} = \left(T_{skin\ target} - T_{skin}\right)_{end\ of\ run} \tag{5.1}$$

the resulting $\Delta T_{skin\ end\ of\ run}$ [°C] is divided by the remaining number of days in the run n_{days}. The obtained result, $\Delta T_{skin\ day}$ [°C]\ is added cumulatively to each day, taking into account the past increases. This process yields the optimized value of the skin temperature, T_{skin}^{opt} [°C], which enables us to achieve the target end of run skin temperatures.

$$\Delta T_{skin\ day} = \frac{\Delta T_{skin\ end\ of\ run}}{n_{days}} \tag{5.2}$$

$$T_{skin}^{opt} = T_{skin} + \sum_{k=1}^{n_{days}} k \cdot \Delta T_{skin\ day} \tag{5.3}$$

the output generated by the long-term optimization is T_{skin}^{opt}, which serves as the set-point for the APC controller. The controller, driven by the short-term models, makes the necessary adjustments to attain the optimal operating conditions. The graphical representation of this optimization on day 100 of the run length is presented in Figure 5.2.

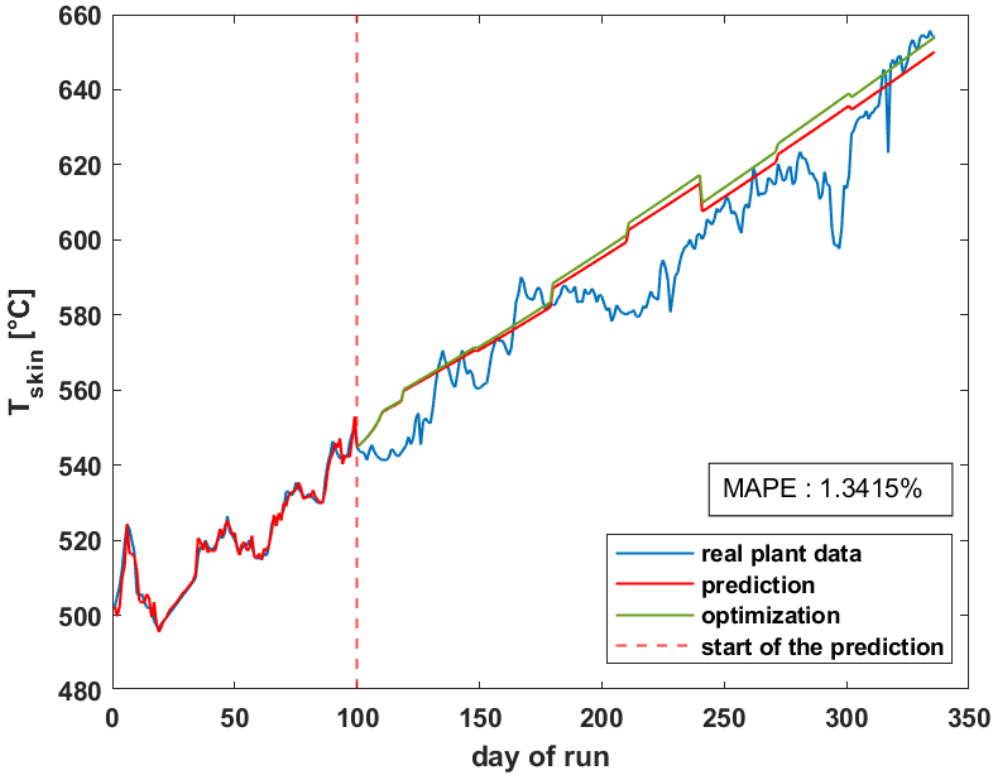

Figure 5.2 Prediction and optimization of the skin temperatures of the 1st pass of the thermal cracking (soaking) at day 100 of run length of the year 2022.

The figure illustrates the margin between the prediction based on scheduled data (the red curve) on the last day of the run, which, in this comparison, has been set to match the actual plant data (the blue curve) at the end of the run, and the target temperature at the end of the run. The optimized curve (the green curve) exhibits a slight increase over time compared to the prediction, allowing it to align with

the set constraints required for the optimizer. In Figure 5.3, the overall simulated behavior of the optimizer is presented, considering day-by-day optimization as it would be when using the APC from the beginning of the run length.

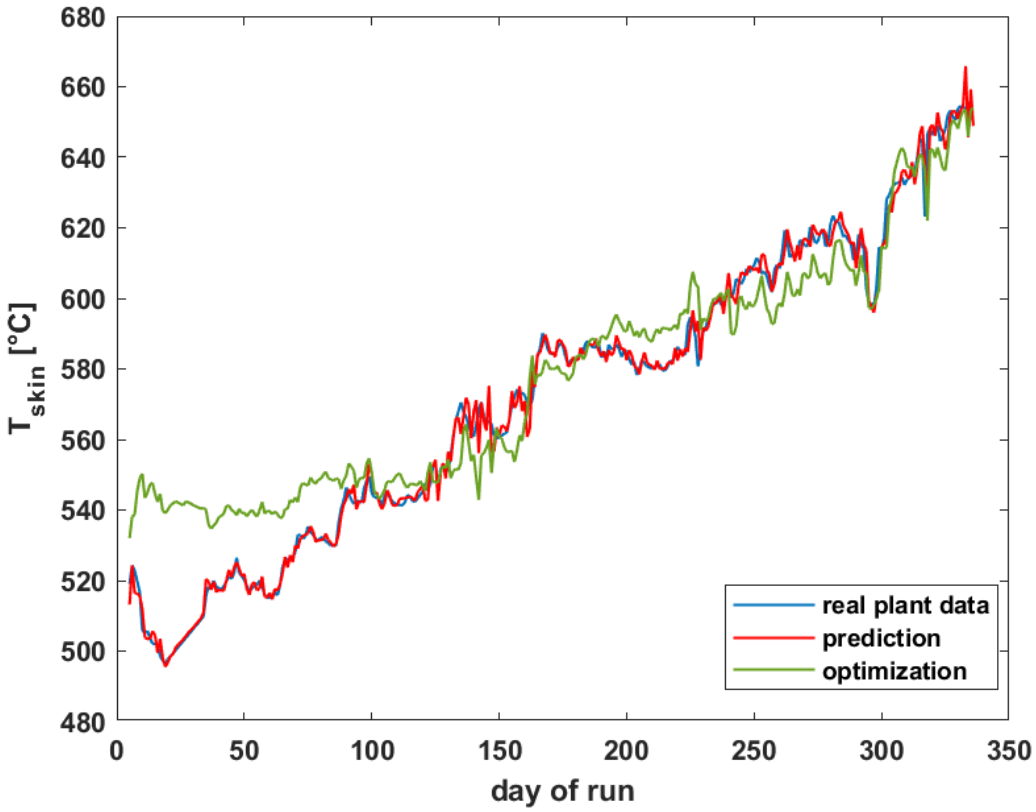

Figure 5.3 Simulated comparison between the optimized value (green) of the skin temperature of the thermal cracking furnace (soaking) and the predicted value (red) obtained from the time series model simulation.

The optimized values for the first 100 days of the run are higher than the actual ones because the optimization aims to enhance the overall run length. As evident, the gradual increase in skin temperatures suggested by the optimizer results in improved furnace management, leading to increased conversion and more stable control throughout the entire run, minimizing temperature spikes over short periods.

5.3 Yield and economic benefits

An estimate of the yields and potential economic gains achievable through the application of optimization with a predictive fouling model for the thermal cracking furnace has been conducted. This estimate is a prerequisite for the preliminary feasibility analysis of the project, as outlined in the construction procedure of an APC in §3.4.1. The optimization, in this case, pertains to long-term optimization and has been initially applied for an economic assessment of the project's profitability using a static yield model. This assessment is based on the long-term optimization described in §5.2 for the operational cycle of the year 2022. As shown in Figure 5.4, the first 67 days of operation were excluded from the analysis to mitigate the impact of transients, upset conditions, and potential activity of the HPTC (high-pressure thermal cracking) unit. The results were evaluated by comparing the real data trend (represented by the orange line) with the optimized trend (shown in green). The ultimate

goal was to achieve a skin temperature of 645°C at the end of the run. To account for potential variability, a wide margin of error of 15°C was considered, relative to the typical end-of-operation target of 660°C. This approach adopted a conservative stance to prevent the possibility of exceeding the target. Any discrepancies were to be corrected through daily optimization to reach the end-of-operation target. For instance, if skin temperatures increased beyond expectations, the optimization would ensure that the daily temperature increase decreased while maintaining the same target. The reference skin temperature for this evaluation was TI18555, 1st pass, which achieved higher temperatures on average throughout the run and reached the highest temperature at the end of the run. This observation suggests that achieving a more balanced furnace management, through the use of short-term optimization in the advanced control system, could lead to more uniform temperatures between the three passes, ultimately increasing the yield.

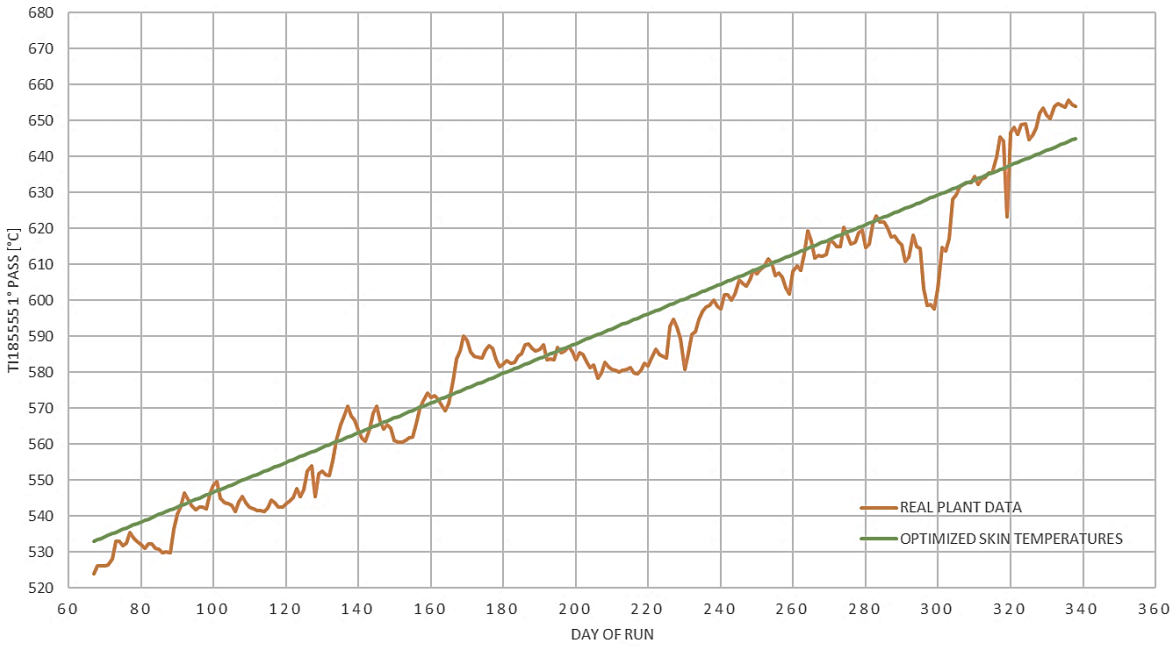

Figure 5.4 Plot of the real skin temperature (orange line) for the thermal cracking furnace (soaking) and the optimized trend (green line). Optimized trend obtained from the optimization of the static model described in §4.2.

The results of the analysis reveal an average daily increase in skin temperature of 2.35%. For comparison, the reference temperature used is the estimated starting temperature for the cracking reactions in the examined furnace, set at approximately 450°C. It is assumed that this temperature marks the point at which the cracking reactions start, as described in Chapter 1.

5.3.1 Evaluation procedure

To perform the estimation, it was necessary to consider the impact of increasing the furnace skin temperature on distillate production and, consequently, on yields, while keeping the feedstock unchanged. However, it is important to note that providing a precise and unequivocal estimate of yields solely for the thermal cracking unit is not possible. This limitation arises from the absence of flow indicators in the subsequent separation section of the plant, with the exception of the main T-1801 separation column. This column also receives feed from the fractionation column connected to

the visbreaking plant. Therefore, there is a risk of error if the evaluation does not take into account the assessment under constant operating conditions of the VB unit. Hence, the historical data analysis considered the following:

- data from periods when the HPTC unit was not in operation;
- data from the thermal cracking furnace when the VB unit was set to produce road bitumen and fuel oil, excluding the industrial bitumen production setting. This exclusion assumes a constant contribution from the VB in yields;
- data from the beginning and end of each operating cycle, accounting for the impact of fouling, which results in different yields during these distinct periods;
- data at a consistent feedstock rate within each evaluation of the effect of increasing the skin temperatures (of the soaking chamber of the furnace) on yields.

This comprehensive analysis of historical data factors in various variables and conditions, ensuring a more accurate assessment of the impact of increased skin temperatures on yields.

To determine the impact on yields resulting from a 1°C increase in skin temperatures, it was necessary to evaluate the steady-state gain terms of the transfer functions. These terms were derived from the analysis of historical data using DMC3 software. The gain, which quantifies the steady-state effect of a 1°C increase in skin temperature on the FOT (furnace outlet temperature) as an operational variable of the furnace, is expressed as follows:

$$K_1 = \frac{\Delta FOT}{\Delta T_{skin}} = 0.5\ °C/°C \tag{5.4}$$

The corresponding yields resulting from a 1°C increase in the FOT of the thermal cracking unit were then determined. The graphs in Figure 5.5 are related to the data at the end of the run, which represents a more conservative approach and results in lower yields. In this case, the following gains are obtained:

$$K_{benzina} = \frac{\Delta benzina}{\Delta TUF} = \frac{7.269 - 6.896}{486.088 - 482.417} = 0.1\frac{t}{°C} \tag{5.5}$$

$$K_{gas} = \frac{\Delta gas}{\Delta TUF} = \frac{3.622 - 3.339}{486.088 - 482.417} = 0.08\frac{t}{°C} \tag{5.6}$$

$$K_{kerosene} = \frac{\Delta kerosene}{\Delta TUF} = \frac{3.269 - 6.896}{486.088 - 482.417} = -0.008\frac{t}{°C} \tag{5.7}$$

$$K_{LGO} = \frac{\Delta LGO}{\Delta TUF} = \frac{13.007 - 13.17}{486.088 - 482.417} = -0.044\frac{t}{°C} \tag{5.8}$$

The most significant contribution comes from the production of gasoline and gas, the primary products of the thermal cracking process. Consequently, as conversion increases, yields of other distillates like kerosene and light diesel decrease.

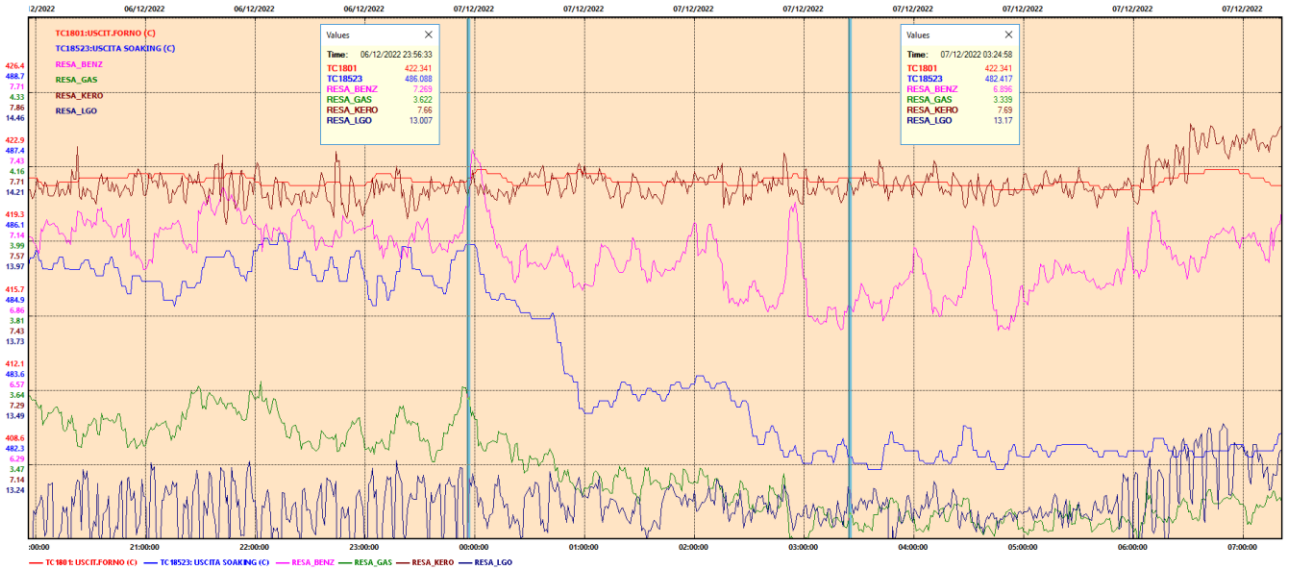

Figure 5.5 Trends of the variables of FOT and the individual percentage yields at the exit of the fractionation column T-1801.

Figure 5.6 Trends of the variables of FOT and the cumulative percentage yield of distillates specifically related to thermal cracking under the same conditions.

In summary, the cumulative percentage yield, as depicted in Fig. 5.6, is illustrated. A 1°C increase in FOT, under identical feed and VB operating conditions, leads to a 0.17% increase in overall yields when considering the year-end of the run, which represents an even more conservative approach. In contrast, when the initial run length period is considered, implying less fouling, the yield value is higher. In this case, a 1°C increase in FOT corresponds to double the overall percentage yields compared to the year-end of the run, resulting in a total yield increase of 0.3%.

5.3.2 Results

The results obtained for the 2022 operating cycle in 271 operational days (excluding the first 67 days for the reasons mentioned in §5.3.1) are presented in Table 5.1 as variations resulting from increasing skin temperature to the optimal operational value, considering the static predictive model.

Table 5.1 Summary of optimized yields achievable starting from the 68th day of the 2022 cycle run for the thermal cracking unit, considering the static predictive model.

Product	ΔFlowrate [ton]	%ΔYield
gas	+8512	+0.57%
gasoline	+10640	+0.71%
kerosene	-851	-0.06%
light gas-oil	-4681	-0.31%
total	+13619	+0.91%

It is important to note that the results should be interpreted in relation to ΔT, which is defined as the difference between the optimized skin temperature and the actual skin temperature. Therefore, the negative sign in Table 5.1 for kerosene and light gas-oil should be attributed to the decrease in flow rates (and yields) of these distillates compared to the actual obtained values, resulting in an increase in gasoline and gas yields. The total economic gain has been estimated based on the total sum of the overall flow rate variations. These variations are not calculated as averages but represent the sum of daily contributions, taking into account the varying daily yields. The economic result obtained is the most conservative one. If we consider setting the optimal target at the end of the run (i.e., 660°C as the skin temperature), which means operating the system at the limits of optimization with an average daily increase in skin temperatures of 6.78%, it leads to an overall 3.31% increase in yield and a substantial economic gain. This demonstrates the system's potential for optimization. However, it's worth highlighting that the economic analysis is based on a static model that doesn't account for the dynamic behavior of the system. Nonetheless, it provides valuable insights into the possibilities the system can offer.

After the development of the time series model, the same evaluation has been carried out also by it. The results, reported in Tab. 5.2, of the optimization were obtained using the same procedure reported previously, but with some considerations. The comparison of the time series model with real plant data are affected by changes in the operating conditions at which the process is carried out for different needs in terms of reaching the goal at the end of run, as mentioned in the description of the furnace management, thus of the skin temperatures as described in §4.2, in the initial days of run up to 150 days of run length, the severity of the furnace is kept at minimum condition with a slightly increase up to the final days of run were the temperatures are increased to reach the target end of run temperatures. This approach, leads to a very high margin of optimization in the first half of the run

length of the furnace and less margin in the second half since the furnace is pushed towards the edge of the operating conditions. Thus, as can be observed from Figure 5.3, when comparing the time series model optimization with real plant data, it's essential to emphasize the need to keep the optimization as active as possible during the initial period of the run to achieve significant improvements in yields and benefits. The simulation of long-term optimization results in a +1.75% increase in yields. This occurs when the optimization remains active throughout the entire year of the run after the initial transient days, with an end-of-run target set as the real end-of-run skin temperature (654°C).

Table 5.2 Summary of optimized yields achievable during the 2022 cycle run for the thermal cracking unit, considering a time series predictive model.

Product	**ΔFlowrate [ton]**	**%ΔYield**
gas	+15320	+0.83%
gasoline	+19150	+1.04%
kerosene	-1532	-0.08%
light gas-oil	-766	-0.04%
total	+32172	+1.75%

However, when optimization is initiated later in the run length, achievable yields decrease. This decrease is due to the reduced margin for optimization, and the operating conditions become closer to the limiting conditions. It's important to note that the comparison in the case of a time series model is not precise, as there are differences in how the long-term optimizer operates compared to the actual control system. In the first case, it aims to maintain the system at optimal operating conditions from the beginning of the run to reach the end-of-run conditions as specified. In the second case, the system deviates from optimal operating conditions in the first half of the run and then moves toward them in the second half, potentially leading to the previously mentioned issues of coke cross-linking.

It is important to note that the results mentioned account only for the part related to the APC working with the long-term optimizer. The implementation of both short-term and long-term optimization will lead to increased yields and benefits. These benefits can be summarized as follows:

- increased overall yield across the run length, thanks to the long-term optimization for fouling control and short-term optimization for balancing the three passes of the furnace;
- reduced utility consumption and optimal $\%O_2$ to the stack, thanks to the short-term model, which allows for achieving the optimal air/fuel ratio in the heating and soaking section, thereby increasing furnace efficiency;
- prevention of high cross-linking of the coke, thanks to the long-term optimization, which controls coke development and avoids steep temperature increases in short periods;

- avoidance of under-cracking by maximizing conversion in the short-term, while also preventing over-cracking conditions that can shorten the furnace run length;
- automation of unit control, reducing the potential for errors.

Overall, the use of APC with a dual-horizon optimizer for the thermal cracking furnace is a solution that enhances furnace management, resulting in increased yields and income while adhering to safety, environmental, and process constraints. Due to the positive results of this analysis and the benefits provided by APC, the project has received approval for commissioning and will be implemented at the API refinery in Ancona.

Conclusions

The presented project originated from a request by the API S.p.A. refinery in Falconara Marittima (Ancona) to control the severity of the thermal cracking process. Specifically, the objectives are to:

- maximize unit conversion, thereby increasing overall refinery conversion;
- control furnace tube fouling to ensure the completion of the run;
- enhance furnace efficiency by balancing the passes and optimizing utility consumption (e.g., minimizing $\%O_2$ to the flue stack);
- stabilize the process by avoiding under/over-cracking conditions and managing disturbances;
- comply with safety, environmental, and process constraints.

To address the issue, the working team considered the application of an optimization and supervisory control system for the plant. As of the present moment when this work was delivered, the plant has only a basic control layer. Therefore, a step-by-step design of the advanced process control (APC) system based on model predictive control (MPC) was carried out up to the final project stage. The initial step involved a preliminary analysis, which focused on the process and process units, particularly the reactions and fouling (coke formation) related to thermal cracking. The following observations were made:

- increasing process severity leads to higher conversion but also increased coke formation;
- the characteristics of the crude oil, and thermal cracking feedstock in general, determine the tendency to form more or less coke under the same severity conditions. Thus, it is essential to consider the quality of the feedstock;
- the thermal cracking plant unit at the API refinery cannot be controlled as a whole, as the separation section (fractionator columns) is coupled with the visbreaking unit. Therefore, the design must focus solely on the thermal cracking furnace;
- the analysis of the variables, including manipulated variables (MVs), controlled variables (CVs), and disturbances (DVs), must account for the presence of the current feedback control system, which could distort the interpretation of the relationships between variables;
- fouling can be primarily monitored through the skin temperatures of the furnace, particularly in the soaking section, where cracking severity is higher than in other sections of the furnace.

It has been concluded that the project can be carried out using an approach that consists of designing an APC with a dual-horizon optimizer, including a predictive model of fouling. In particular, the designed APC consists of:

- short-term models for each relationship between the identified variables in the plant's step testing phase to meet the objectives of multivariate predictive control;
- a long-term model based on a statistical approach, specifically using a time series linear model that predicts the skin temperatures of the furnace's soaking section to forecast the residual run length in terms of the end-of-run temperature on a fixed day of the run;

- optimization of the short-term models using set constraints and variable rankings, enabling the APC to reach the optimal operating region for economic efficiency. This optimization is related to the capability of maximizing yields and furnace efficiency while maintaining compliance with safety, environmental, and process constraints;
- an optimizer for the long-term model using the predictive long-term fouling model. It retrieves the optimal operating conditions in terms of the allowable maximum daily skin temperature, facilitating the achievement of specified end-of-run conditions and control of fouling buildup throughout the run.

The overall APC system has been built inside the DMC3 software provided by Aspen Technology, with whom the project is in collaboration. The short-term models were constructed using identification algorithms provided by the DMC3 software after the plant step-tests. The short-term optimization was also implemented in the software by defining the gain matrix, CV rankings, and limit constraints. On the other hand, the long-term model was designed for a preliminary evaluation of its usability using MATLAB software. Initially, a static model was created to perform a profitability analysis of the project, incorporating a static model to control fouling. After a positive result from the economic evaluation, a time series model was developed. The time series model is composed of two parts:

- a black-box part of the model that depends on the feed-flowrate to the single pass of the furnace and the fuel gas flowrate to the soaking chamber. The coefficients of the linear equations were derived from the steady-state gain coefficients of the mathematical models between the skin temperatures and these two variables;
- a time series part of the predictive model developed using an ARIMAX model on the prediction error not accounted for by the black-box part of the model. This part is influenced by the quality of the feedstock to the furnace, represented by the VGC parameter and the pressure drops (ΔP), which is the difference between the inlet and outlet pressure of the furnace.

The results of the long-term model with respect to past run length show a low mean average percentage error (MAPE), less than 3%, with a reduction of up to 0.4% as more data are collected and precise forecasting is achieved. Once the model's validity was proven, the optimizer for the long-term model was built with the need to implement a reliable and easy-to-use optimization in an APC. Therefore, an optimization that evaluates daily increases in skin temperatures based on the margin between the estimated residual run length and the set end-of-run conditions (day and temperature) was designed. A final yield and economic analysis were performed using a suitable method based on mathematical relationships between skin temperatures, outlet temperature, and distillate yields at set conditions, allowing for a precise estimation. The results show an increase in yields ranging from 1% to 3%, highlighting that as optimization improves yields, economic gains also increase. It should be noted that this evaluation did not include a quantitative estimation of the overall APC application, which could potentially lead to further yield increases and process management improvements, including full automation of unit control. Further possible project developments were suggested by AspenTech, which proposed evaluating model performance over one run length and further

developing the predictive model through the application of neural networks. The evaluation also considered the possible implementation of reaction kinetics if there is stabilization of the feedstock quality for thermal cracking. The work presented here and the results obtained have allowed the project to move into the commissioning phase, with completion of its online implementation expected by 2024. This will allow for the evaluation of the actual results generated by the application in the future.

References

Asinger, F. (1968). *Mono-olefins. Chemistry and technology*. Pergamon Press, Oxford (U.K), p.9-24.

Bauer, M. and I. K. Craig (2008). Economic Assessment of Advanced Process Control—A Survey and Framework. *J. Process Control*, **18**, 2-18.

Bemporad, A. and M. Morari (1999). Robust model predictive control: A survey. In: *Robustness in identification and control* (A. Garulli, A. Tesi), Springer, Berlin (Germany), p.207-226.

Box, G.E.P., Jenkins, G.M., Reinsel, G.C., Jung, G.M. (2015). *Time Series Analysis: Forecasting and Control* (5th ed.). Wiley, New York (U.S.A.), p.2-11, p.88-119.

Coats, H. B. and J. B. Hill (1928). The Viscosity-Gravity Constant of Petroleum Lubricating Oils. *Ind. Eng. Chem.*, **20**, 641-644.

Murphree, E. V. and G. Ciprios (1962). *Cracking and reforming.* Institute of Petroleum, London (U.K.), p.313-364.

Nelson, W. L. (1958). *Petroleum Refinery Engineering* (4th ed.). McGraw-Hill Book Co., New York (U.S.A.), p.626-693.

Reyniers, G. C., Froment, G. F., Kopinke, F.D. and G. Zimmerman (1994). Coke Formation in the Thermal Cracking of Hydrocarbons — Modelling of Coke Formation in Naphta Cracking. *Ind. Eng. Chem. Res.*, **33**, 2584-2590.

Sachanen, A. N. (1940). *Conversion of Petroleum.* Reinhold Publishing Co., New York (U.S.A.), p.9-186.

Sachanen, A. N. and M. D. Tilicheyev (1927). Influence of High Pressure Cracking. *Oil Gas J.*, **28** p.46.

Speight, J. G. (2007). *The Chemistry And Technology of Petroleum* (4ª ed.). CRC Press, Boca Raton (U.S.A.), p.40

Treccani (2005). *Enciclopedia degli Idrocarburi*, Capitolo 5.2, p.233.

Web site

`https://www.e-education.psu.edu/fsc432/content/chemistry-thermal-cracking-0`

(ultimo accesso: 15/07/2023)